Sorgenti di Radiazione Thomson/Compton e Collisori Fotonici

Luca Serafini – INFN-Milan and University of Milan
luca.serafini@mi.infn.it
also thanks to V. Petrillo, F. Broggi, A. Bacci, A.R. Rossi, I. Drebot, C. Curatolo, M. Rossetti

Seminar Outline

- **Overview of Compton Sources and Applications**
- **Linear Quantum Theory of Inverse Compton Scattering of Beams and Paradigms for Compton Sources**
- **Photon-Photon Colliders at low energy (MeV) for Breit-Wheeler and photon-photon scattering experiments**
- **Hadron-Photon Colliders as muon photo-cathodes for TeV photons, neutrino and pion/muon low emittance beams**

Inverse Compton Sources, Overview, Theory, Main Technological Challenges – Photonic Colliders

- **New Generation of X/γ ray beams via electron-photon beam collisions for advanced applications in medicine/biology-material science/cultural heritage/national security *and* fundamental research in nuclear physics and high energy physics (e-γ, γ-γ colliders, pol. e^+ beams, hadron. physics, etc)**
- **Inverse Compton Sources (ICS) are e^-/photon colliders aimed at producing secondary beams of photons**
- **Several Test-Facilities world-wide: after a decade of machine test&development we are entering the era of User Facilities in X-ray imaging and γ-ray Nuclear Physics and Photonics**

Inverse Compton Sources, Overview, Theory, Main Technological Challenges – Photonic Colliders

- **Hadronic Physics was the original motivation for Compton back-scattering experiments (cfr. Ladon at INFN-LNF, Graal at ESRF, etc): single photon per bunch collision at energies > 50 MeV with tagging (quite popular decades ago)**
- **Recent Proposals (*R.Hajima et al., PRAB 19, 020702, 2016*) for high flux (5000 / s) GeV photons using FELs and 7 GeV e$^-$ E.R.L.**
- **Combination at this Lab (CERN, SPS and LHC) of TeV-class proton beams and (possible) X-ray FELs ⇒ TeV-class photons (the role in beam-beam collisions of beam phase space quality on TeV photon spectra and fluxes (100 / s))**

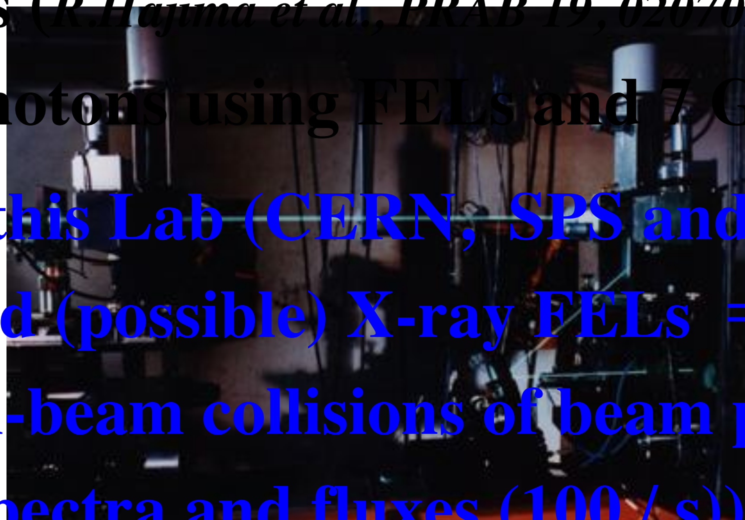

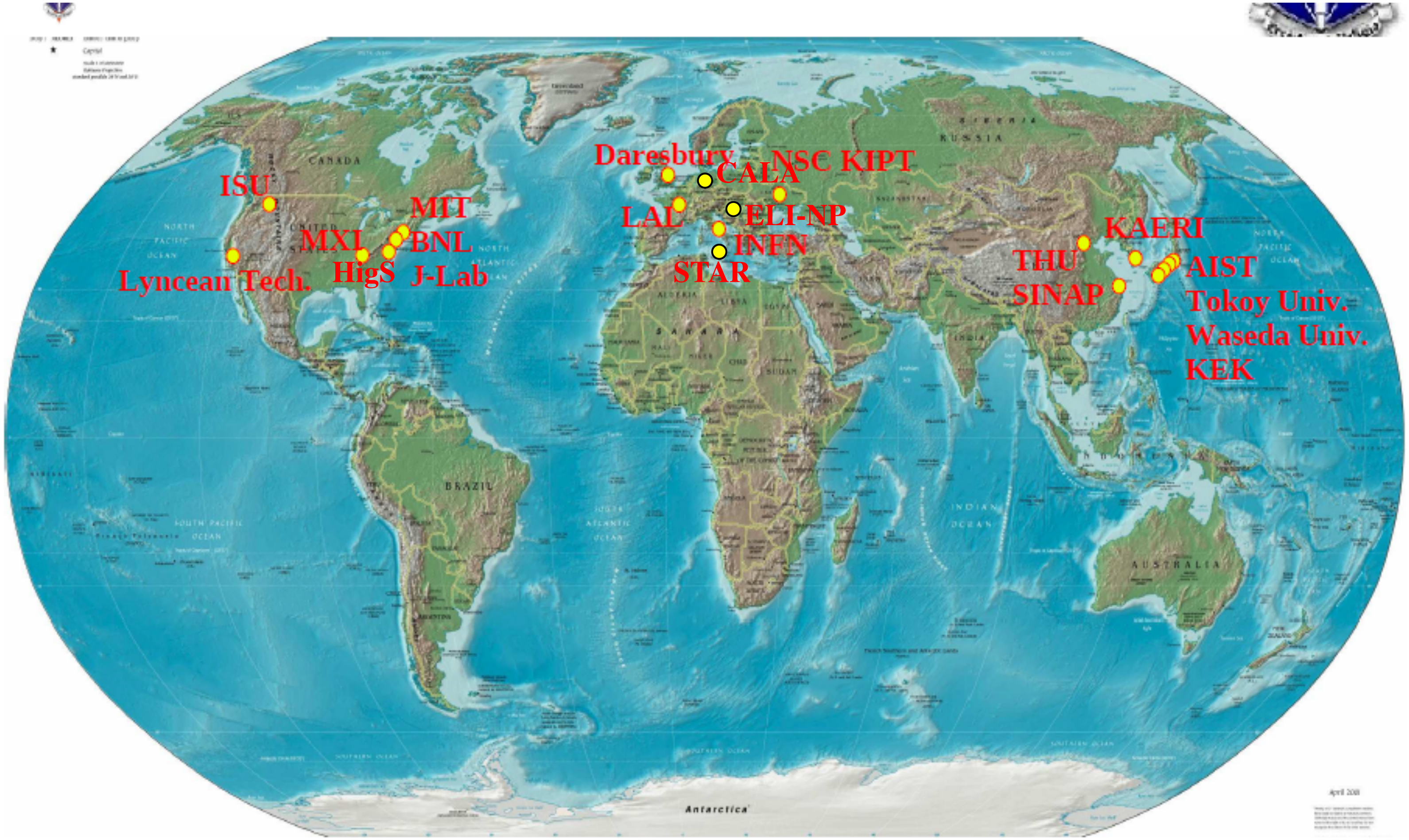

ICS are the most effective "photon accelerators" (boost twice than FELs)

"4γ² boost effect" $$E_{X/\gamma} = 4\gamma^2 E_{laser}$$

$$with\ T = 100\,MeV\ (\gamma = 197)\ E_{laser} = 1.2\ eV \Rightarrow E_{X/\gamma} = 186\ keV$$

Courtesy A. Variola

Existing and planned Thomson sources

	Type	Energy [KeV]	Flux (@ 10% bandwidth)	Source size (μm)
*PLEIADES (LLNL) [11,12]	Linac	10-100	10^7 (10 Hz)	18
*Vanderbilt [13,14]	Linac	15-50	10^8 (few Hz)	30
*SLAC [15]	Linac	20-85		
*Waseda University [16,17]	Linac	0.25-0.5	$2.5\ 10^4$ (5 Hz)	
*AIST, Japan [18]	Linac	10-40	10^6	30
*Tsinguha University [19]	Linac	4.6	$1.7\ 10^4$	
*LUCX (KEK) [20]	Linac	33	$5\ 10^4$ (12.5 Hz)	80
+ UTNL, Japan [21,22]	Linac	10-40	10^9	
MIT project [23]	Linac	3-30	$3\ 10^{12}$ (100 MHz)	2
MXI systems [24]	Linac	8-100	10^9 (10Hz)	
SPARC –PLASMONX [25]	Linac	20-380	$2\ 10^8$ -$2\ 10^{10}$	0.5-13
Quantum Beam (KEK) [26,27]	Linac		10^{13}	3
*TERAS (AIST) [28]	Storage ring	1-40	$5\ 10^4$	2
*Lyncean Tech [29,30,31]	Storage ring	7-35	~ 10^{12}	30
Kharkov (SNC KIPT) [32]	Storage ring	10-500	$2.6\ 10^{13}$ (25 MHz)	35
TTX (THU China) [33,34]	Storage ring	20-80	$2\ 10^{12}$	35
ThomX France [35]	Storage ring	50	10^{13} (25 MHz)	70

Table 3: Compact Compton X ray sources. Symbols * and + refers respectively to machines in operation and to machines in construction.

STAR (Calabria) Linac 20-100 10^{11} (100 Hz) 18

From **THOMX** Conceptual Design Report, A.Variola, A.Loulergue, F.Zomer, LAL RT 09/28, SOLEIL/SOU-RA-2678, 2010

highly asymmetric compact*

electron-photon colliders

***10 m, 10 M$**

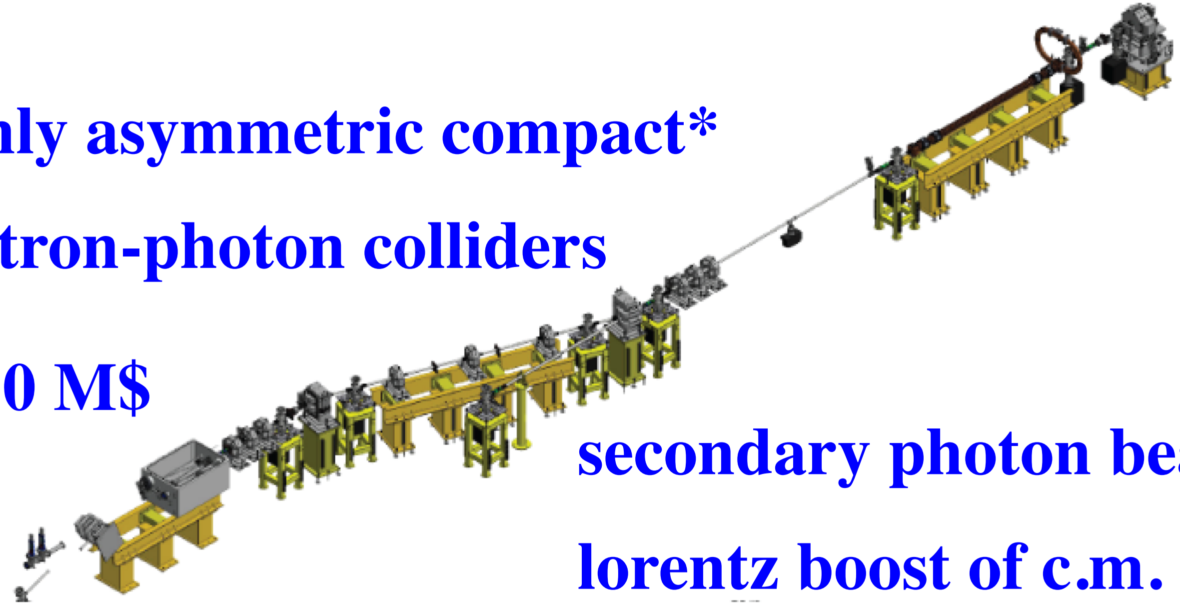

secondary photon beams via large

lorentz boost of c.m. reference frame

Fig.2 – STAR machine as an example of Paradigm A. Overall length about 12 m.

MeV/GeV's electrons

eV's photons

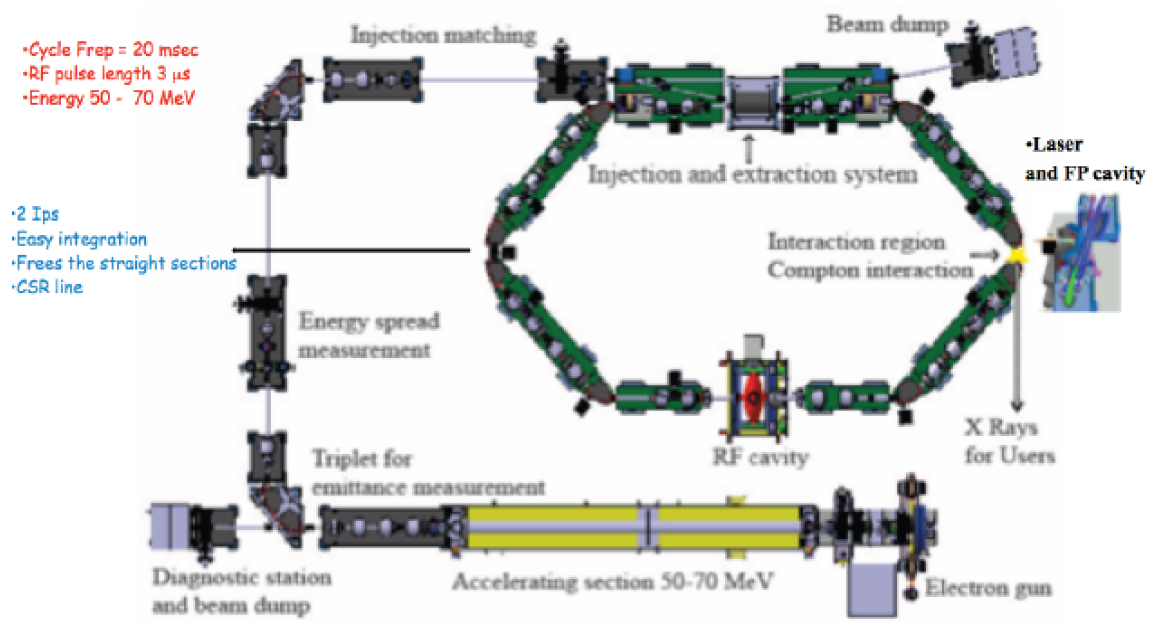

Fig.3 – ThomX as an example of Paradigm B. Size is about 10x10 m^2.

MariX/BriXS Program at Universita' degli Studi di Milano and INFN

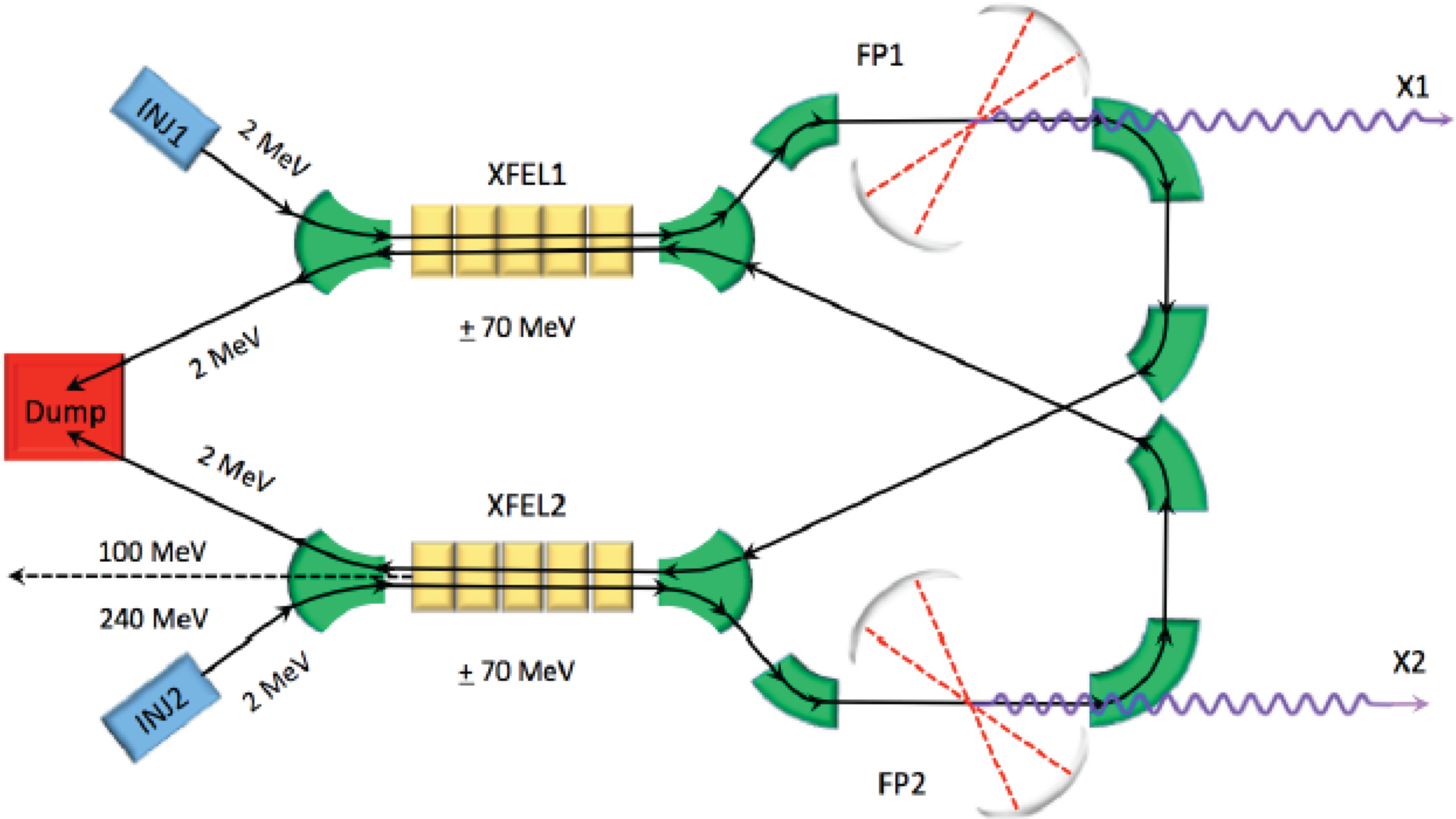

Fig.6 – BriXS conceptual lay-out, based on a wrapped push-and-pull modified Tigner-Variola scheme.

Courtesy V. Petrillo

Biomedical imaging with the lab-sized laser-driven synchrotron source Munich Compact Light Source

Klaus Achterhold

Biomedical Physics, Physics-Department E17, Technische Universität München

Compact machine
10x10 m^2
In operation since early 2015

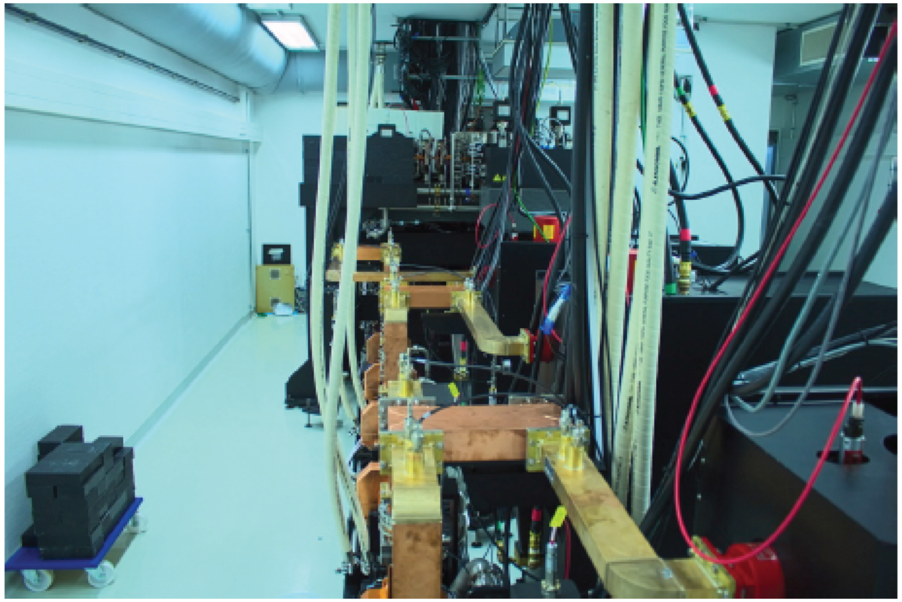

Klaus.Achterhold@tum.de

$$E_x(\Theta,\alpha,E_L,T)=\frac{(1+\beta\cos\alpha)E_L}{1-\beta\cos\Theta+(E_L/mc2)(1+\cos(\Theta+\alpha))}$$

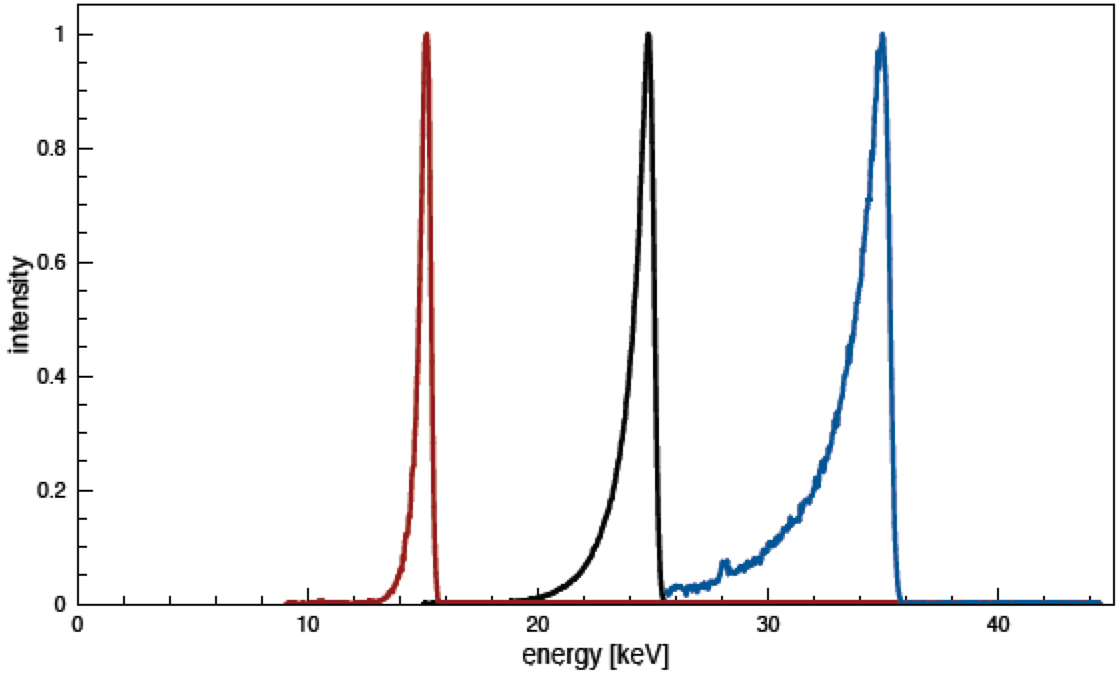

measured Spectrum of X-rays into +/- 2 mrad

Bandwidth

$35000+0.0016\cdot\Delta T$ with $\Delta T/T=0.3\%$
$35000+30000\cdot\Delta E_L$ with $\Delta E_L/E_L=10^{-12}$

$35000-9000\cdot\Delta\alpha^2$ with $\Delta\alpha=0.03$

Measured $5\cdot10^{10}$ ph/sec with 20 mA

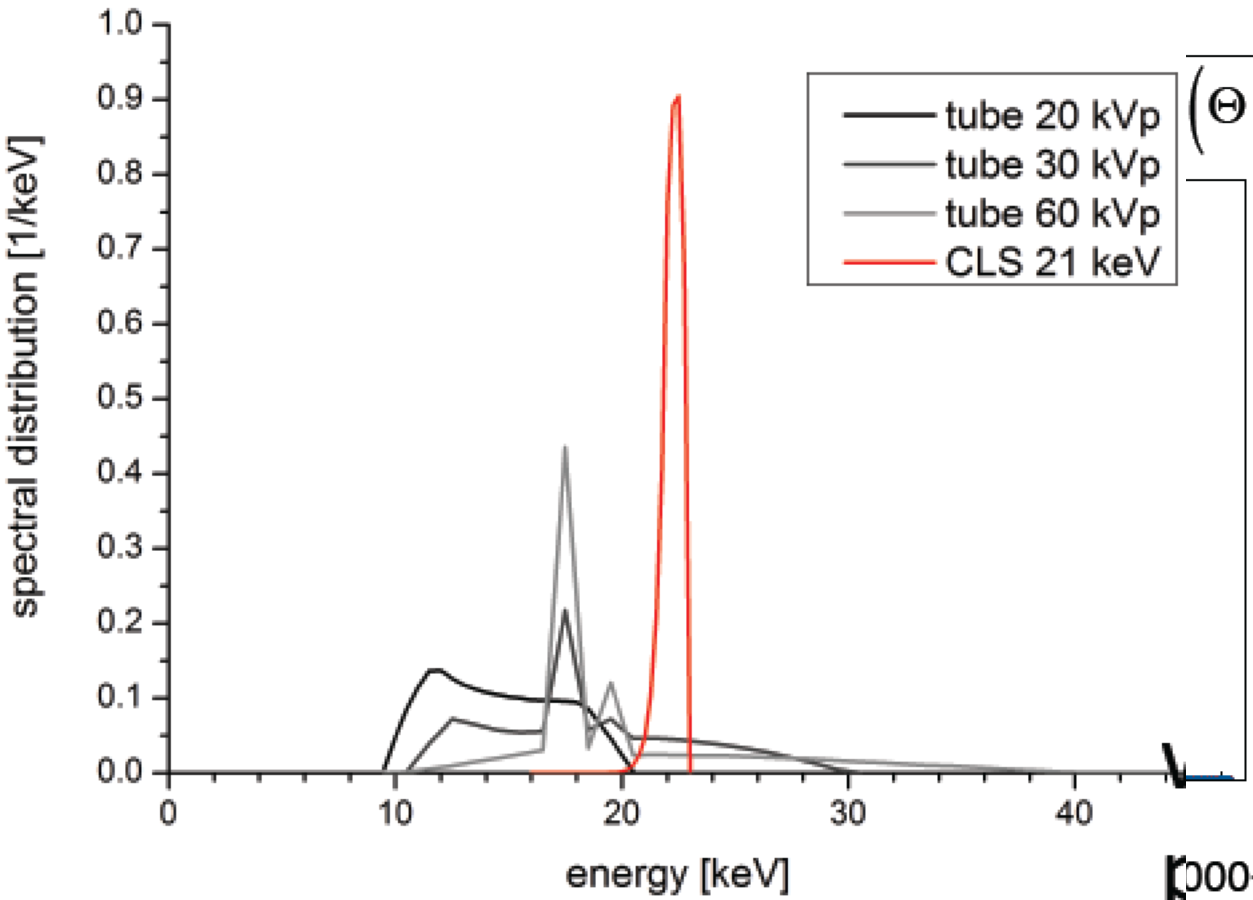

$(\Theta+\alpha))$

measured
Spectrum of X-rays
into +/- 2 mrad

Bandwidth

000+0.0016 · ΔT with ΔT/T=0.3%

35000+30000 · ΔE_L with $\Delta E_L/E_L=10^{-12}$

35000-9000 · $\Delta\alpha^2$ with $\Delta\alpha$=0.03

Measured $5{\cdot}10^{10}$ ph/sec with 20 mA

Great example of Radio-logical imaging applied to mass screening over population: mammography

Conventional X-ray tube for mammography

Spatial resolution ~100 μm

High Flux ~10^7 $\gamma/(mm^2 s)$ equivalent to ~$5 \cdot 10^{11}$ γ/s over 20x20 cm^2 area.

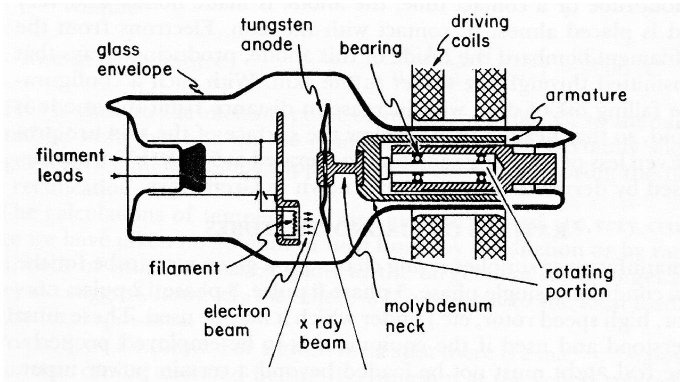

Anode Material	Molybdenum
Anode Angle	12°
Anodic Voltage	28 kV
Filtrations	1 mm Be 0.03 mm Mo 600 mm Air

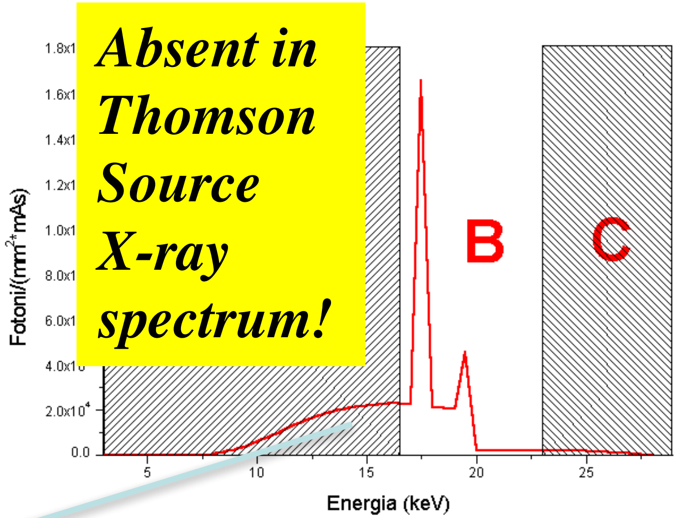

Low energy photons in the spectrum are absorbed by tissue, delivering radiation dose without bringing informations to detector. Risk of inducing secondary tumors increases without increasing the benefit of detecting early tumors

Mammography with Mono-chromatic X-rays at 20 keV has been proven far superior in Signal-to-Noise-Ratio w.r.t. conventional mammographic tubes, with a considerably lower radiation dose to the tissue

Conventional
X-ray tube 26 kVp
MGD 1 mGy

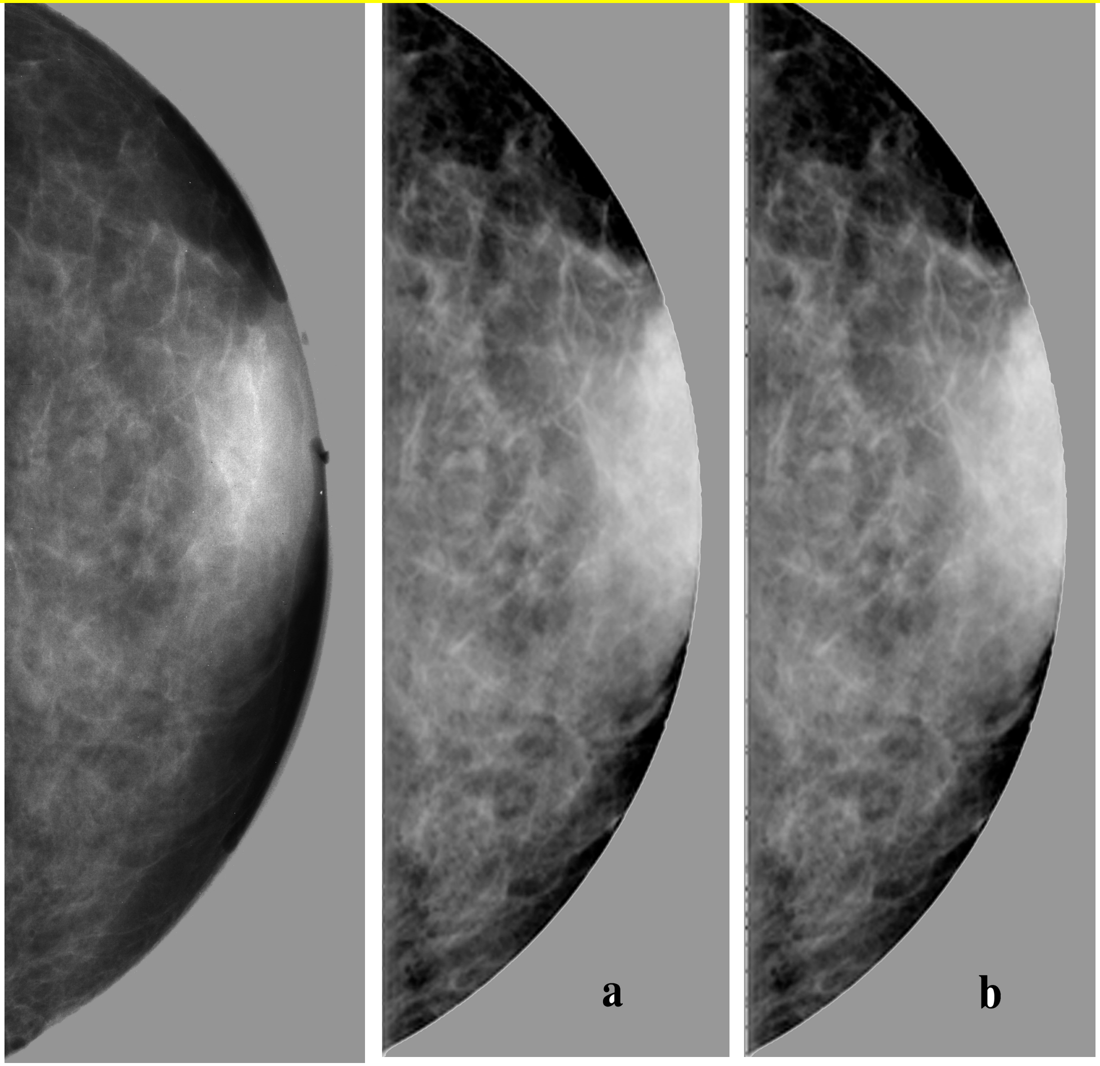

a) SR digital image
Energy 17 keV
Scan step 100 mm
MGD 1 mGy

b) SR digital image
Energy 20 keV
Scan step 100 mm
MGD 0.33 mGy

3 cm thick in vitro human breast tissue

Compact Thomson X-ray Sources could be located inside hospitals to diagnose and treat patients directly at the hospital site (unlike Synchrotrons…)

IOP Publishing | Institute of Physics and Engineering in Medicine Physics in Medicine & Biology

Phys. Med. Biol. 61 (2016) 1634–1649 doi:10.1088/0031-9155/61/4/1634

Towards breast tomography with synchrotron radiation at Elettra: first images

R Longo[1,2], F Arfelli[1,2], R Bellazzini[3,4], U Bottigli[5], A Brez[3,4], F Brun[2,6], A Brunetti[7], P Delogu[4,8], F Di Lillo[9], D Dreossi[10], V Fanti[11], C Fedon[1,2], B Golosio[7], N Lanconelli[12], G Mettivier[9], M Minuti[3,4], P Oliva[7], M Pinchera[3,4], L Rigon[1,2], P Russo[9], A Sarno[9], G Spandre[3,4], G Tromba[10] and F Zanconati[13]

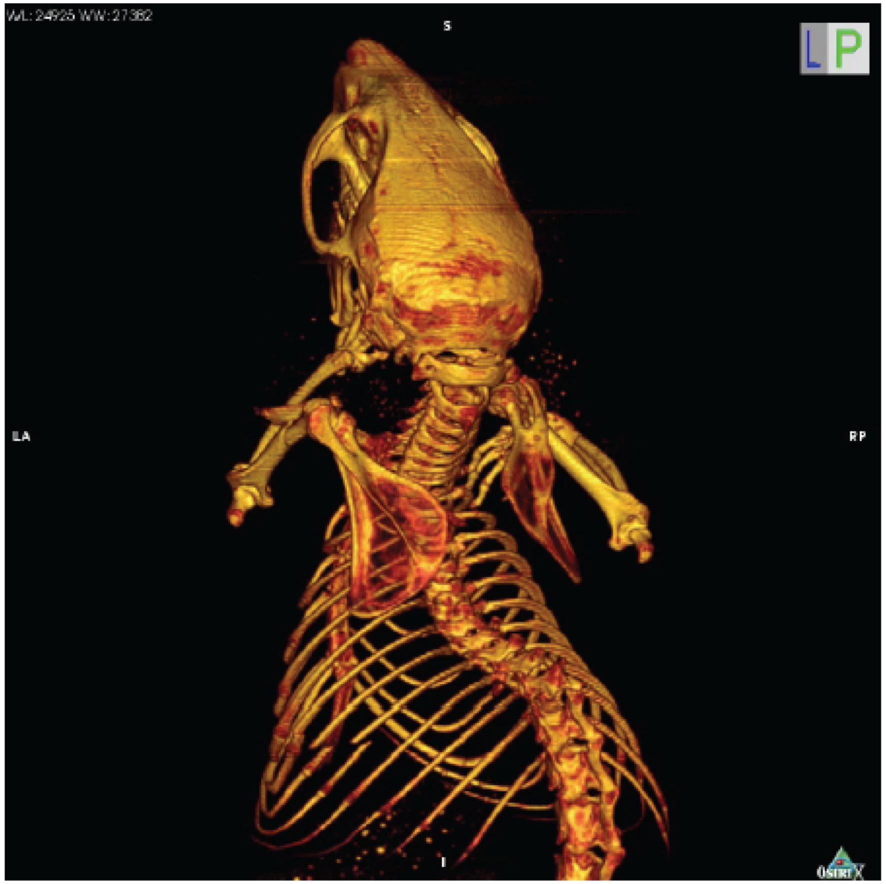

small source size → high resolution (81 μm)
monochromatic → no beam hardening artefacts

Klaus.Achterhold@tum.de

Phase Contrast Imaging made possible by small round source spot size (< 20 μm)

courtesy of A. Bravin (ESRF)

Bio-Medical Advanced Imaging with Mono-chromatic X-rays, demonstrated at Synchrotrons, is possible also with High Flux Thomson X-ray Sources in 20 keV-100 keV energy range

Cortical brain imaging: Characterization of brain vascular network and transport after injection of barium

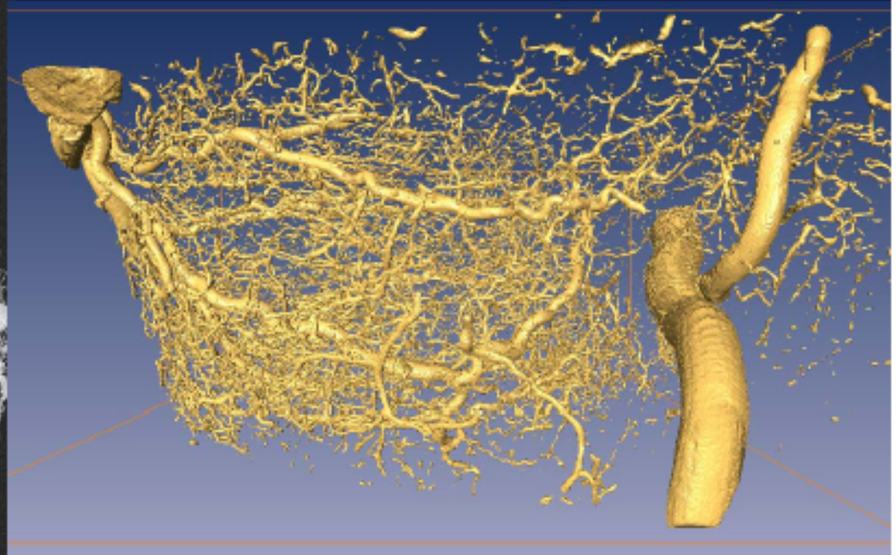

Sample size: 1.5x1.5x1 mm^3

frontal cortex: y-z plane

3D iso-surface frontal cortex y-z plane

Rat cortical brain. Barium (600 mg*mL^{-1}), 20 keV in absorption; voxel size = 1.4 μm.

F. Pouraboué et al. J. of Microscopy, Vol. 215, August 2004,139–148

Bio-Medical Advanced Imaging with Digital Subtraction of Mono-chromatic X-ray shots are also possible with High Flux Thomson X-ray Sources with picosecond to millisecond time resolution

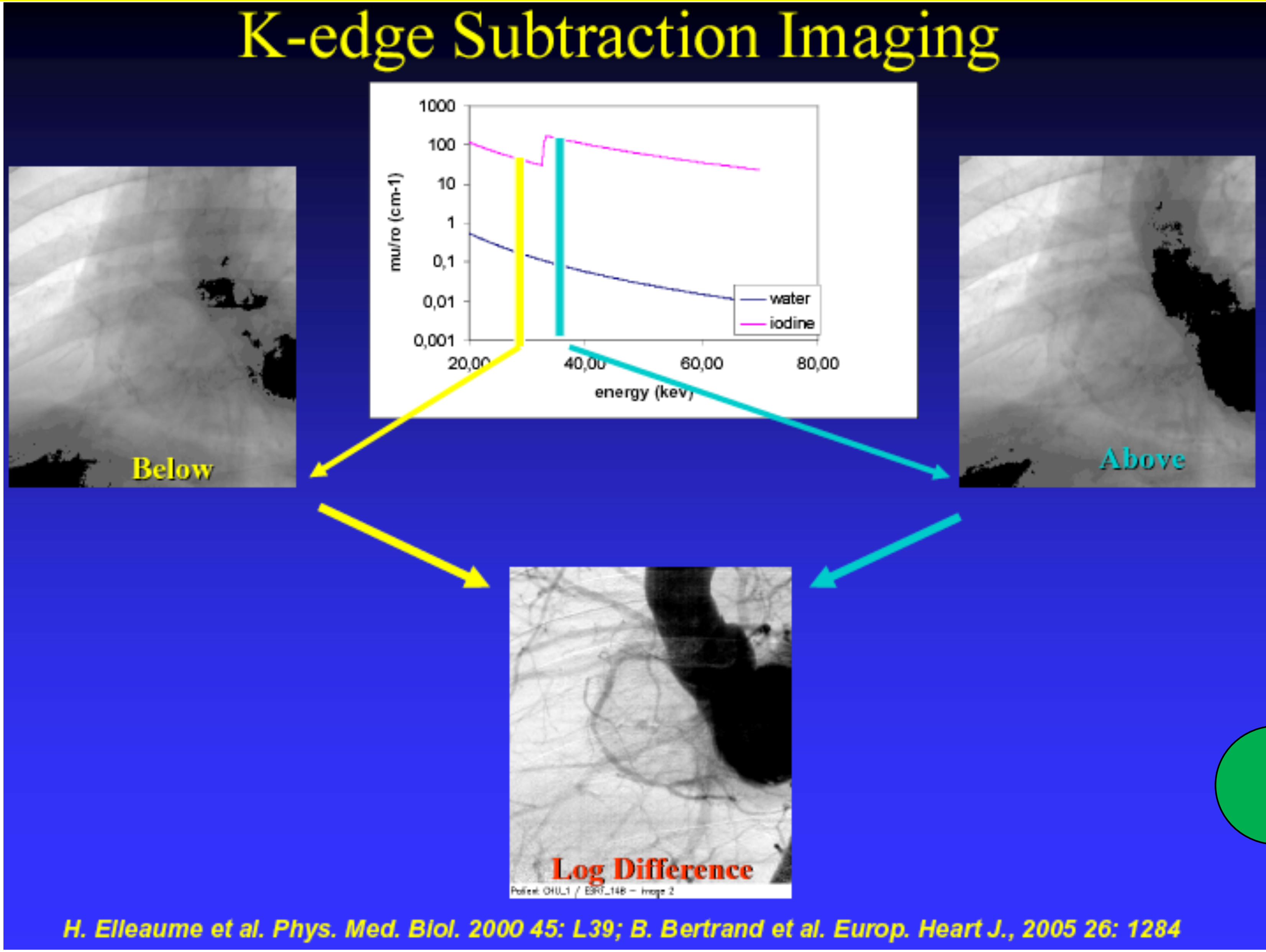

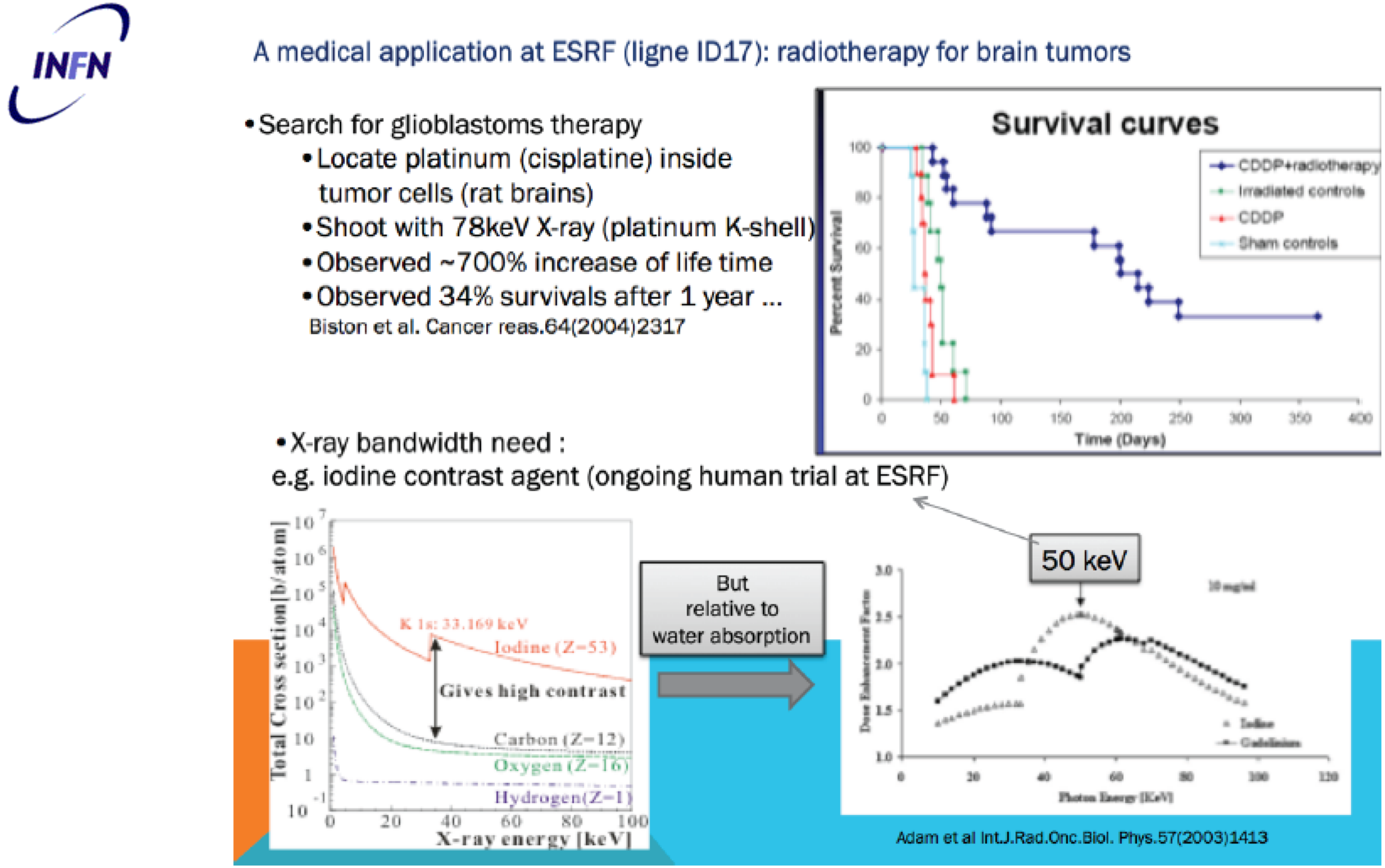

Fig.10 *– Radio-Therapy using mono-chromatic X-rays joined to cisplatine chemio-therapy for selected X-ray absorption inside tumoral cells.*

comprehensive overview recently presented at the PAHBB-2016 Workshop (see https://conferences.pa.ucla.edu/hbb/index.html) by A. Variola (INFN-LNF)

Advancing Thomson X Ray Sources for Bio/Medical Imaging Applications and Matter Science

NUCLEAR INSTRUMENTS & METHODS IN PHYSICS RESEARCH

Section A: accelerators, spectrometers, detectors and associated equipment

Volume 608 (2009), Issue 1S
Supplement

COMPTON 2008

Compton sources for X/γ rays:
Physics and applications
Alghero, Sardinia, Italy, September 7–12, 2008

Edited by Massimo Carpinelli, Luca Serafini

Abstracted/Indexed in: Current Contents: Engineering, Computing and Technology; Current Contents: Physical, Chemical and Earth Sciences; EI Compendex Plus; Engineering Index; INSPEC. Also covered in the abstract and citation database SCOPUS®. Full text available on ScienceDirect®.

0168-9002(20090901)608:1s;1-V

608 1S NUCLEAR INSTRUMENTS AND METHODS IN PHYSICS RESEARCH (SECTION A)–VOL. 608/1S (2009) S1–S120 ELSEVIER

ELSEVIER

Volume 608, Issue 1S Supplement
September 1, 2009
ISSN 0168-9002

COMPTON 2008

**Compton sources for X/γ rays:
Physics and applications**

**Alghero, Sardinia, Italy
September 7–12, 2008**

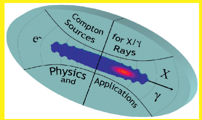

Guest Editors

Massimo Carpinelli
Luca Serafini

Accelerator and Equipments
in ELI-NP Building
100 m, 100 M$ scale

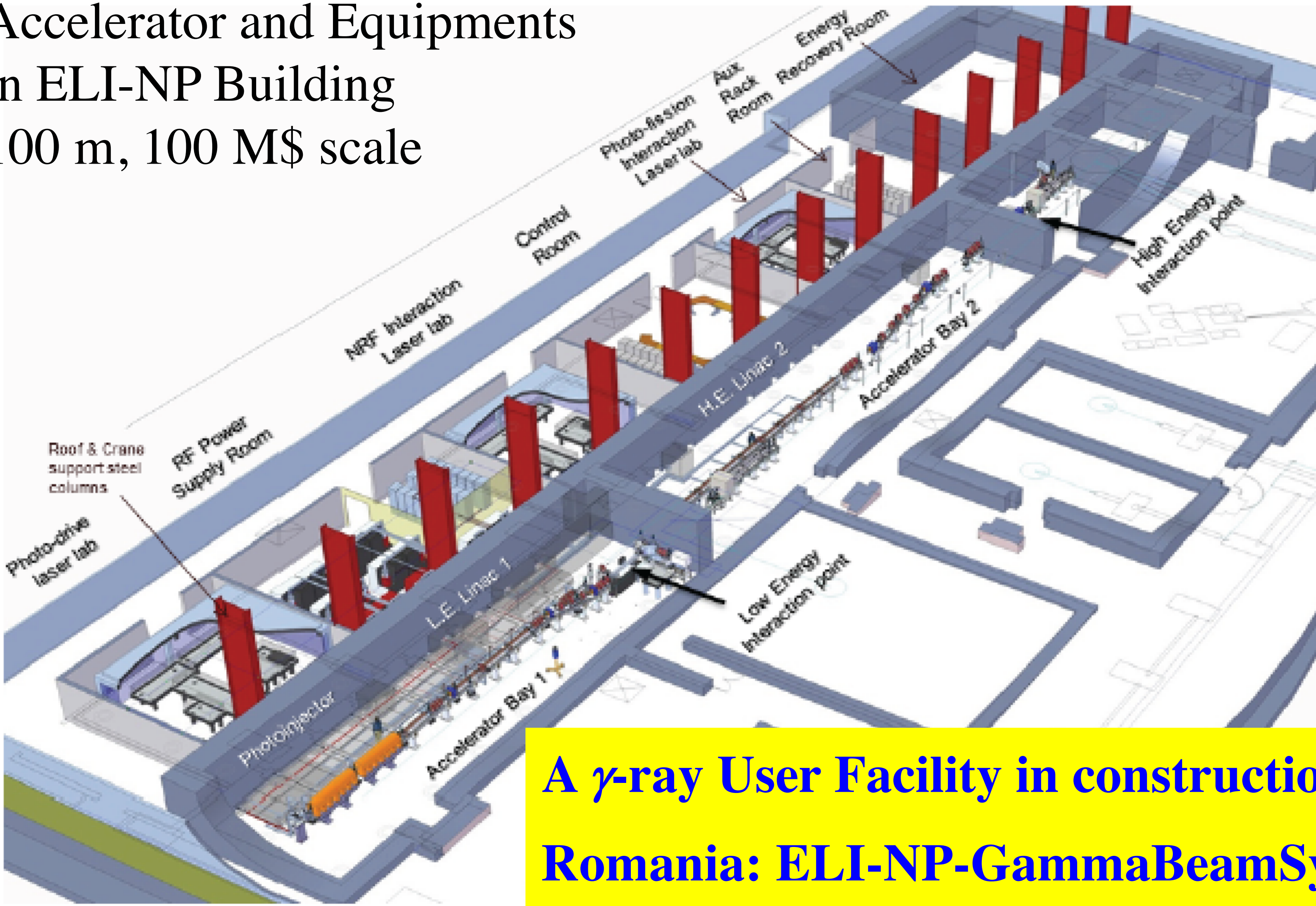

A γ-ray User Facility in construction in Romania: ELI-NP-GammaBeamSystem

Fig. 197. Isometric 3D view of Building Layout of the Accelerator Hall & Experimental Areas

European Collaboration for the proposal of a Gamma-Beam System to the ELI-NP Project

Technical Design Report

EuroGammaS proposal for the ELI-NP Gamma beam System

With 73 tables and 230 figures

O. Adriani, S. Albergo, D. Alesini, M. Anania, D. Angal-Kalinin, P. Antici, A. Bacci, R. Bedogni, M. Bellaveglia, C. Biscari, N. Bliss, R. Boni, M. Boscolo, F. Broggi, P. Cardarelli, K. Cassou, M. Castellano, L. Catani, I. Chaikovska, E. Chiadroni, R. Chiche, A. Cianchi, J. Clarke, A. Clozza, M. Coppola, A. Courjaud, C. Curatolo, O. Dadoun, N. Delerue, C. De Martinis, G. Di Domenico, E. Di Pasquale, G. Di Pirro, A. Drago, F. Druon, K. Dupraz, F. Egal, A. Esposito, F. Falcoz, B. Fell, M. Ferrario, L. Ficcadenti, P. Fichot, A. Gallo, M. Gambaccini, G. Gatti, P. Georges, A. Ghigo, A. Goulden, G. Graziani, D. Guibout, O. Guilbaud, M. Hanna, J. Herbert, T. Hovsepian, E. Iarocci, P. Iorio, S. Jamison, S. Kazamias, F. Labaye, L. Lancia, F. Marcellini, A. Martens, C. Maroli, B. Martlew, M. Marziani, G. Mazzitelli, P. McIntosh, M. Migliorati, A. Mostacci, A. Mueller, V. Nardone, E. Pace, D.T. Palmer, L. Palumbo, A. Pelorosso, F.X. Perin, G. Passaleva, L. Pellegrino, V. Petrillo, M. Pittman, G. Riboulet, R. Ricci, C. Ronsivalle, D. Ros, A. Rossi, L. Serafini, M. Serio, F. Sgamma, R. Smith, S. Smith, V. Soskov, B. Spataro, M. Statera, A. Stecchi, A. Stella, A. Stocchi, S. Tocci, P. Tomassini, S. Tomassini, A. Tricomi, C. Vaccarezza, A. Variola, M. Veltri, S. Vescovi, F. Villa, F. Wang, E. Yildiz, F. Zomer

109 Authors, 327 pages
published today on ArXiv
http://arxiv.org/abs/1407.3669

Photonuclear Reactions

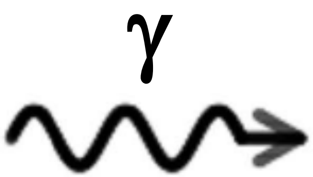

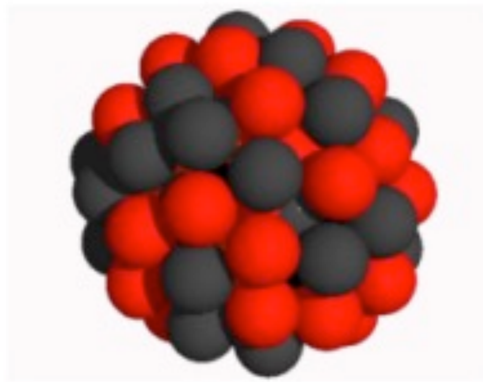

What happens?

Narrowband gamma-ray absorption and re-radiation by the nucleus is an “isotope-specific” signature

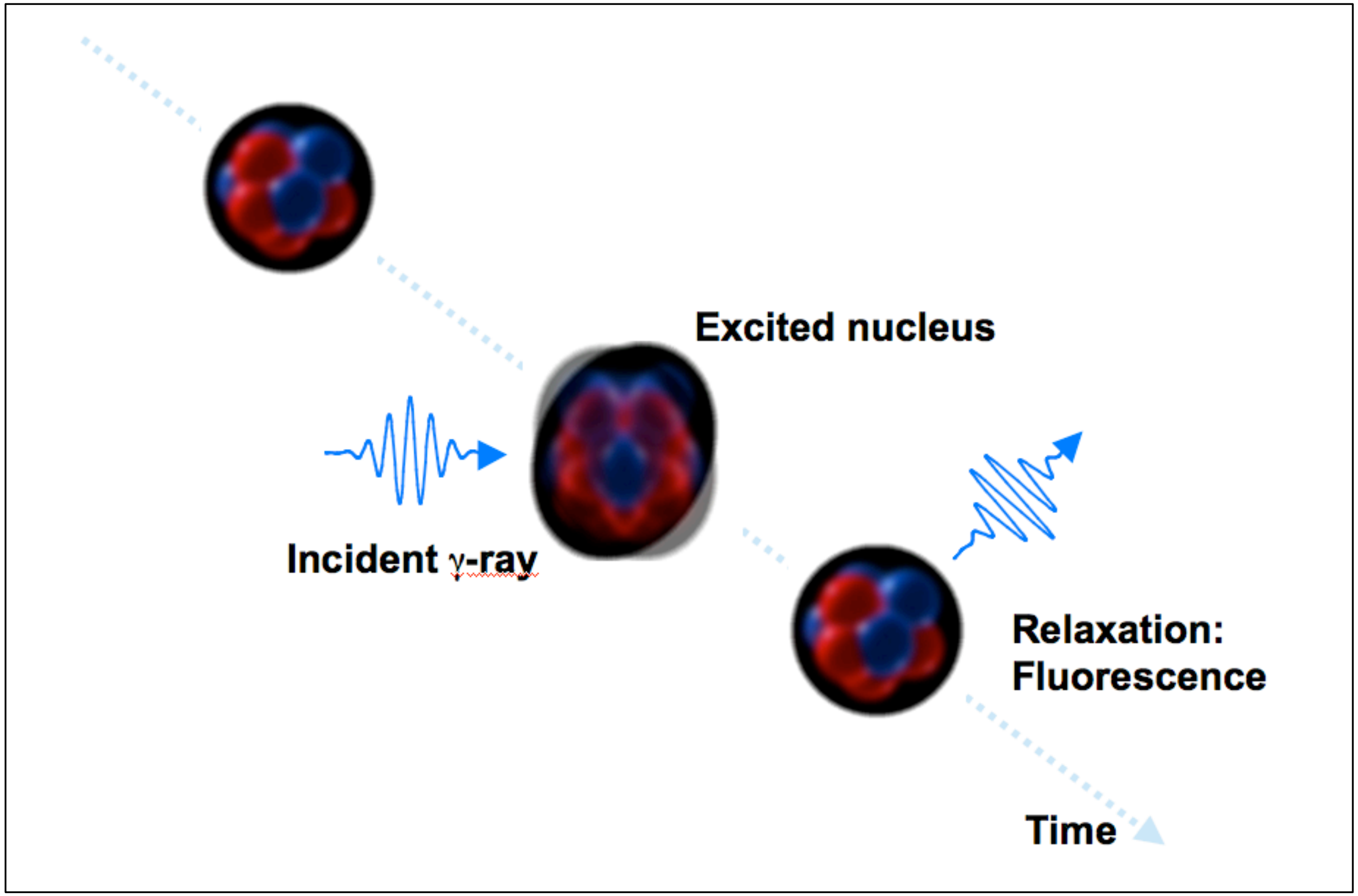

Nuclear Resonance Fluorescence (NRF) is analogous to atomic resonance fluorescence but depends upon the number of protons AND the number of neutrons in the nucleus

Courtesy C. Barty - LLNL

Photonuclear Reactions

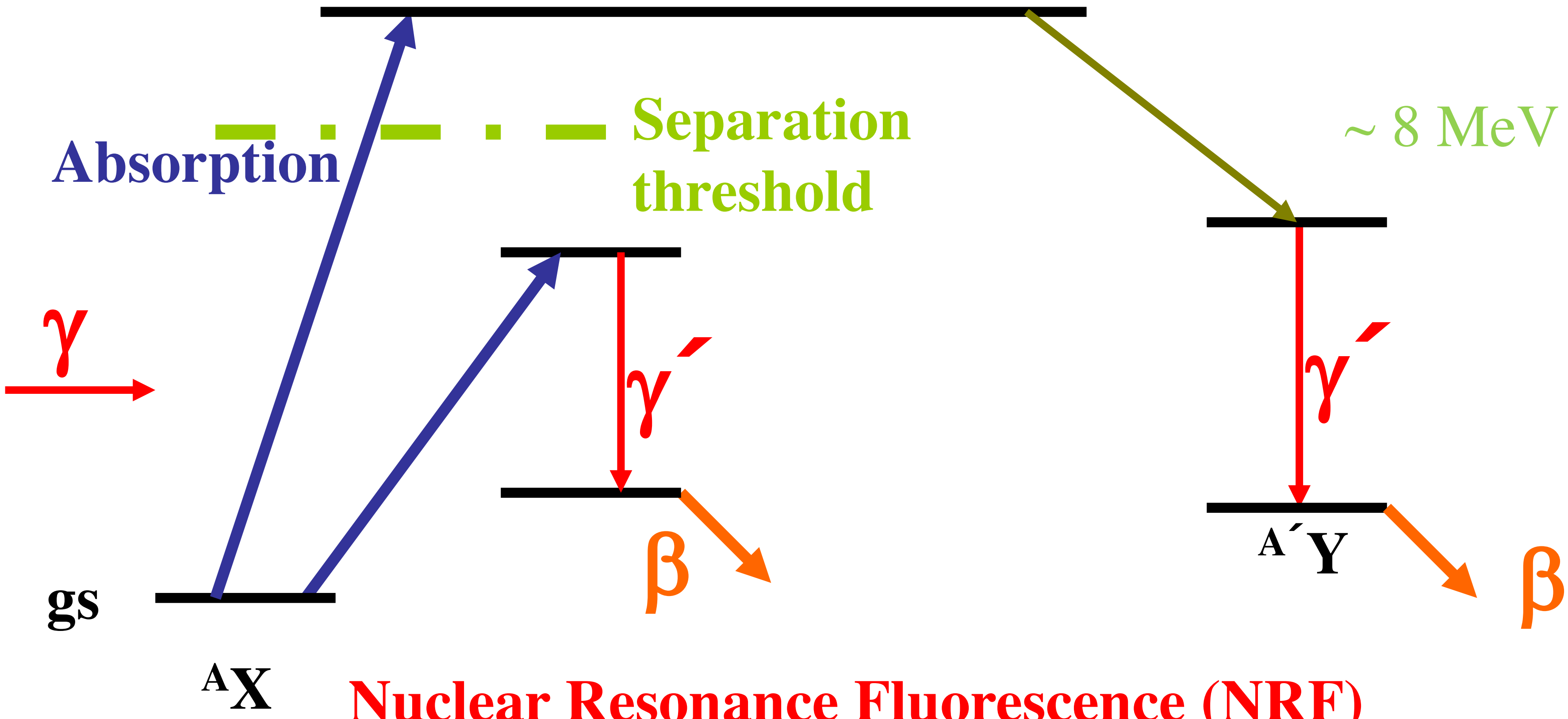

Nuclear Resonance Fluorescence (NRF)

Photoactivation

Photodisintegration (-activation)

Nondestructive Assay by Nuclear Resonant Fluorescence

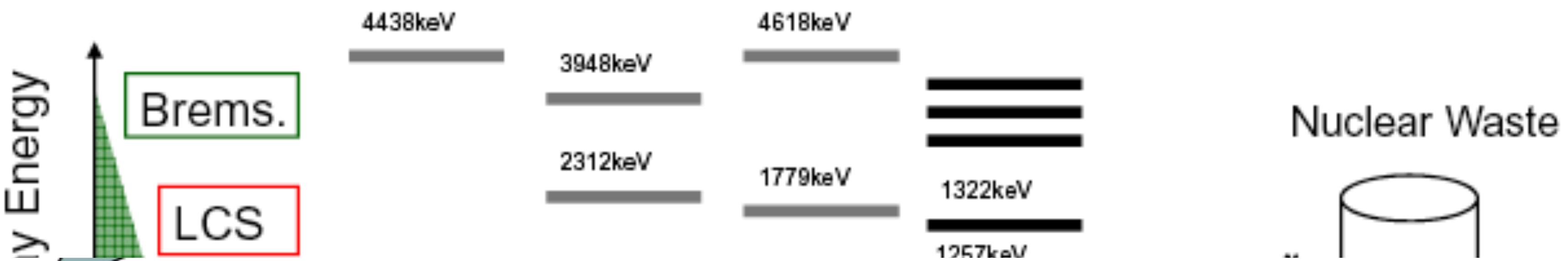

Mono-energetic & tunable γ-ray beam
(unlike bremsstrahlung)

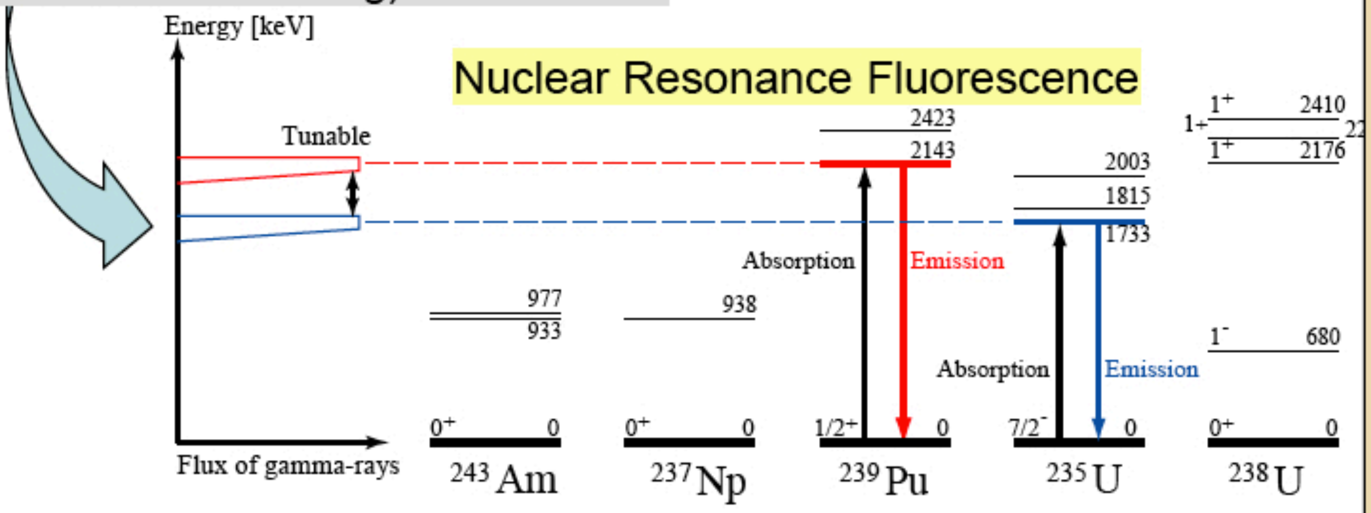

R. Hajima et al., J. Nuclear Science and Technology, 45, 441-451 (2008).

Simulation 2: 2-D Mapping of Shielded Isotopes

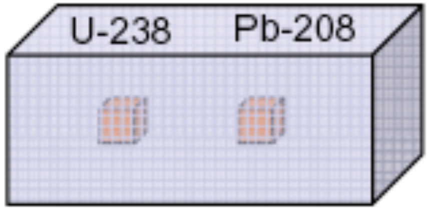

Metal objects
in a concrete block

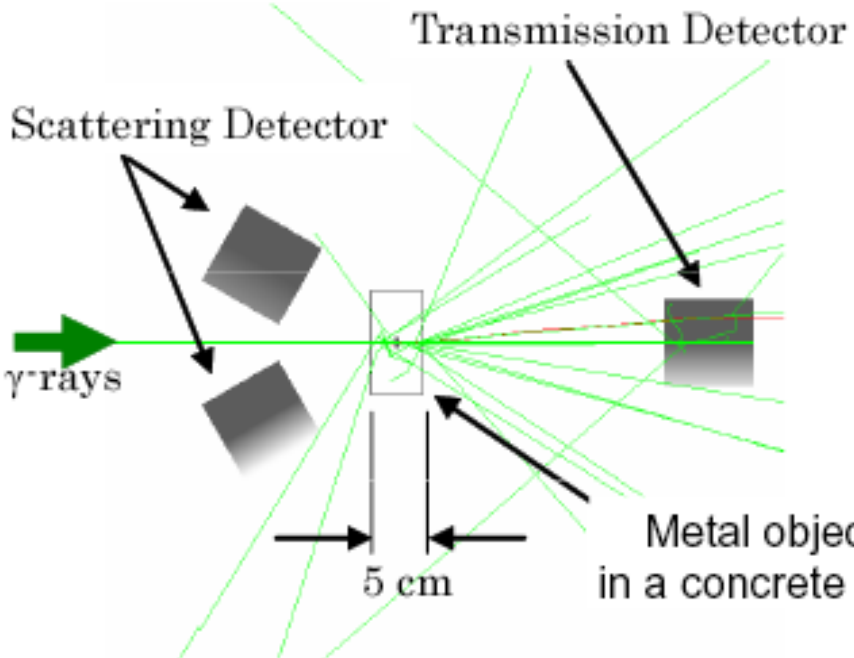

Metal objects
in a concrete block

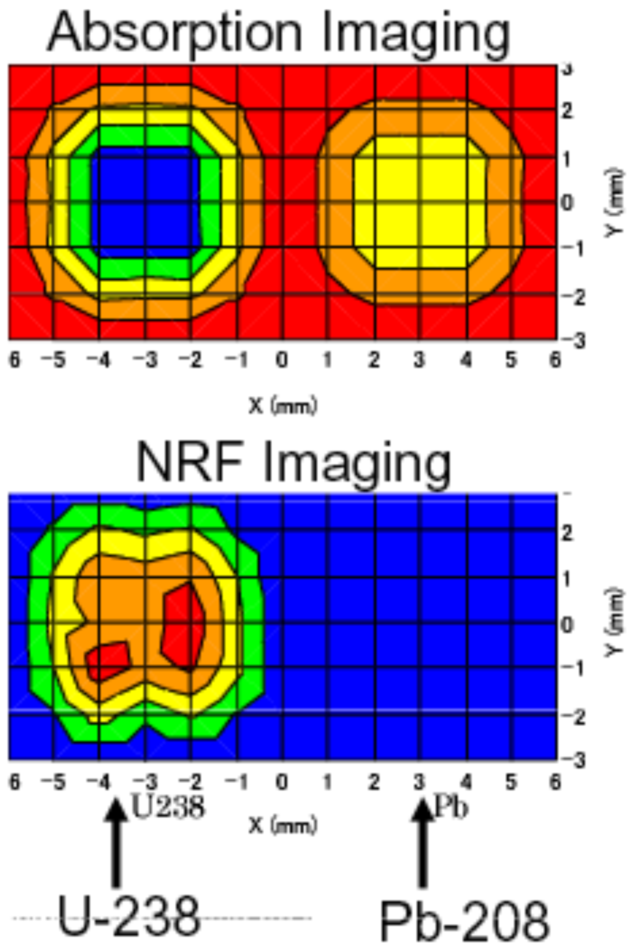

The IGS performance requirements are severe

Up to 10^{13}, 10 MeV gammas/sec

Producing 10 MeV gammas requires
~500 MeV electrons
(assuming green drive laser)

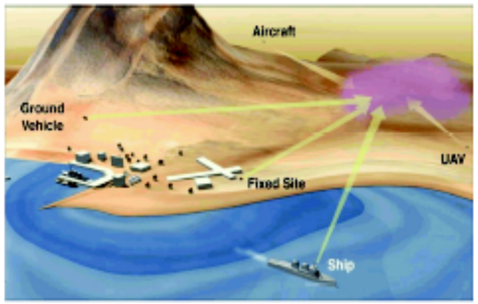

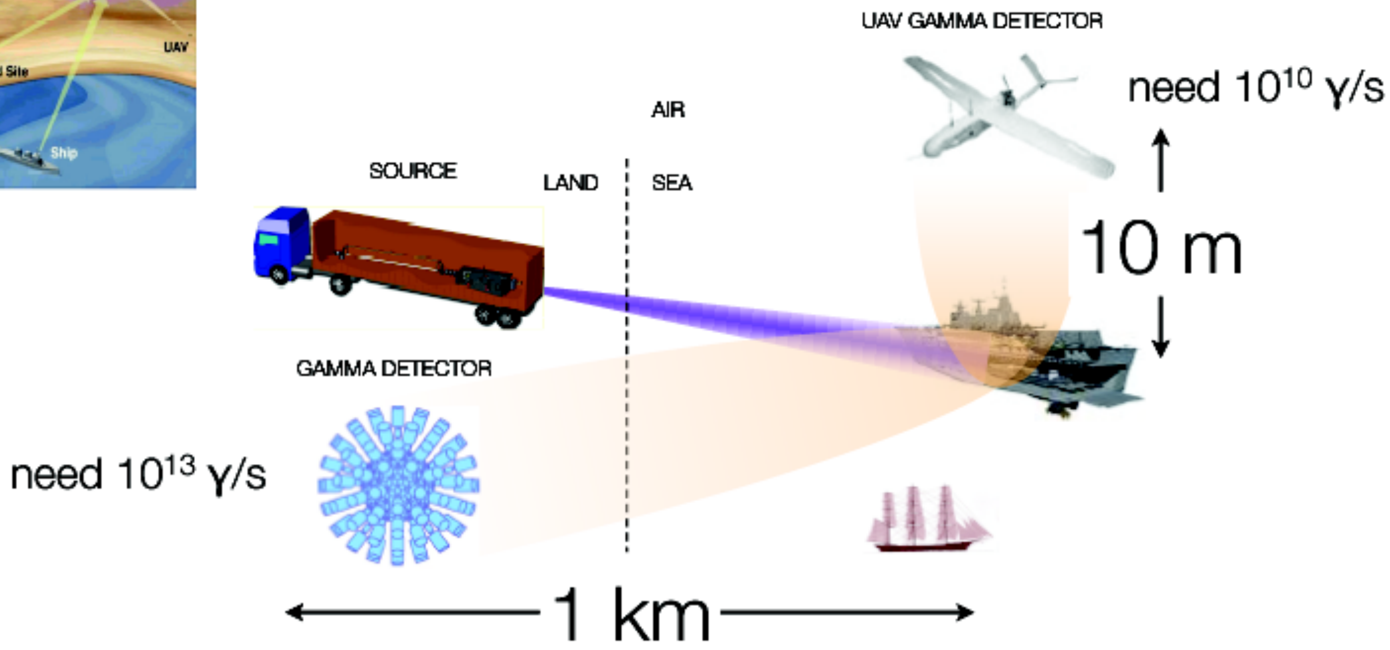

courtesy of G. Travish (UCLA)

“Evil doers” obtaining Special Nuclear Materials (SNR) is considered a high likelihood.

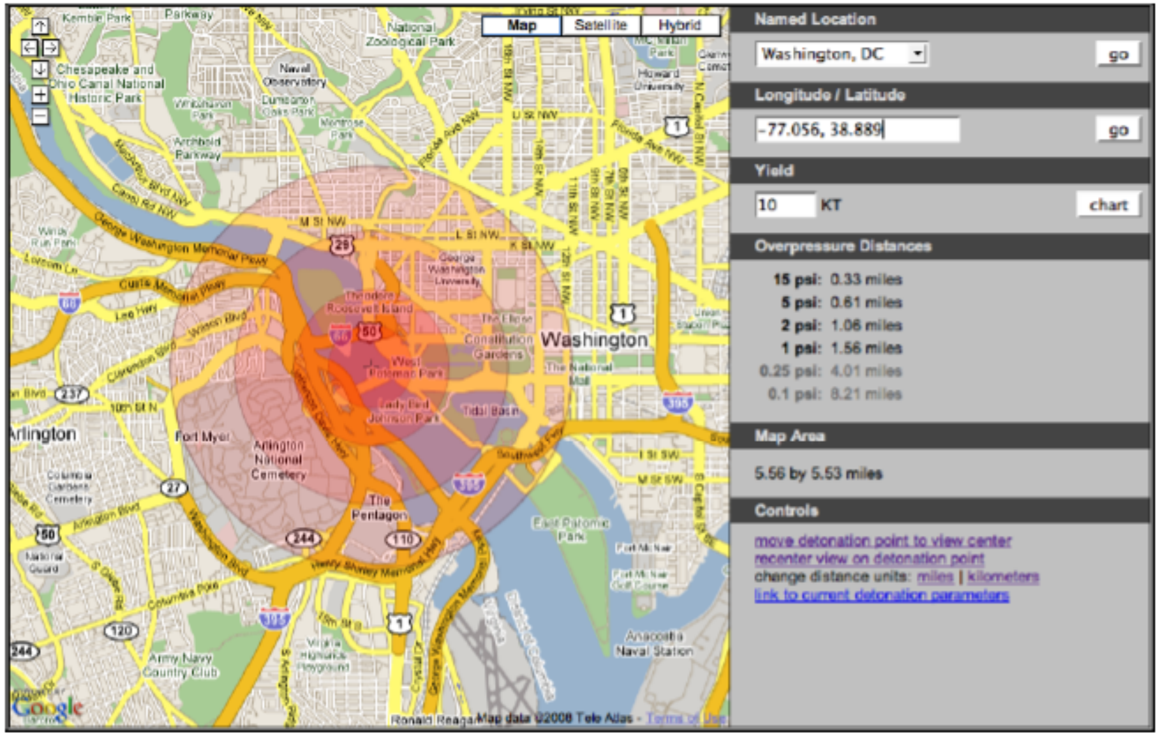

In this post-Cold War world, nuclear terrorism may be the single most catastrophic threat that any nation faces - we must do everything we can to ensure against its occurrence.

-- Joseph Krol, Associate Administrator, NNSA

courtesy of G. Travish (UCLA)

Photofission is a promising means of detecting SNM with high confidence.

❶ 6+ MeV gammas induce fission in actinides
❷ Prompt neutrons and gammas immediately emitted
❸ Fission fragments decay, emitting delayed gammas and neutrons

➡ Delayed gammas and neutrons are a positive signal

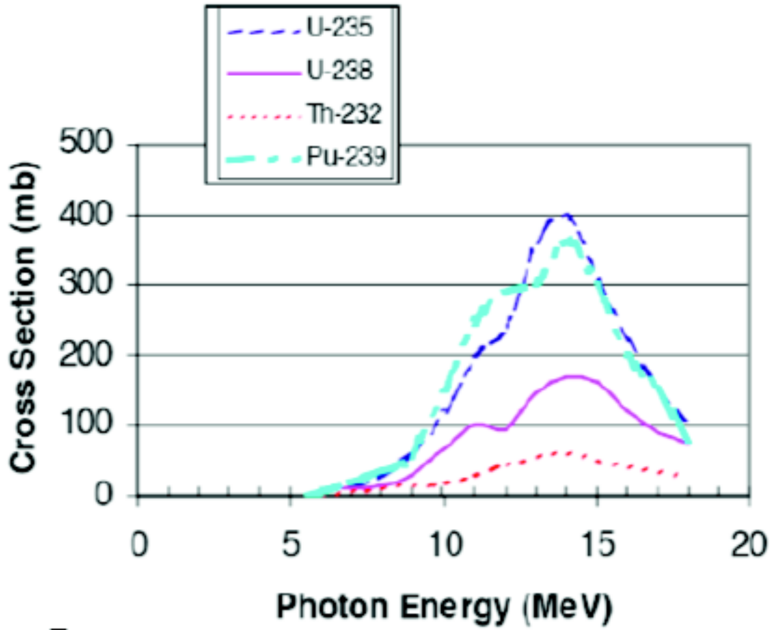

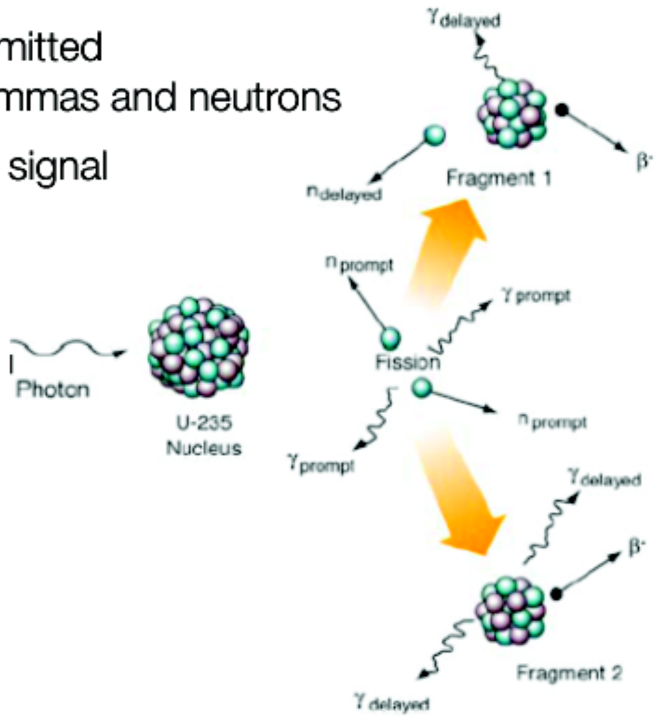

courtesy of G. Travish (UCLA)

Challenges of *electron-(optical)photon colliders* as *X/γ* beam Sources using Compton back-scattering

- Need of *high peak brightness/high average current* electron beams (cmp. FEL's drivers) *fsec-class* synchronized and *μm-μrad-scale* aligned to *high peak/average power* laser beams
- Main goal for Nuclear Physics and Nuclear Photonics:
  Spectral Densities > 10^4 $N_{ph}/(s \cdot eV)$
  photon energy range 1-20 MeV, *bandwidths* 10^{-3} class
- Main goal for Medical Applications with *X*-rays: tunability in the 20-120 keV range, good mono-chromaticity (1-10 %), high flux (10^{11} min., 10^{12} for radio-imaging, 10^{13} for radio-therapy)

- **Main goal for *MeV-class* $\gamma - \gamma$ and *TeV* γ - nucleon colliders:**
  ***Peak Brilliance* > 10^{21}** $N_{ph}/(s \cdot mm^2 \cdot mrad^2 \cdot 0.1\%)$ **$10^9 < N_{ph} < 10^{13}$**
  Source spot size μm-scale (low diffraction, few μrad)
  Tunability, Mono-chromaticity, Polarization (H,V,C)
- **Photon-Photon scattering (+ Breit-Wheeler: pair creation in vacuum) is becoming feasible with this new generation γ-beams: a γ-γ low energy collider**

3^{rd}-4^{th} Generation Light Sources

- Synchrotron light sources: < 50 keV, > 50 ps (100 m, 300 M$)
- X-ray FEL (LCLS): energy ≤25 (50?) keV, 1-100 fs (1 km, 1 G$)

- **New approach: inverse Compton scattering (ICS) 20-200 keV , sub-ps, (10 m , 10 M$) – sometimes called Laser Synchrotron since a laser pulse substitutes the magnetic undulators**

Brilliance of Lasers and X-ray sources

$$N_{ph} = 10^{19} - 10^{20}$$

$$\sigma_t = 10 - 20 \quad fs$$

ELI

BELLA

$$B = \frac{N_{ph}}{\sqrt{2\pi}\sigma_t \left(M^2\lambda\right)^2 \frac{\Delta\lambda}{\lambda}}$$

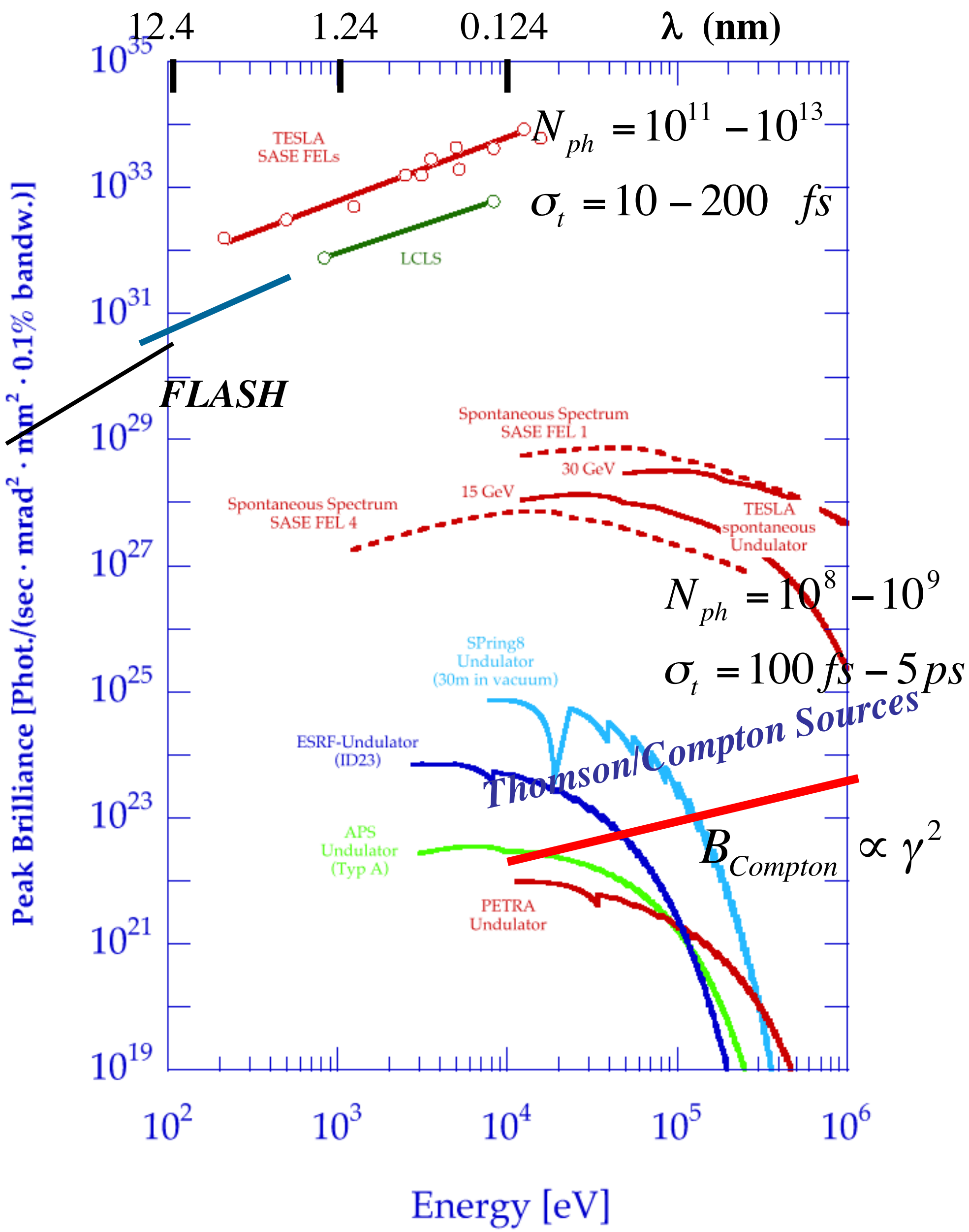

$$B_{peak} = \frac{N_{ph}}{\sqrt{2\pi}\sigma_t \varepsilon_x^2 \frac{\Delta E_X}{E_X}}$$

$$B_{av} = \frac{N_{ph} f}{\varepsilon_x^2 \frac{\Delta E_X}{E_X}}$$

Rivaling with Synchr. Light Sources for energies above 50 keV

ICS vs. other sources

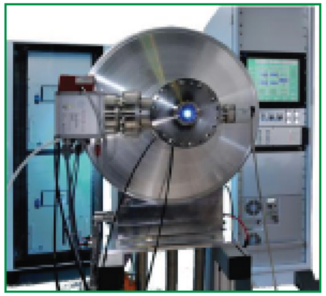

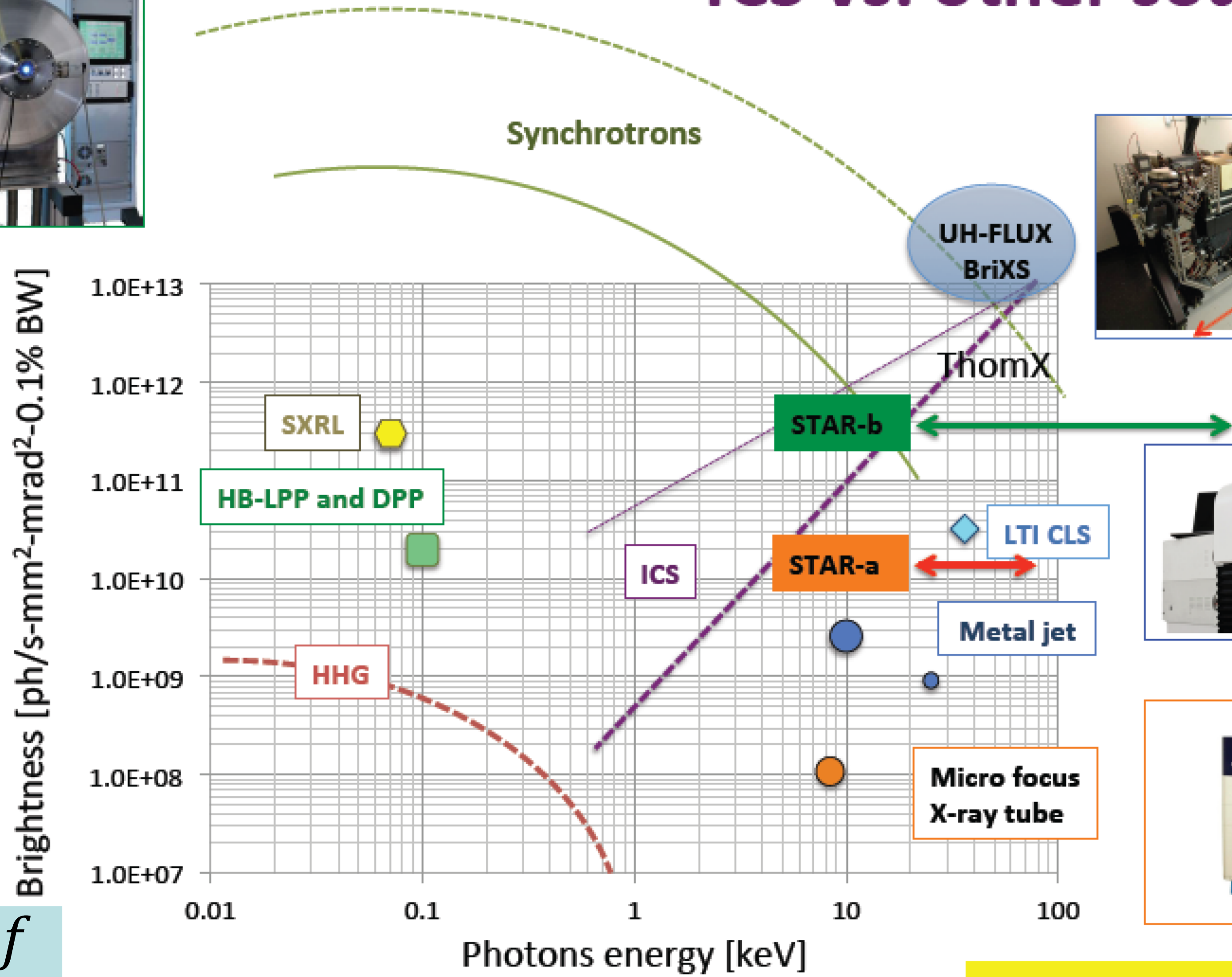

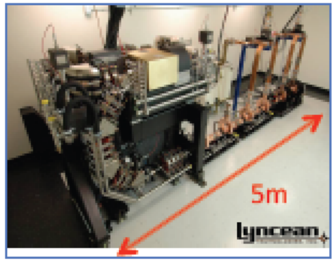

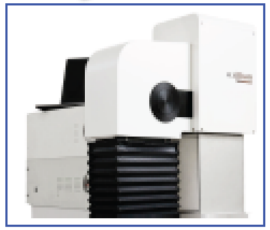

$$B_{av} = \frac{N_{ph} f}{\varepsilon_x^2 \frac{\Delta E_X}{E_X}}$$

High Brightness Beams, Havana, Cuba

Courtesy of A. Murokh
RadiaBeamTechnology

highly asymmetric compact*

elecron-photon colliders

*10 m, 10 M$

secondary photon beams via large

lorentz boost of c.m. reference frame

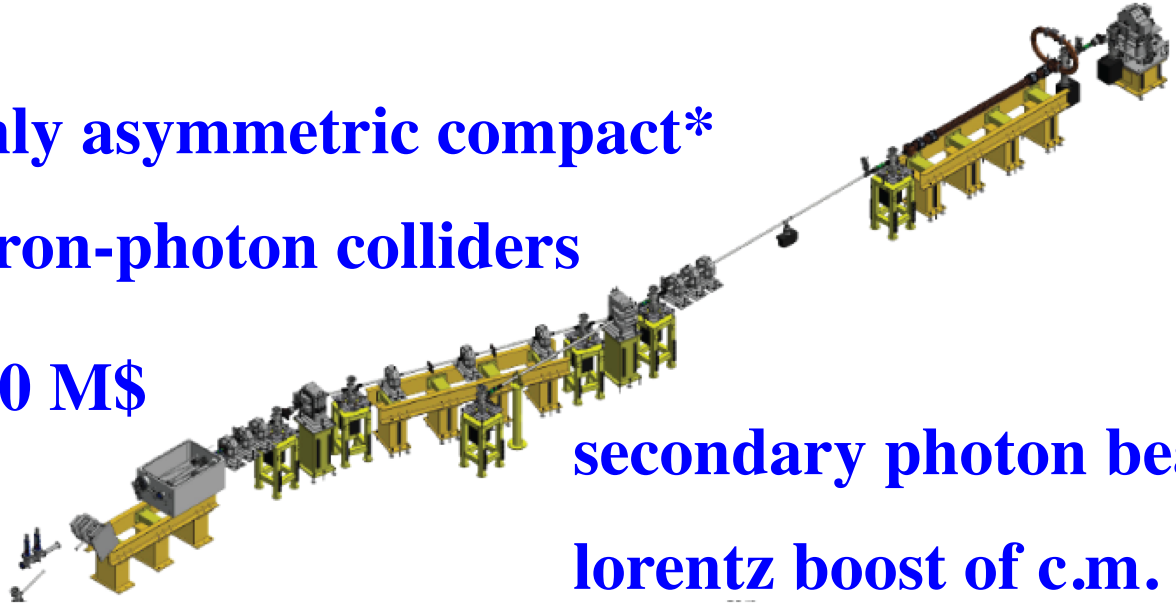

Fig.2 – *STAR machine as an example of Paradigm A. Overall length about 12 m.*

MeV/GeV's electrons

eV's photons

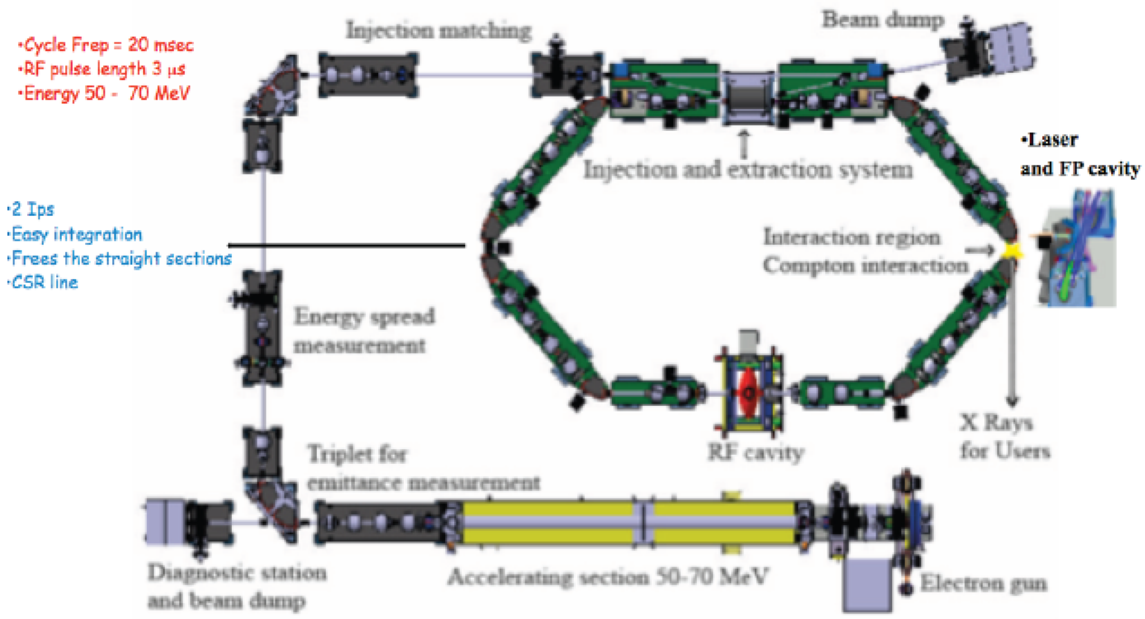

Fig.3 – *ThomX as an example of Paradigm B. Size is about 10x10 m^2.*

STAR – Southern europe Thomson source for Applied Research

is a good example of research infrastr. based on X-ray beam lines

for a regional facility to be built in an developing region/country

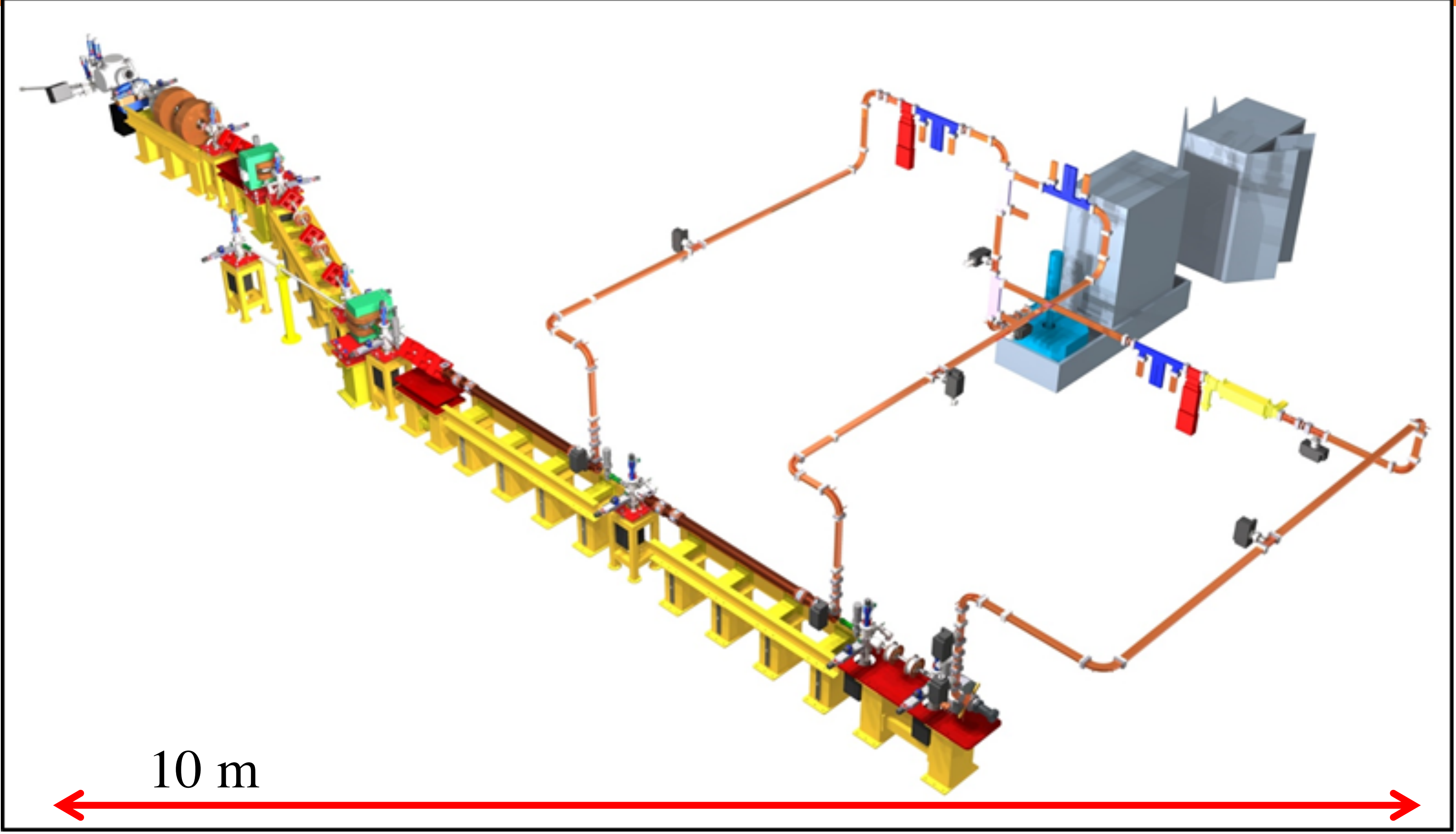

Calabria

Convergency regions

Funds for development from the European Community, including research infrastructures

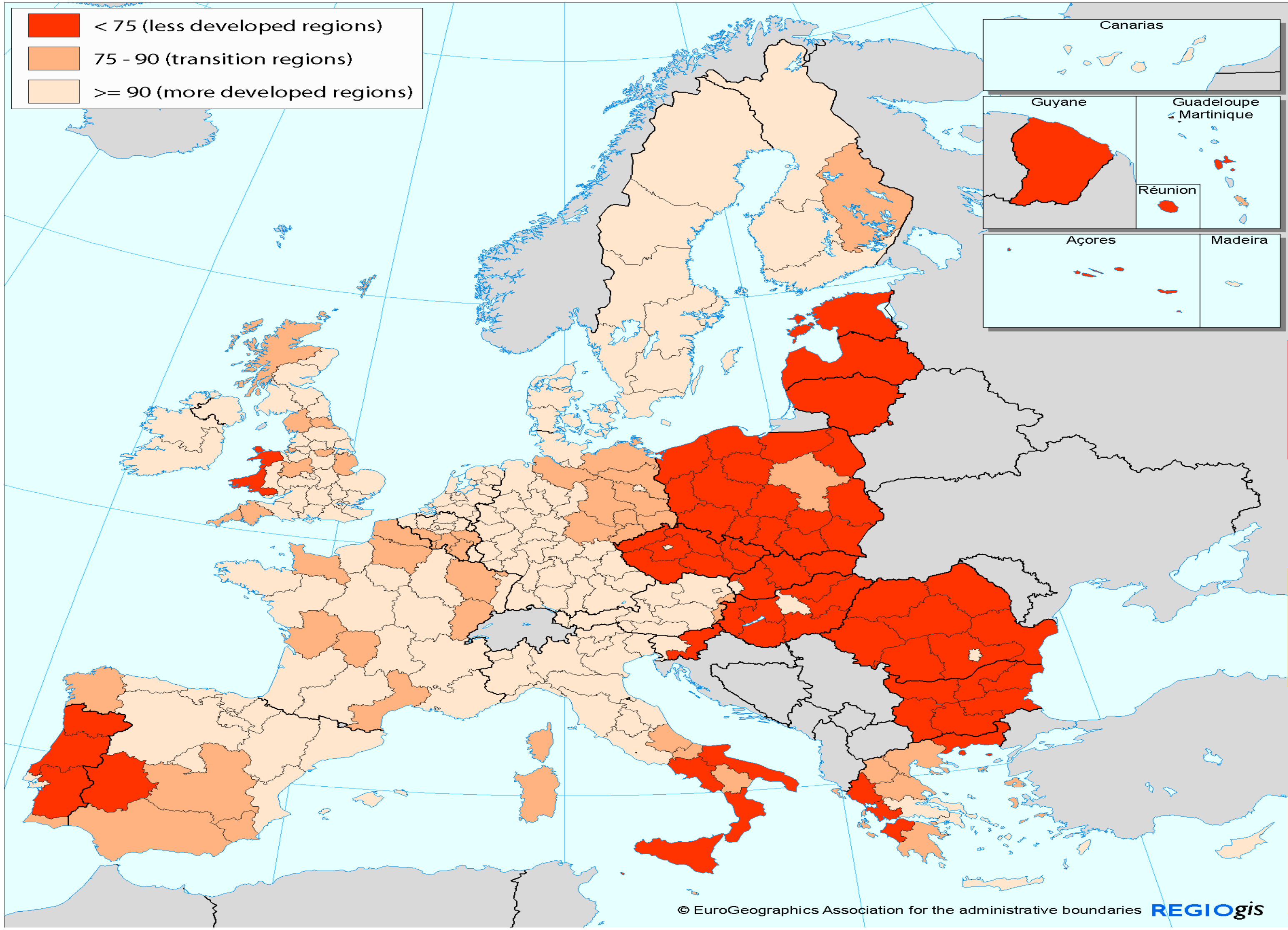

2014-2020

(indicativa)

Regioni meno sviluppate

Regioni in transizione

Regioni piú sviluppate

University of Calabria

- 35.000 students
- Strong physics department

The STAR Project
A TBS (IC) user facility

UniCal, The University of Calabria

CNISM, Italian Consortium on Physical Sciences of Matter (1300 reasercher from 39 universities)

Funding €15.700.000

| 8.4 M€ STAR source - CNISM
| 6.6 M€ Laboratories and building - UniCal
| 0.7 M€ Master program – UniCal

In collaboration with **INFN** and **Elettra – Sincrotrone di Trieste**

STAR Hangar and Bunker

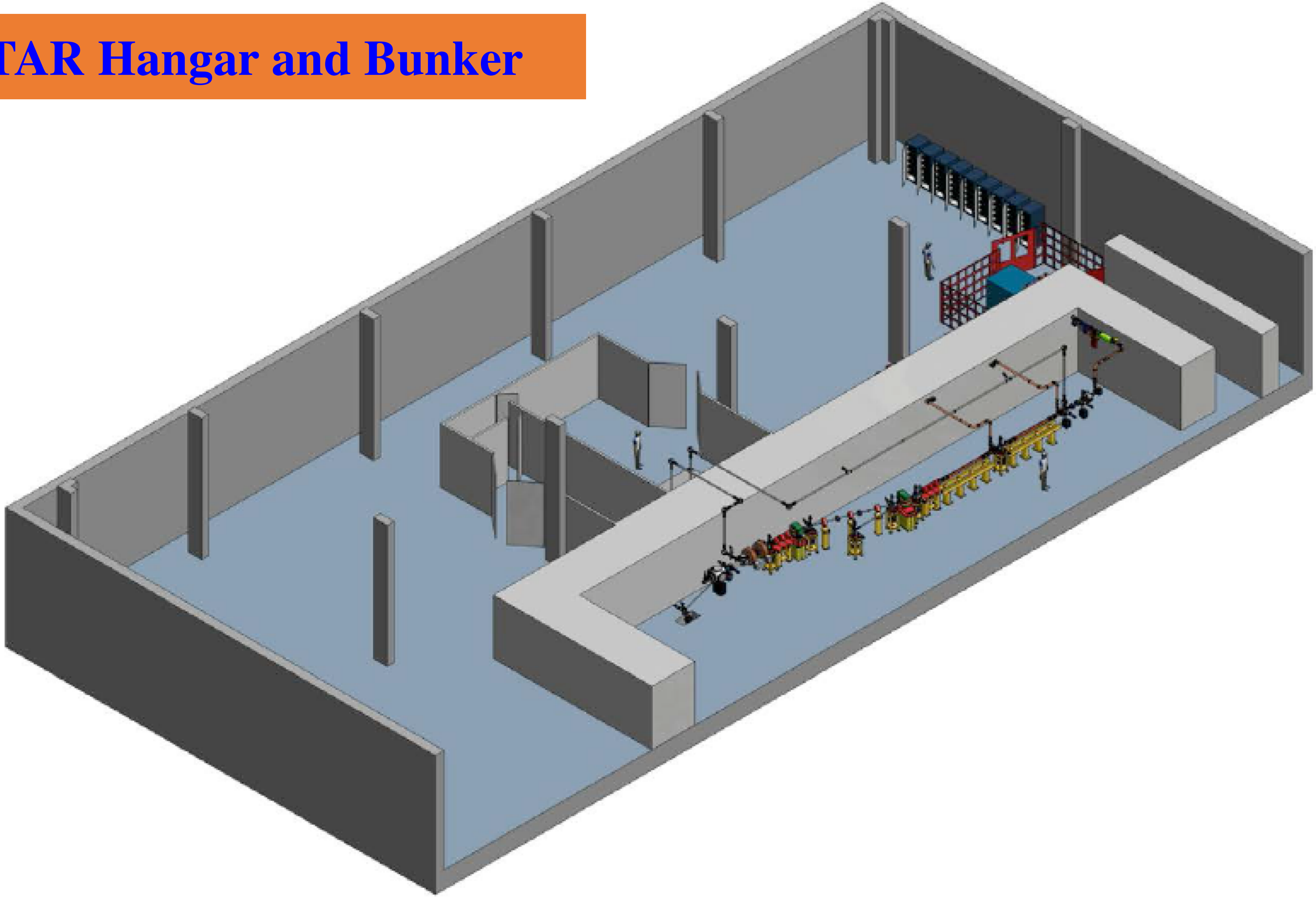

October 2013


AdR CNR
Ingegneria
STAR
MaTeRiA
SILA
Dip Fisica
INFN

Stato Bunker STAR a Gennaio 2016

Stato Bunker STAR a fine Maggio 2017

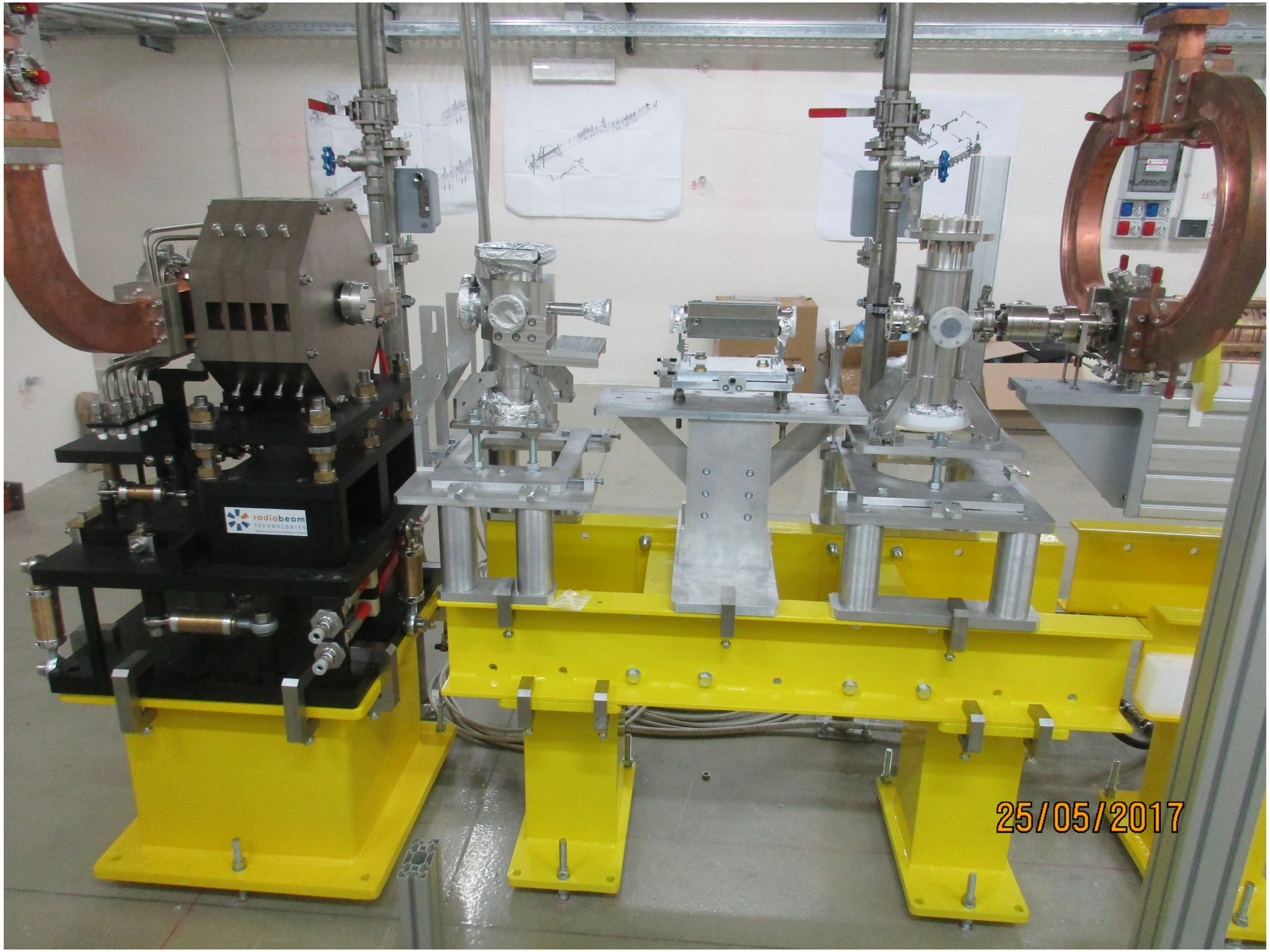


25/05/2017

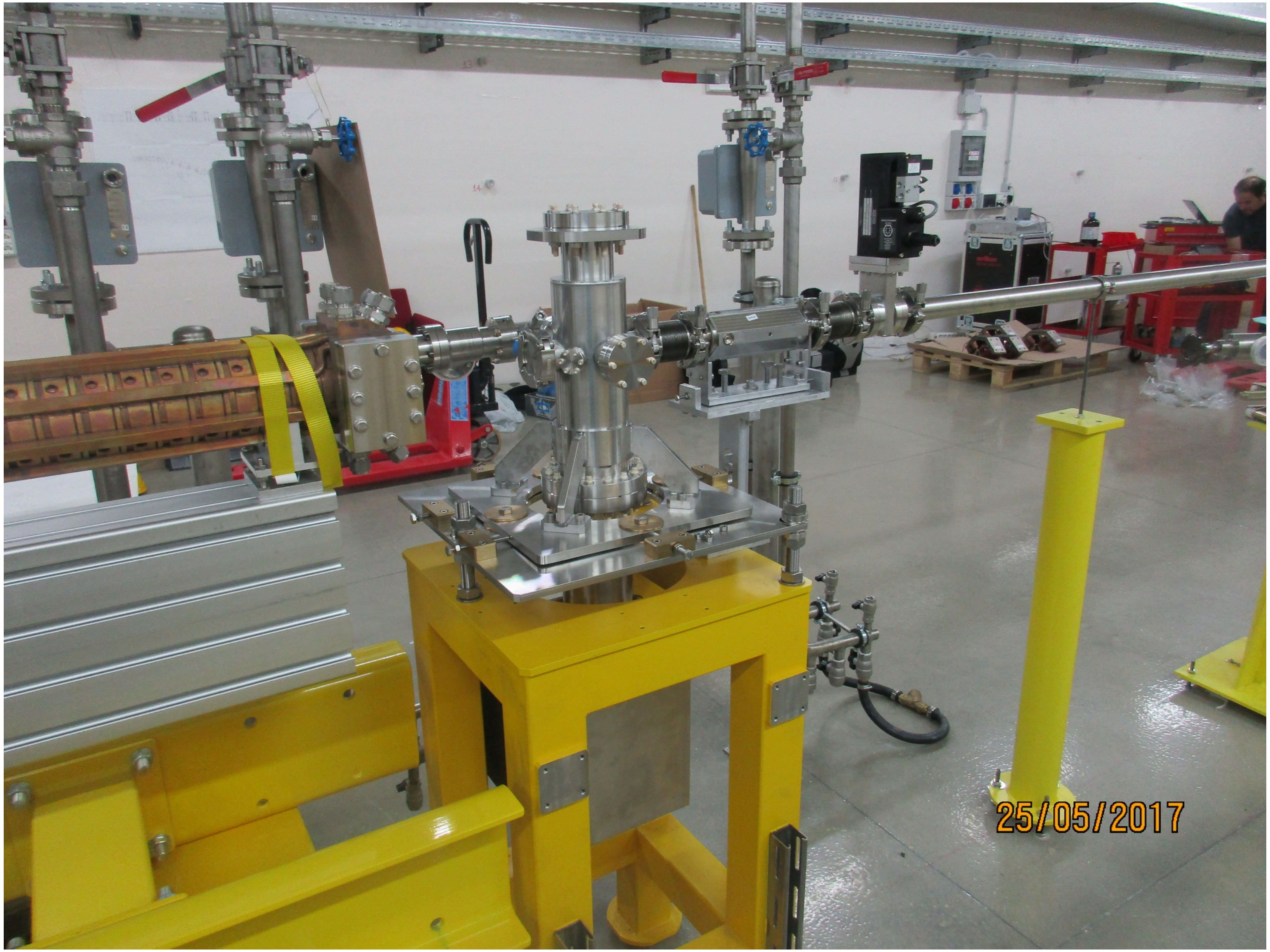
25/05/2017


25/05/2017


25/05/2017

Commissioning will start soon - first beams expected within end of 2018

Inverse Compton Sources, Overview, Theory, Main Technological Challenges – Photonic Colliders

Luca Serafini – INFN-Milan and University of Milan

4 Lecture Outline

- **Overview of Projects/Proposal for ICS' and Applications**
- **Classical e.m. and Linear Quantum Theory of Inverse Compton Sources (ICS) and paradigms for ICS**
- **Photon-Photon Colliders at low energy for Breit-Wheeler and photon-photon scattering experiments**
- **Hadron-Photon Colliders as muon photo-cathodes for TeV photons, neutrino and pion/muon low emittance beam generation**

If the Physics of Linear Compton/Thomson back-scattering is well known….

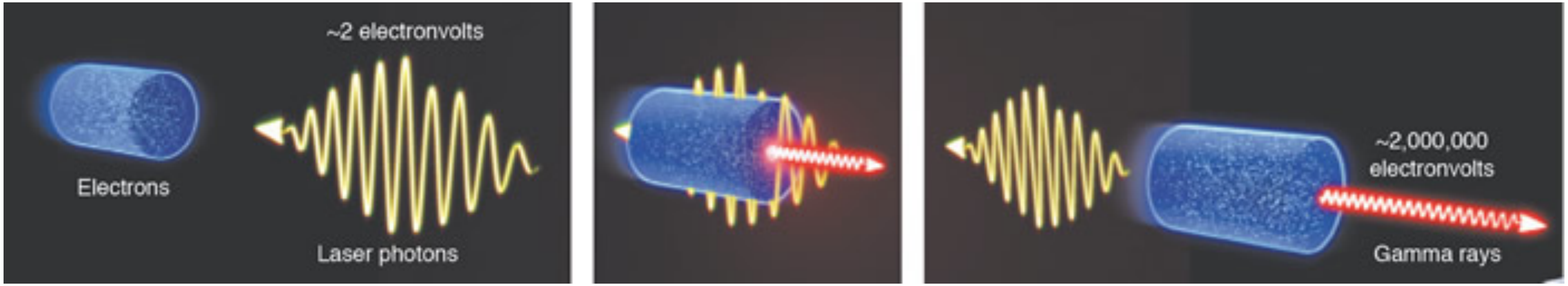

the Challenge of making a Compton Source running as an electron-photon Collider with maximum Luminosity, to achieve the requested Spectral Density, Brilliance, narrow Bandwidth of the generated *X/γ* ray beam, is a completely different issue/business !

Re-visiting the Physics of Compton back-scattering with an eye to effects impacting the quality and behavior of the photon (and electron) beam phase space distributions

Courtesy L. Palumbo

2 Approaches to describe the Physics of I.C.S.
A) (linear) Quantum B) Classical

- A) Quantum: linear QED of electron-photon 2-body kinematics and Klein-Nishina cross section

Limitation of (linear) quantum description: does not take into account the coherent organization of photons in the e.m. field of the laser pulse (intensity field, no phase)

- Effect of electron recoil on *X*/γ ray bean (spectral density, bandwidth broadenin beam (emittance dilution in multiple scattering and incoherent energy spread due to scattering stochasticity)

- B) Classical:
- No Energy/M collective effe absorption/er

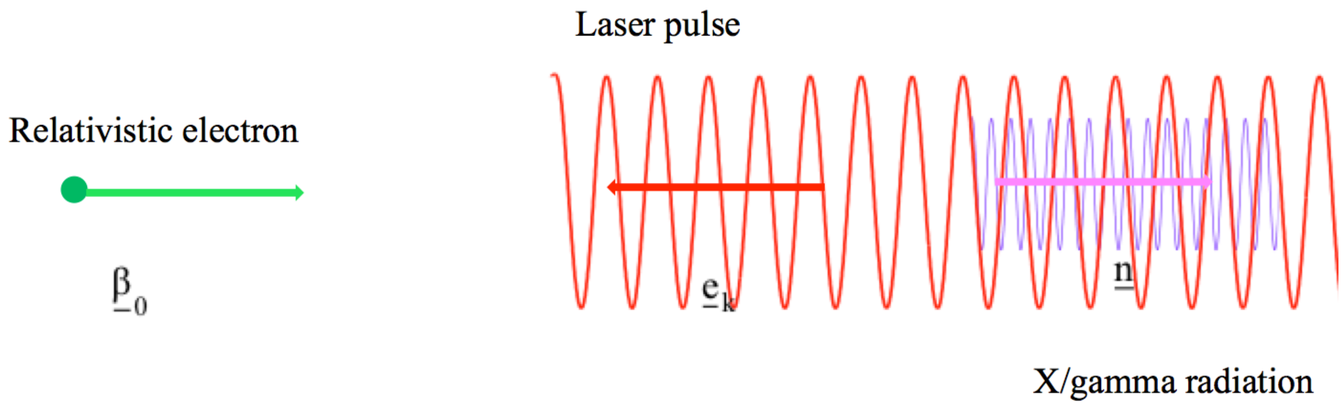

The Classical E.M. view (Maxwell eq.): Thomson Sources as synchrotron radiation sources with electro-magnetic undulator

FEL's and Thomson/Compton Sources common mechanism:
collision between a relativistic electron and a (pseudo)electromagnetic wave

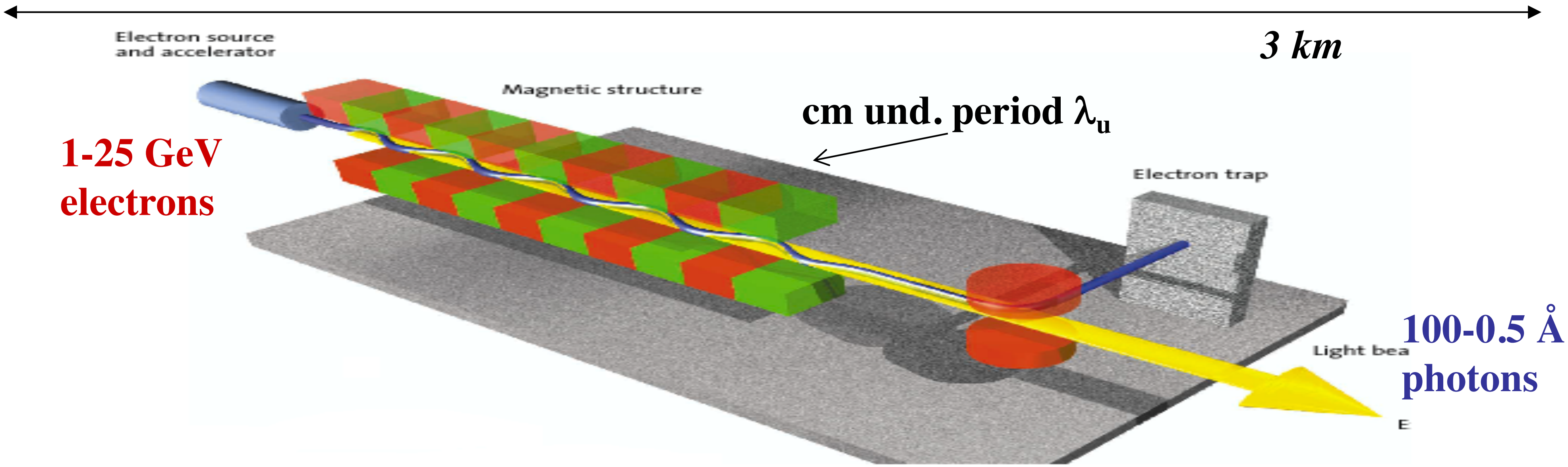

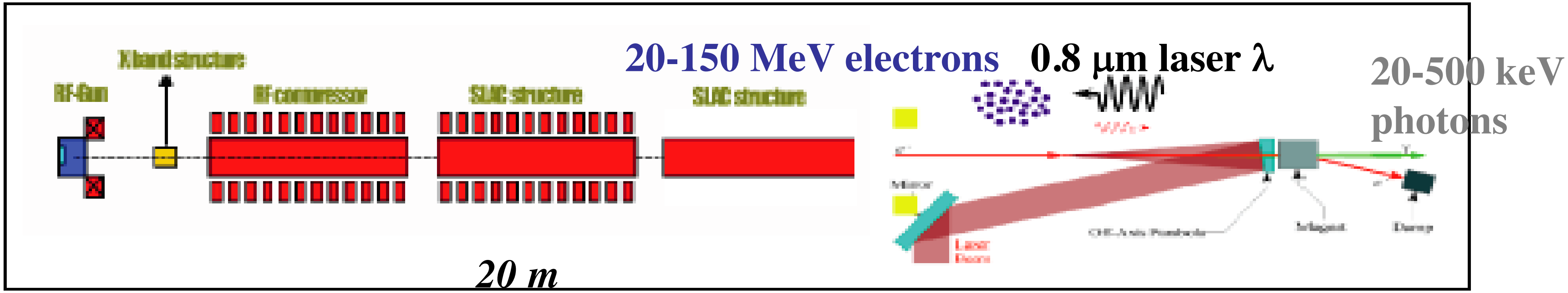

Classical model

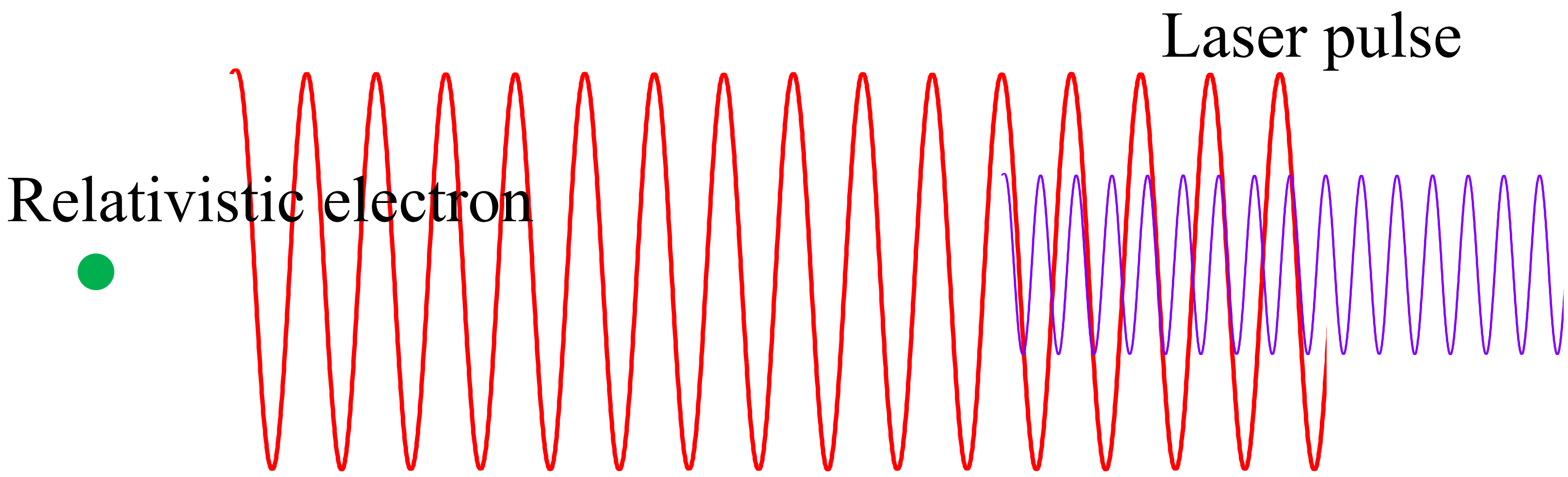

Courtesy V. Petrillo

Let us analyze in details similarities and differences between otpical and magnetic undulators (see also ref.1): the field on axis of a magnetostatic undulator is given by $B_w = B_{0w} e^{ik_w z}$, associated to a vector potential of normalized amplitude $a_w = \dfrac{eB_{0w}}{mck_w}$.

The field on axis of an optical undulator (under the approximation of a plane wave) is $B_L = B_{0L} e^{i(k_L z + \omega_L t)}$, $E_L = E_{0L} e^{i(k_L z + \omega_L t)}$, with $E_{0L} = cB_{0L}$: the associated normalized vector potential is $a_0 = \dfrac{eB_{0L}}{m\omega_L}$ with $\omega_L = ck_L = \dfrac{2\pi c}{\lambda}$. The two undulators apply, to a relativistic electron traveling on axis with $z = \beta_{//} ct$, a transverse force given by

$$F_\perp^L = mca_0\omega_L \left(1 + \beta_{//}\right) e^{i(1+\beta_{//})\omega_L t} \tag{1a}$$

and

$$F_\perp^w = mc^2 a_w \beta_{//} k_w e^{i\beta_{//} k_w ct} \tag{1b}$$

respectively. From $\dot{p}_\perp = F_\perp$ and $p_\perp = mc\beta_\perp \gamma$ we derive $\beta_\perp^L = \dfrac{a_0}{\gamma} e^{i\omega_L (1+\beta_{//})t}$ and $\beta_\perp^w = \dfrac{a_w}{\gamma} e^{i\beta_{//} k_w ct}$.

In case of a helical magnetic undulator, as well as for a cicrcularly polarized laser pulse acting as an optical undulator, we are in a simple situation of constant transverse and longitudinal momentum components, so that we can write $\beta_\perp^L = \dfrac{a_0}{\gamma}$ and $\beta_\perp^w = \dfrac{a_w}{\gamma}$, while $\beta_{//}^w = \sqrt{1 - \dfrac{1 + a_w^2}{\gamma^2}}$ and $\beta_{//}^L = \sqrt{1 - \dfrac{1 + a_0^2}{\gamma^2}}$.

In case of a helical magnetic undulator, as well as for a cicrcularly polarized laser pulse acting as an optical undulator, we are in a simple situation of constant transverse and longitudinal momentum components, so that we can write $\beta_\perp^L = \frac{a_0}{\gamma}$ and $\beta_\perp^w = \frac{a_w}{\gamma}$, while $\beta_{//}^w = \sqrt{1 - \frac{1+a_w^2}{\gamma^2}}$ and $\beta_{//}^L = \sqrt{1 - \frac{1+a_0^2}{\gamma^2}}$.

In order to derive the resonance expression for the radiation emitted in the forward direction on axis, we note that the angular frequency ω_e of the oscillating electron in the field of the optical undulator (see Eq.1a) is $\omega_e = \left(1+\beta_{//}^L\right)\omega_L$, *i.e.* almost double than the laser frequency. The typical FEL slippage condition will therefore set the resonance frequency for the radiation emitted by the electron at: $n\lambda_R = cT_e - \beta_{//}^L cT_e$ ($\omega_R = ck_R = \frac{2\pi c}{\lambda_R}$), which can be trasformed into

$$\lambda_R = \frac{\lambda}{n}\frac{1-\beta_{//}^L}{1+\beta_{//}^L} \tag{2a}$$

This expression comes out to be equal (for *n=1*) to the expression of a Thomson backscattered radiation of a laser of wavelength λ by an electron travelling on axis at speed $\beta_{//}^L c$. Expanding uo to second order in the small value $\delta = \frac{1+a_0^2}{\gamma^2}$ we obtain

$$\lambda_R = \frac{\lambda}{4n\gamma^2}\left(1+a_0^2\right)\left(1+\frac{1+a_0^2}{2\gamma^2}\right) \tag{2b}$$

In the case of a magnetic undulator the resonance condition is derived considering that the angular frequency of the oscillating electron in the field of the undulator (see Eq.1b) is $\omega_e = \beta_{//} c k_w$, so the resonance condition

$n\lambda_R = cT_e - \beta_{//}^w cT_e$ now becomes

$$\lambda_R = \frac{\lambda_w}{n}\frac{1-\beta_{//}^w}{\beta_{//}^w} \tag{3a}$$

which is equivalent to

$$\lambda_R = \frac{\lambda_w}{2n\gamma^2}\left(1+a_w^2\right)\left(1+3\frac{1+a_w^2}{4\gamma^2}\right) \tag{3b}$$

It is well known[1] that there is an equivalence between a magnetic and an optical undulator: if the conditions

$$\left(1+\beta_{//}^L\right)\omega_L = c\beta_{//}^w k_w \quad ; \quad a_0 = a_w \tag{4}$$

are satisfied, the two undulators apply the same force on any electron travelling on axis and, furthermore, the emitted radiation in the forward direction on axis has the same frequency as far as we neglect the small red-shift ($\delta/2$ for the optical and $3\delta/4$ for the magnetic undulator). For an ultrarelativistic beam $\beta_{//} \approx 1$, the equivalence principle can be cast in the much simpler form

$$\lambda_w = \lambda/2 \quad ; \quad a_0 = a_w \tag{4b}$$

Therefore, we can say that if two undulators are equivalent, *i.e.* apply the same force and produce the same radiation, the two are undistinguishable by the electron beam.

LINEAR (a_0<<1, single photon) THOMSON BACK-SCATTERING

$$\nu_X = \nu_L \frac{1-\beta\cos\alpha_L}{1-\beta\cos\theta} \approx \nu_L \frac{4\gamma^2}{1+\theta^2\gamma^2} \approx 4\gamma^2\nu_L$$

$$for\ \alpha_L = \pi\ (scatt.\ angle) \qquad and$$

$$\theta << 1 \quad or \quad \theta = 0\ (obs.\ angle)$$

e^- (1 GeV); λ_0=1μm, E_0=1.24 eV ⟶ λ_T=6 x10^{-8}μm, E_T=20 MeV

e^- (200 MeV); λ_0=1μm, E_0=1.24 eV ⟶ λ_T=1.56 x10^{-6}μm, E_T=800 KeV

e^- (29 MeV); λ_0=0.8μm, E_0=1.5 eV ⟶ λ_T=0.5 x10^{-4}μm, E_T=20 KeV

From the electron orbits and the Liénard-Wiechert potentials **in the far zone** one can write the expression of the electric field [Jackson..]:

$$\mathbf{E} = \frac{e}{c}\left[\frac{\mathbf{n}\times\left[(\mathbf{n}-\boldsymbol{\beta}(t'))\times\dot{\boldsymbol{\beta}}(t')\right]}{R(1-\mathbf{n}\cdot\boldsymbol{\beta}(t'))^3}\right]_{ret}$$

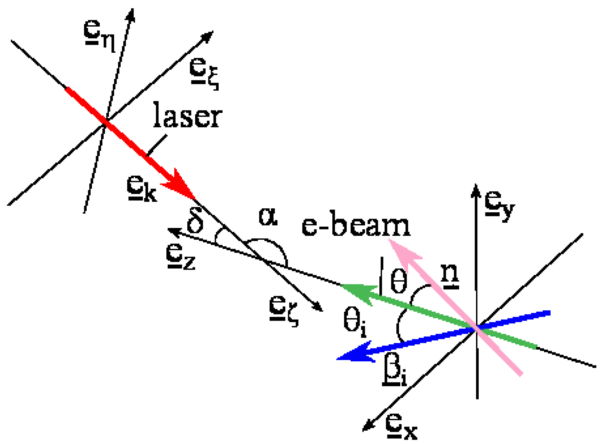

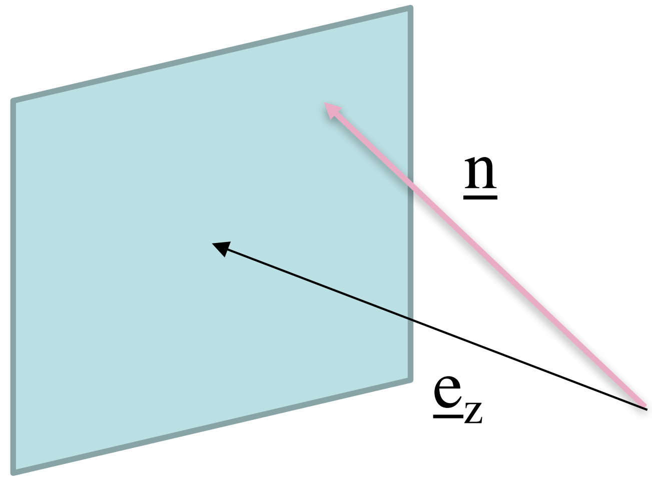

Courtesy V. Petrillo

From the motion equation of the electrons

$$\frac{d\mathbf{p}}{dt} = -e(\mathbf{E}_L + \boldsymbol{\beta} \times \mathbf{B}_L)$$

If **E** and **B=k**x**E** are electric and magnetic field of the incoming laser,

$$\dot{\boldsymbol{\beta}} = \frac{d\boldsymbol{\beta}}{dt} = -\frac{e}{mc\gamma}(\mathbf{E}_L(1-\boldsymbol{\beta}\cdot\mathbf{e}_k) + \boldsymbol{\beta}\cdot\mathbf{E}_L(\mathbf{k}-\boldsymbol{\beta}))$$

Courtesy V. Petrillo

Classical double differential spectrum

The double differential spectrum for **one electron** is:

$$\frac{d^2W_i}{d\omega d\Omega} = \frac{e^2}{4\pi^2 c}\left|\int_{-\infty}^{+\infty} dt e^{i\omega t}\,\frac{\mathbf{n}\times\left[(\mathbf{n}-\beta(t'))\times\dot{\beta}(t')\right]}{(1-\mathbf{n}\cdot\beta(t'))^3}\right|^2 = \hbar\omega\frac{\mathrm{d}^2\mathrm{N}_\mathrm{i}}{\mathrm{d}\omega\mathrm{d}\Omega}$$

And for all the beam:

$$\hbar\omega\frac{\mathrm{d}^2\mathrm{N}}{\mathrm{d}\omega\mathrm{d}\Omega} = \hbar\omega\sum_i\frac{\mathrm{d}^2\mathrm{N}_\mathrm{i}}{\mathrm{d}\omega\mathrm{d}\Omega}$$

$\Psi \equiv \gamma\vartheta_M$

$$N(\Psi) \cong \pi\alpha\Im N_e\left(\frac{cT}{\lambda}\right)a_0^2\Psi^2\,\frac{(1+\Psi^2+\frac{2}{3}\Psi^4)}{\left(1+\Psi^2\right)^3}$$

Full treatement of linear and nonlin. TS for a plane-wave laser pulse with analytical expression of the distributions in ***P. Tomassini et al.***, Appl. Phys. B **80**, 419 (2005).

$$\Psi \equiv \gamma\vartheta_M$$

$$N(\Psi) \cong \pi\alpha\Im N_e \left(\frac{cT}{\lambda}\right) a_0^2 \Psi^2 \frac{(1+\Psi^2+\frac{2}{3}\Psi^4)}{(1+\Psi^2)^3}$$

$$a_0 = 4.3\frac{\lambda}{w_0}\sqrt{\frac{U_L[J]}{\sigma_t[ps]}}$$

$a_0 \equiv e^2 A/(m_e c^2) = 8.5 \times 10^{-10}\sqrt{I\lambda_0^2}$, I being the peak intensity in W/cm^2 and λ_0 the wavelength in μm, the pulse

$$N_l a_0^2 \propto \frac{U_L}{w_0^2}$$

Total intensity and Stokes parameter $|E_x|^2-|E_y|^2$ on the screen at 1 m, $\gamma=1200$

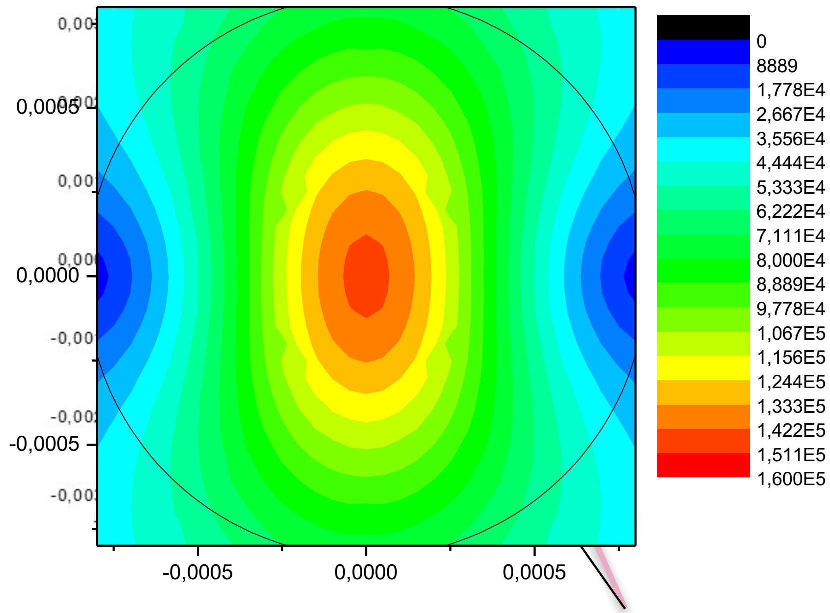

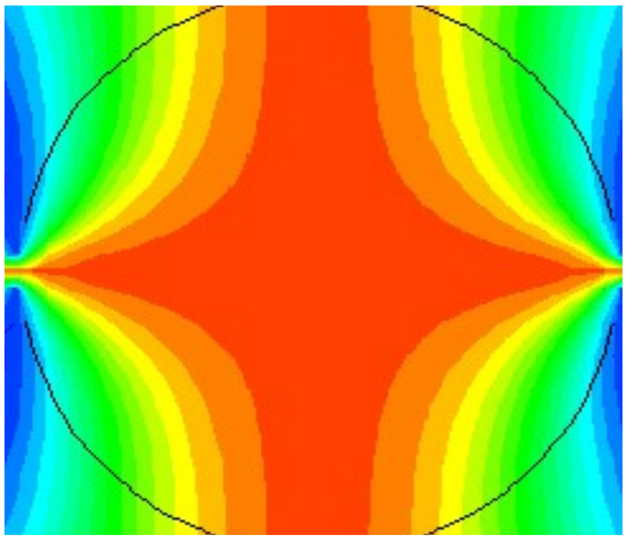

Linear and Nonlinear Thomson Scattering for Advanced X-ray Sources in PLASMONX

Paolo Tomassini, A. Bacci, J. Cary, M. Ferrario, A. Giulietti, Danilo Giulietti, L. A. Gizzi, Luca Labate, L. Serafini, Vittoria Petrillo, and C. Vaccarezza

***Abstract*—Thomson scattering of laser pulses onto ultrarelativistic e-bunches is becoming an advanced source of tunable, quasi-monochromatic, and ultrashort X/gamma radiation. Sources aimed at reaching a high flux of scattered photons need to be driven by high-brightness e-beams, whereas extremely short (femtosecond scale or less) sources need to make femtosecond-long e-beams that collide with the laser pulses. In this paper, we explore the performance of the PLASMONX TS source in several operating regimes, including preliminary results on a source based on e-bunches produced by laser wakefield acceleration and controlled injection via density downramp.**

***Index Terms*—Compton scattering, Thomson scattering (TS), X-ray sources.**

I. Introduction

FUNDED by the Istituto Nazionale di Fisica Nucleare (INFN), the PLasma Acceleration at Sparc and MONOfield acceleration (LWFA) with internal/external injection or Thomson scattering (TS) physics and applications. TS X-ray sources are attracting strong attention because of their flexibility and potential compactness with respect to conventional synchrotron sources. A TS source driven by high-quality e-beams can be switched on in several operating modes, namely, the high-flux-moderate-monochromaticity mode (HFM2), the moderate-flux-monochromatic mode (MFM), and the short-and-monochromatic mode (SM). The HFM2 mode is suitable, e.g., for medical imaging, when high-flux sources are needed and a moderate monochromaticity is useful to improve the detection/dose performance. The MFM mode is useful for static probing when high monochromaticity and, possibly, tunability are needed (e.g., imaging with subtraction of images taken with different energies). The SM mode is finally u
pump-and-probe experiments, e.g., in physical chem

the Compton process). If the electrons are ultrarelativistic, the scattered radiation looks frequency-upshifted and is mostly emitted forward with respect to the motion of particles in a small cone of aperture roughly given by the inverse of their Lorentz gamma.

The physics of TS is quite complex in the nonlinear regime, i.e., when the laser pulse strength $a0 = 8.5 \cdot 10^{-10}(I\lambda^2)^{1/2}$ approaches or exceeds unity. At intensities above the so-called "relativistic intensity" $I\lambda^2 = 10^{18}\ \mu\mathrm{m}^2 \cdot \mathrm{W/cm}^2$, the extremely intense electric field makes the electrons' quivering speed approach the light speed, making the magnetic field relevant for dynamics, thus generating a complex particle motion.

The computation in the far field of the scattered photons' distribution N_λ of pulsation ω can be performed in the classical regime provided that the energy of the electrons is far below tens of gigaelectronvolts, as it is the case for this paper, by using

$$\frac{d^2N_\gamma}{d\omega d\Omega} = \frac{\alpha}{4\pi^2}\omega\left|\vec{J}(\vec{n},\omega)\right|^2$$
$$\vec{J}(\vec{n},\omega) = \vec{n} \times \left(\vec{n} \times \int dt\vec{\beta}(t)e^{i\omega\left(t-\frac{\vec{n}\cdot\vec{r}(t)}{c}\right)}\right) \qquad (1)$$

where r and β represent the particle position and speed, respectively, and $\vec{n}$ is the emitted photon unit versor. By taking the retarded effects into account, which are the nonlinear quivering and secular motion of each electron in the bunch due to pulse longitudinal ponderomotive forces, an analytical computation

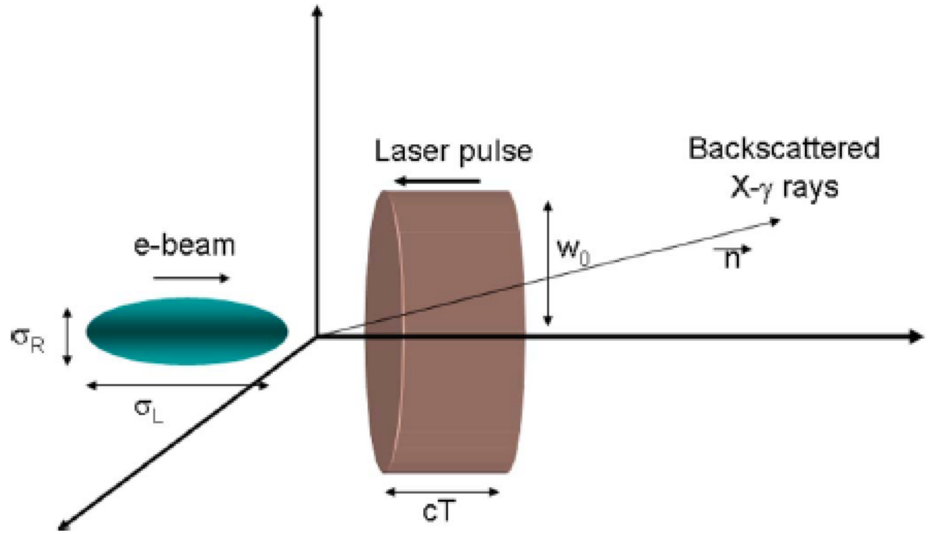

Fig. 1. Thomson backscattering geometry. The electron beam of longitudinal and transverse sizes σ_L and σ_R, respectively, is moving at a relativistic speed from left to right, colliding with a photon beam of waist size w_0 and duration T, thus emitting scattered radiation mainly in the direction of motion of the electron beam.

electron bunch parameters considered in this paper; see [4]). Considering that the analytical outcome sketched in (2) and (3) are valid only for the case of planar long flattop laser pulse, the code decomposes the pulse in a sequence of single cycles, with each cycle having its own phase shift and intensity. While the particle is moving along its secular path, it interacts with different cycles of the pulse, and the coherent summa
the radiation emitted in each cycle gives rise to the ra
emitted during the entire interaction.

Example

Quasi head-on collision of a 5 MeV electron ($\theta_e = 50$ mrad, $\phi_e = \pi/2$) on a flat-top pulse of normalized ampliude a_0=1.5, λ = 1μm and T = 20 fs

P. Tomassini et al., Appl. Phys. B 80, 419 (2005)

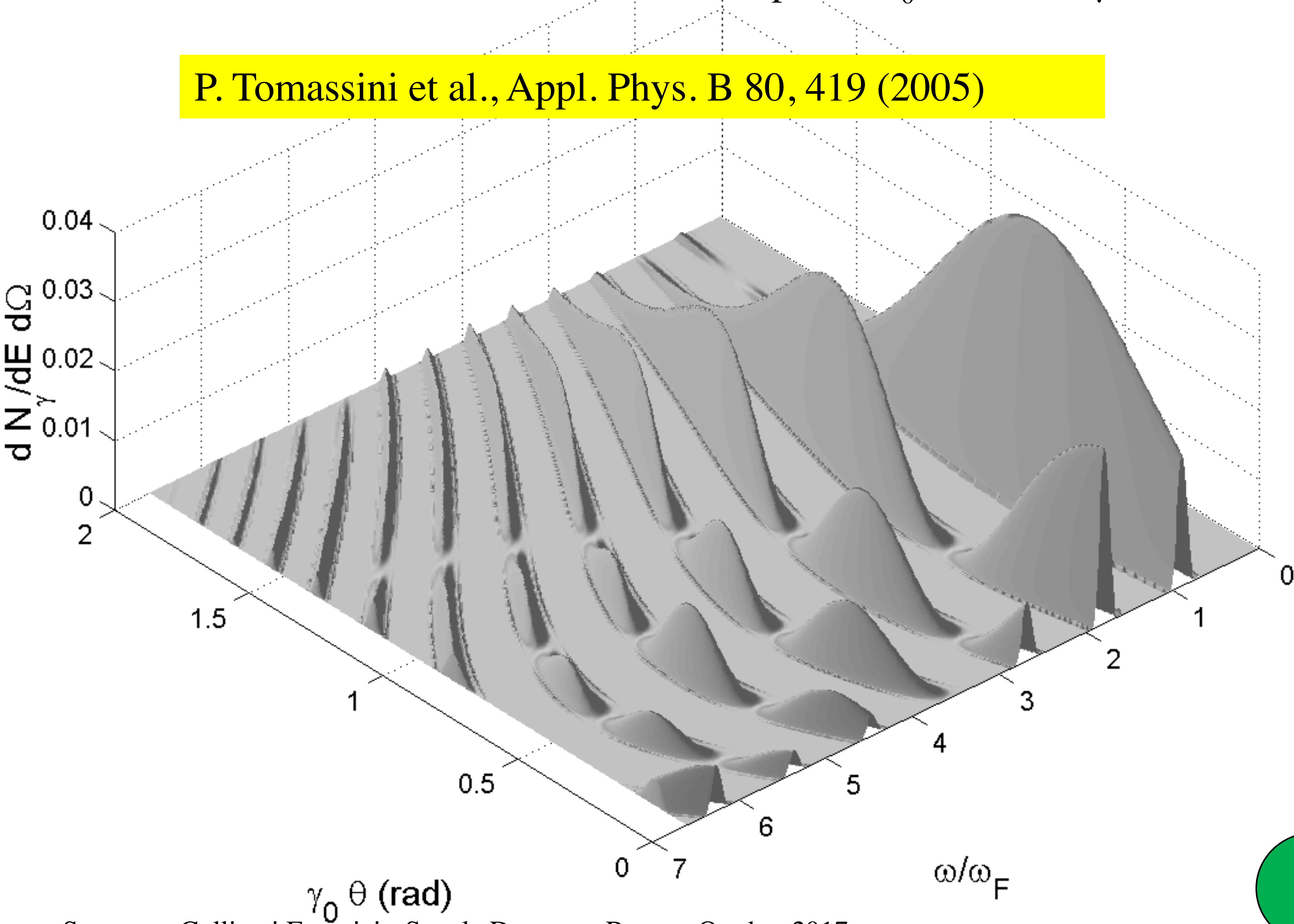

FEL resonance condition

$$\boxed{\lambda_R = \lambda_w \frac{\left(1+a_w{}^2\right)}{2\gamma^2}}$$

(magnetostatic undulator)

Example : for λ_R=*1A*, λ_w=*2cm*, *E=7 GeV*

$$a_w = 0.93\lambda_w[cm]B_w[T]$$

Violation of Energy-Momentum Conservation !!

$$\cancel{\lambda_R = \lambda \frac{\left(1+a_0^2/2\right)}{4\gamma^2}}$$

(electromagnetic undulator)

Example : for λ_R=*1A*, λ=*0.8μm*, *E=25MeV*

Example : for *hν=10 MeV*, λ=*0.4μm*, *E=530 MeV*

$$a_0 \propto \frac{\lambda[\mu m]\sqrt{P[TW]}}{R_0[\mu m]}$$

laser power

laser spot size

L. Serafini et al., Proceedings of the SPIE, Volume 6634, article id. 66341G (2007)

Compton Inverse Scattering Physics is clear: recall some basics

Quantum model

Laboratory ref. system

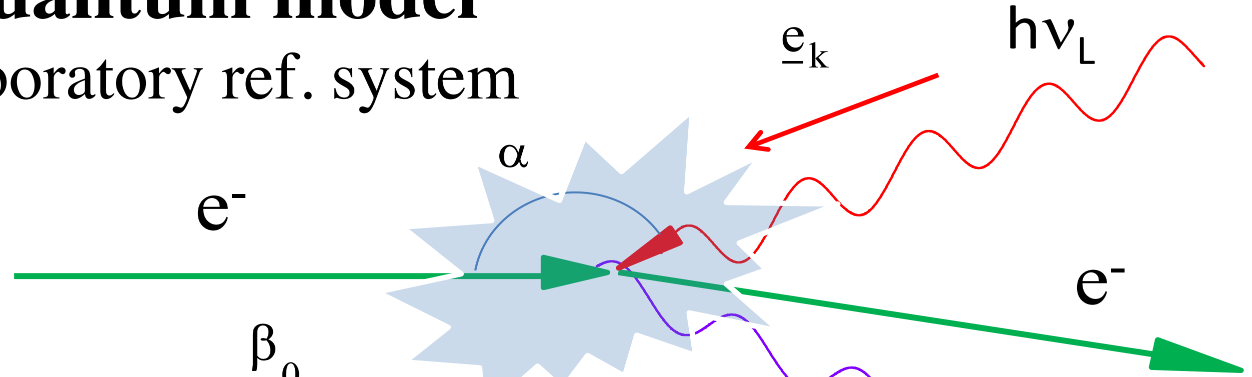

3 regimes: a) Elastic, Thomson b) Quasi-Elastic, Compton with Thomson cross-section c) Inelastic, Compton, recoil dominated

$$\begin{cases} mc^2(\gamma-\gamma_0)=-h(\nu-\nu_L) \\ mc(\underline{\beta}\gamma-\underline{\beta}_0\gamma_0)=-h(\underline{k}-\underline{k}_L)/2\pi \end{cases}$$

Energy and momentum conservation laws

γ_0:initial Lorentz factor

$$\nu = \nu_L \frac{1-\underline{e}_k\cdot\underline{\beta}_0}{1-\underline{n}\cdot\underline{\beta}_0 \boxed{+\dfrac{h\nu_L}{mc^2\gamma_0}(1-\underline{e}_k\cdot\underline{n})}}$$

$$\lambda = \boxed{\lambda_L\frac{1-\underline{n}\cdot\underline{\beta}_0}{1-\underline{e}_k\cdot\underline{\beta}_0}} + \boxed{\frac{h}{mc\gamma_0}\frac{1-\underline{e}_k\cdot\underline{n}}{1-\underline{e}_k\cdot\underline{\beta}_0}}$$

Petrillo V. and al., NIM A **693** (2012)

Sun C. and Wu Y. K., PRSTAB **14** (2011) 044701

Courtesy V. Petrillo

Quantu ens in the

Center nematics)

ref.

Analytical description of photon beam phase spaces in Inverse Compton Scattering sources

C. Curatolo,[1] I. Drebot,[1] V. Petrillo,[1,2] and L. Serafini[1]

[1] *INFN-Milan, via Celoria 16, 20133 Milano, Italy*

[2] *Università degli Studi di Milano, via Celoria 16, 20133 Milano, Italy*

(Dated: 22 May 2017)

We revisit the description of inverse Compton scattering sources and the photon beams generated therein, emphasizing the behavior of their phase space density distributions and how they depend upon those of the two colliding beams of electrons and photons. Main objective is to provide practical formulas for bandwidth, spectral density, brilliance, which are valid in general for any value of the recoil factor, i.e. both in the Thomson regime of negligible electron recoil, and in the deep Compton recoil dominated region, which is of interest for gamma-gamma colliders and Compton Sources for the production of multi-GeV photon beams. We adopt a description based on the center of mass reference system of the electron-photon collision, in order to underline the role of the electron recoil and how it controls the relativistic Doppler/boost effect in various regimes. Using the center of mass reference frame greatly simplifies the treatment, allowing to derive simple formulas expressed in terms of rms momenta of the two colliding beams (emittance, energy spread, etc.) and the collimation angle in the laboratory system. Comparisons with Monte Carlo simulations of inverse Compton scattering in various scenarios are presented, showing very good agreement with the analytical formulas: in particular we find that the bandwidth dependence on the electron beam emittance, of paramount importance in Thomson regime, as it limits the amount of focusing imparted to the electron beam, becomes much less sensitive in deep Compton regime, allowing a stronger focusing of the electron beam to enhance luminosity without loss of mono-chromaticity. A similar effect occurs concerning the bandwidth dependence on the frequency spread of the incident photons: in deep recoil regime the bandwidth comes out to be much less dependent on the frequency spread. The set of formulas here derived are very helpful in designing inverse Compton sources in diverse regimes, giving a quite accurate first estimate in typical operational conditions for number of photons, bandwidth, spectral density and brilliance values - the typical figures of merit of such radiation sources.

I. INTRODUCTION

Inverse Compton Scattering sources (ICSs) are becoming increasingly attractive as radiation sources in photon energy regions either not covered by other high brilliance sources (FEL's, synchrotron light sources) or where compactness becomes an important figure of merit, like for advanced X-ray imaging applications to be implemented in university campus, hospitals, museums, etc., i.e. outside of research centers or large scale laboratories [1]. ICSs are becoming the γ-ray sources of reference in nuclear photonics, photo-nuclear [2, 3] and fundamental physics [4], thanks to superior performances in spectral densities achievable. Eventually they will be considered for very high energy photon generation (in the GeV to TeV range) since there are no other competing techniques at present, neither on the horizon, based on artificial tools at this high photon energy [5]. As a consequence, a flourishing of design activities is presently occurring in several laboratories [6–15] and companies [16–19], where ICSs are being conceived, designed and built to enable several domains of applications, and ranging from a few keV photon energy up to GeV's and beyond. Designs of ICSs are carried out considering several diverse schemes, ranging from high gradient room temperature pulsed RF Linacs [3, 20, 21] to CW ERL Super-conducting Linacs [22, 23] or storage rings [2, 24–27], as far as the electron beam generation is concerned, and from single pulse J-class amplified laser systems running at 100 Hz to optical cavities (e.g. Fabry-Perot) running at 100 MHz acting as photon storage rings for the optical photon beams, not to mention schemes based on FEL's to provide the colliding photon beam [22, 28, 29].

In order to assess the performances of a specific ICSs under design, detailed simulations of the electron-photon beam collision are typically carried out using Monte Carlo codes [30–32] able to model the linear and non-linear electron-photon quantum interaction leading to Compton back-scattering events, taking into account in a complete fashion the space-time propagation of the two colliding beams through the interaction point region, including possible multiple scattering events occurring during the overlap of the two pulses. Only in case of negligible electron recoil, i.e. in the so called Thomson regime typical of low energy X-ray ICSs, classical electromagnetic numerical codes (e.g. TSST [33]), modelling the equivalent undulator radiation emitted by electrons wiggling in the electromagnetic field of the incoming laser pulse, allow to analyze particular situations such as the use of chirped [34], tilted [35] and twisted [36] lasers.

In the recent past some efforts have been developed to carry out analytical treatments of the beam-beam collision physics, embedding the single electron-photon collision from a quantum point of view within a rms distribution of the scattered photon beam [27, 37–43], or,

. ref.

$$\vec{p}_e^{\,*} + \hbar\vec{k}_{h\nu}^{\,*} = \vec{0}$$

electron $4-ve$ $E_e^2 / c^2 - m_e^2 c^2 \Big]$

photon $4-vec$ $_L / c\Big]$

Invariant Mass, Lorentz transformation from Lab to c.m. ref. system

$$Total\ 4-vector\ \mathbf{P} = \mathbf{P}_e + \mathbf{P}_{h\nu} = \left[E_e/c + h\nu_L/c, 0, 0, \sqrt{\frac{E_e^2}{c^2} - m_e^2 c^2} - h\nu_L/c \right]$$

$$Invariant\ Mass\ s \equiv c\mathbf{P} \bullet c\mathbf{P} = E_{tot}^{2*} = E_{cm}^2$$

$$\left(4-vector\ product\ \mathbf{P}_1 \bullet \mathbf{P}_2 \equiv \left[E_1 E_2 / c^2 - \vec{p}_1 \cdot \vec{p}_2 \right] \right)$$

$$E_{cm} \cong \sqrt{4E_e h\nu_L + m_e^2 c^4} = m_e c^2 \sqrt{1 + \frac{4\gamma h\nu_L}{m_e c^2}} = m_e c^2 \sqrt{1+\Delta}$$

$$e^-\ recoil\ factor\ \Delta \equiv \frac{4\gamma h\nu_L}{m_e c^2}$$

from $\vec{p}^{\,*}_{tot} = \vec{p}^{\,*}_e + \hbar\vec{k}^{\,*}_{h\nu} = \vec{0}$ $\Rightarrow$ $\left|\vec{p}^{\,*}_e\right| = \hbar\left|\vec{k}^{\,*}_{h\nu}\right|$

and $\boxed{E_{cm} = E^*_e + h\nu^* = m_e c^2\sqrt{1+\Delta}}$ $\left(\begin{array}{l} E^*_e = m_e^2 c^4 + \left|\vec{p}^{\,*}_e\right|^2 c^2 \\ h\nu^* = \hbar\left|\vec{k}^{\,*}_{h\nu}\right| c \end{array}\right)$

$\Downarrow$

$$E^*_e = m_e c^2 \frac{2+\Delta}{2\sqrt{1+\Delta}}$$

$$h\nu^* = m_e c^2 \frac{\Delta}{2\sqrt{1+\Delta}} = \frac{2\gamma h\nu_L}{\sqrt{1+\Delta}}$$

$$\left|\vec{p}^{\,*}_e\right| = m_e c \frac{\Delta}{2\sqrt{1+\Delta}}$$

Holds before and after scattering (c.m ref. system!)

$$\begin{cases} E_{cm} \xrightarrow[\Delta \to 0]{} m_e c^2 \\ E_{cm} \xrightarrow[\Delta \to \infty]{} 2\sqrt{\gamma m_e c^2 h\nu_L} = 2\sqrt{E_e E_{h\nu}} \end{cases}$$

Δ=0 electron as relativ. mirror

Δ>>1 symmetric collider

$$\begin{cases} E_e^* \xrightarrow[\Delta \to 0]{} m_e c^2 \\ E_e^* \xrightarrow[\Delta \to \infty]{} m_e c^2 \dfrac{\sqrt{\Delta}}{2} = \sqrt{\gamma m_e c^2 h\nu_L} \end{cases}$$

$$\begin{cases} h\nu^* \xrightarrow[\Delta \to 0]{} m_e c^2 \dfrac{\Delta}{2} = 2\gamma h\nu_L \\ h\nu^* \xrightarrow[\Delta \to \infty]{} m_e c^2 \dfrac{\sqrt{\Delta}}{2} = \sqrt{\gamma m_e c^2 h\nu_L} \end{cases}$$

$$E_e^* \xrightarrow[\Delta \to \infty]{} h\nu^*$$

symm. collider

before scattering

$$\begin{pmatrix} p^*_{eIN} = \left[0,0,p^*_e\right] \\ \hbar\vec{k}^*_{IN} = \left[0,0,-h\nu^*/c\right] \end{pmatrix}$$

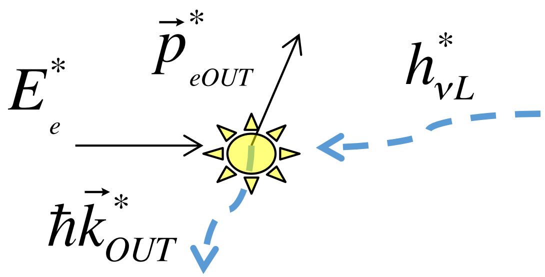

after scatt.

$$\begin{pmatrix} p^*_{eOUT} = \left[p^*_e \sin\vartheta^* \cos\varphi^*, p^*_e \sin\vartheta^* \sin\varphi^*, p^*_e \cos\vartheta^*\right] \\ \hbar\vec{k}^*_{OUT} = \left[-p^*_e \sin\vartheta^* \cos\varphi^*, -p^*_e \sin\vartheta^* \sin\varphi^*, -p^*_e \cos\vartheta^*\right] \end{pmatrix}$$

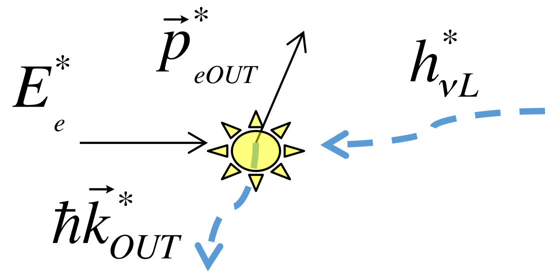

what is the probability of scattering at ϑ^*, φ^* ?
Klein-Nishina differential cross-section

$$\frac{d\sigma}{d\theta' d\phi'} = r_e^2 \left(\frac{2}{2+\Delta(1-cos\theta')}\right)^2 \left(\frac{1+cos^2\theta'}{2}\right) \cdot \left(1+\frac{\Delta^2(1-cos\theta')^2}{2(1+cos^2\theta')(2+\Delta(1-cos\theta'))}\right) sin\theta'$$

$\Delta \to 0$

$$\boxed{\frac{d\sigma}{d\vartheta^* d\varphi^*} = r_e^2 \left(\frac{1+\cos^2\vartheta^*}{2}\right)\sin\vartheta^*}$$

$$\vartheta^* = \vartheta'\sqrt{1+\Delta}$$

To transform to the Lab ref. system we need to compute γ_{cm}

$$\gamma_{cm} = \frac{E_{lab}}{E_{cm}} = \frac{E_e + h\nu_L}{m_e c^2 \sqrt{1+\Delta}} \cong \frac{\gamma}{\sqrt{1+\Delta}}$$

Then apply a Lorentz transformation

$$\begin{cases} E_{ph} = p^*_{ph}\gamma_{cm}\left(1+\sqrt{1-\frac{1}{\gamma^2_{cm}}}\cos\theta^*\right) \\ p_{phx} = p^*_{ph}\sin\theta^*\cos\phi^* \\ p_{phy} = p^*_{ph}\sin\theta^*\sin\phi^* \\ p_{phz} = p^*_{ph}\gamma_{cm}\left(\sqrt{1-\frac{1}{\gamma^2_{cm}}}+\cos\theta^*\right) \end{cases}$$

$$\tan\vartheta = \frac{\sin\vartheta^*}{\gamma_{cm}\left(\beta_{cm} + \cos\vartheta^*\right)} \cong \frac{\sqrt{1+\Delta}\,\sin\vartheta^*}{\gamma\left(1+\cos\vartheta^*\right)}$$

$$\cos\vartheta^* \cong \frac{1-\gamma_{cm}^2\tan^2\vartheta}{1+\gamma_{cm}^2\tan^2\vartheta} = \frac{1+\Delta-\gamma^2\tan^2\vartheta}{1+\Delta+\gamma^2\tan^2\vartheta} \qquad if\ \ \beta_{cm} = 1$$

general solution
see below

considering only $\vartheta \ll 1 \quad (\vartheta < 1/\gamma)$

$$\boxed{E_{ph} = m_e c^2 \frac{\Delta\gamma}{2(1+\Delta)}\left[1+\sqrt{1-\frac{1+\Delta}{\gamma^2}\frac{1+\Delta-\gamma^2\vartheta^2}{1+\Delta+\gamma^2\vartheta^2}}\right]}$$

$\gamma\vartheta < 1$

$$\boxed{E_{ph} = m_e c^2 \frac{\Delta\gamma}{2(1+\Delta)}\left[2-\frac{1+\Delta}{2\gamma^2}-\frac{2\gamma^2\vartheta^2}{1+\Delta}\right]}$$

$$\cos\vartheta^* = \frac{\sqrt{1+tan^2\vartheta}-\gamma_{cm}\sqrt{\gamma_{cm}^2-1}\,tan^2\vartheta}{1+\gamma_{cm}^2 tan^2\vartheta}$$

notation warning $h\nu_x = E_{ph}$

$$E_{ph} = \frac{4\gamma^2 h\nu_L}{1+\Delta}\left[1 - \frac{1+\Delta}{4\gamma^2} - \frac{\gamma^2\vartheta^2}{1+\Delta}\right]$$

$\gamma >> 1 \qquad (1+\Delta)/\gamma^2 << 1$

$$f(\alpha) = \frac{1+\cos\alpha}{2}$$

$$E_{ph} = 4\gamma^2 h\nu_L \frac{1 - \dfrac{\gamma^2\vartheta^2}{1+\Delta}}{1+\Delta} f(\alpha)$$

Deep Compton regime ($\Delta >> 1$ recoil dominated)

$$E_{ph} \xrightarrow[\Delta\to\infty]{} \gamma mc^2\left(1 - \frac{\gamma^2\vartheta^2}{\Delta}\right) f(\alpha)$$

Thomson regime $\Delta = 0$ no recoil

$$E_{ph} \xrightarrow[\Delta\to 0]{} 4\gamma^2 h\nu_L \left(1 - \gamma^2\vartheta^2\right) f(\alpha)$$

$$\Delta \equiv \frac{4\gamma h\nu_L}{m_e c^2}\left(\frac{1+\cos\alpha}{2}\right)$$

Recap
(exact analytical formula, no approximations)

$$\Delta = \frac{4\gamma h\nu_L}{m_e c^2} \qquad \gamma_{cm} = \frac{\gamma}{\sqrt{1+\Delta}}$$

$$E_{ph} = \frac{2\gamma^2 h\nu_L}{1+\Delta}\left[1 + \sqrt{1 - \frac{1+\Delta}{\gamma^2}} \cos\vartheta^*\right]$$

$$\cos\vartheta^* = \frac{\sqrt{1+tan^2\vartheta} - \gamma_{cm} tan^2\vartheta \sqrt{\gamma_{cm}^2 - 1}}{1+\gamma_{cm}^2 tan^2\vartheta} \qquad if \quad \vartheta < \frac{\pi}{2}$$

$$\cos\vartheta^* = \frac{-\sqrt{1+tan^2\vartheta} - \gamma_{cm} tan^2\vartheta \sqrt{\gamma_{cm}^2 - 1}}{1+\gamma_{cm}^2 tan^2\vartheta} \qquad if \quad \vartheta > \frac{\pi}{2}$$

$$E_{ph-max} = \frac{4\gamma^2 h\nu_L}{1+\Delta} = 4\gamma_{cm}^2 h\nu_L$$

Recap (exact analytical formula, example 250 MeV electrons against $h\nu_L$=1.2 eV photons)

$$\gamma = 490. \quad \Delta = 0.0046 \quad \gamma_{cm} = 488.88 \qquad E_{ph}(MeV) = \frac{1.1472}{2}\left[1 + \sqrt{1 - \frac{1+\Delta}{\gamma^2}\cos\vartheta^*}\right]$$

$E_{ph}(eV)$

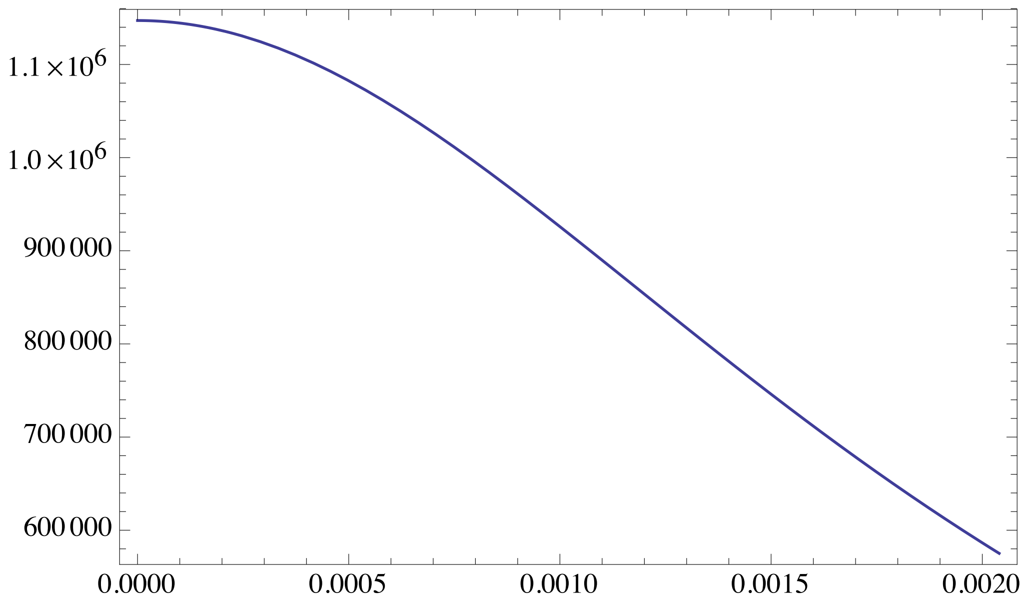

$\vartheta = 1/\gamma$

$E_{ph}(eV)$

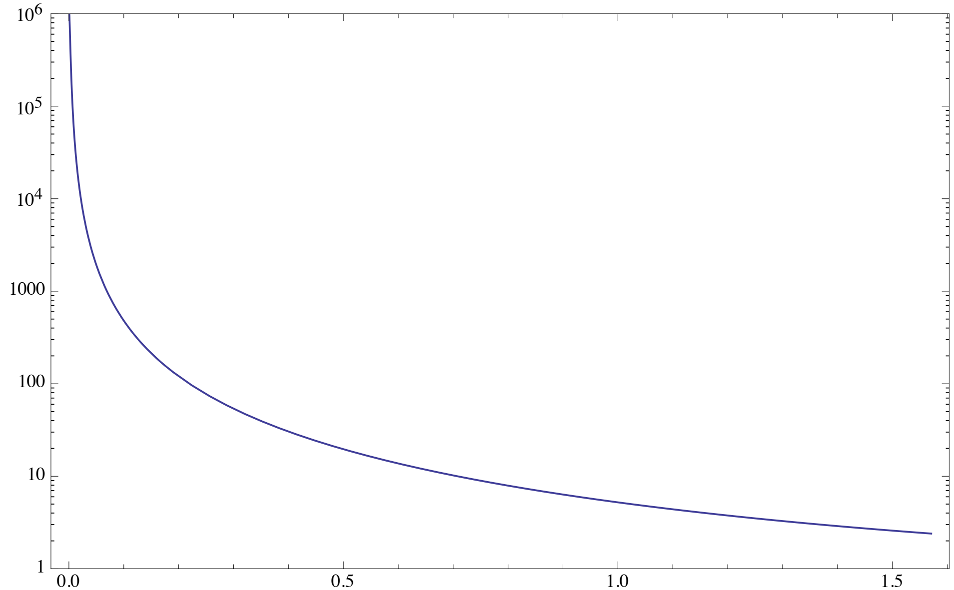

ϑ

Recap (exact analytical formula, example 250 MeV electrons against $h\nu_L$=1.2 eV photons)

$\gamma = 490.$ $\Delta = 0.0046$ $\gamma_{cm} = 488.88$ $E_{ph}(MeV) = \frac{1.1472}{2}\left[1 + \sqrt{1 - \frac{1+\Delta}{\gamma^2}}\cos\vartheta^*\right]$

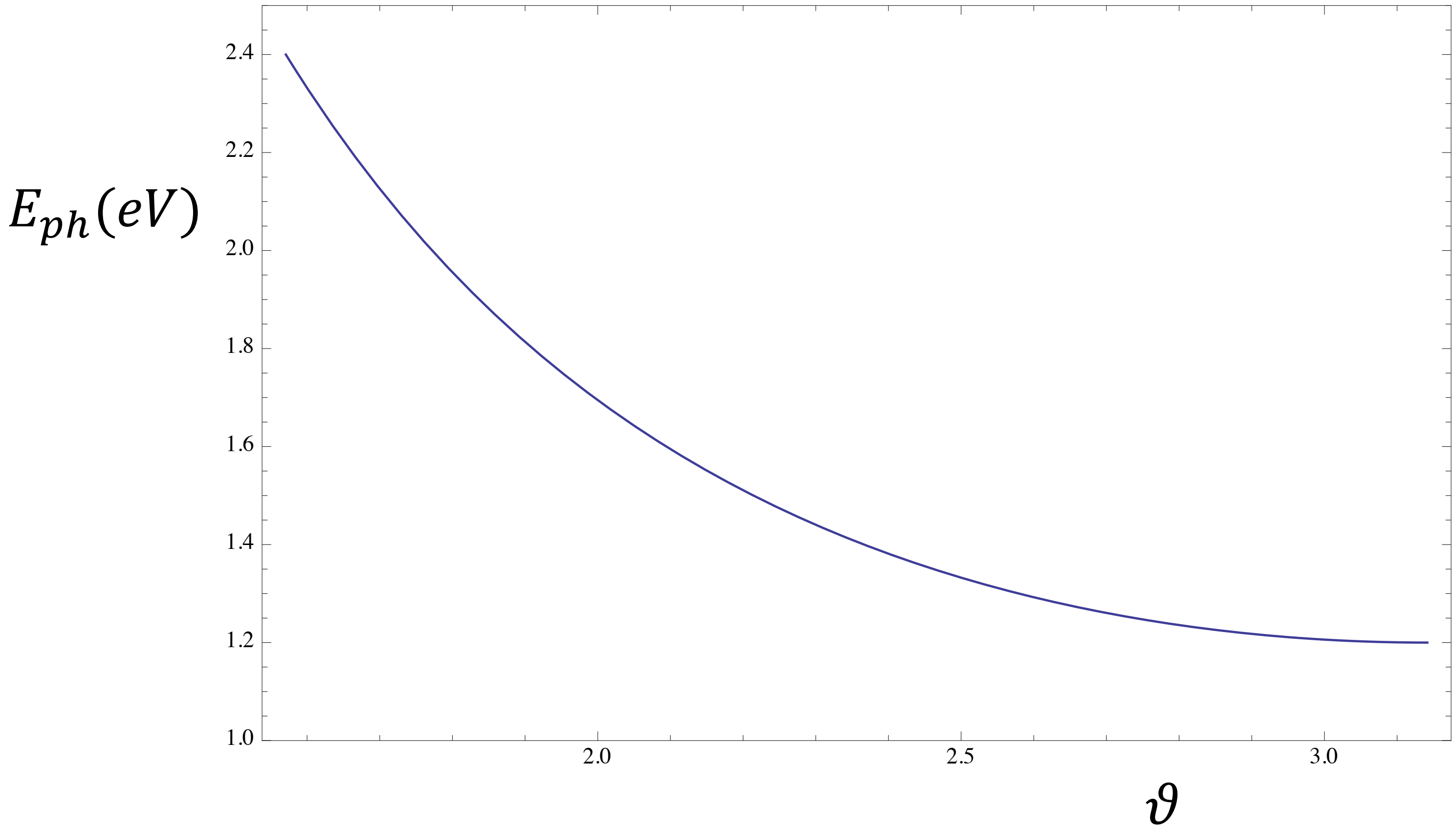

Single electron-photon spectra

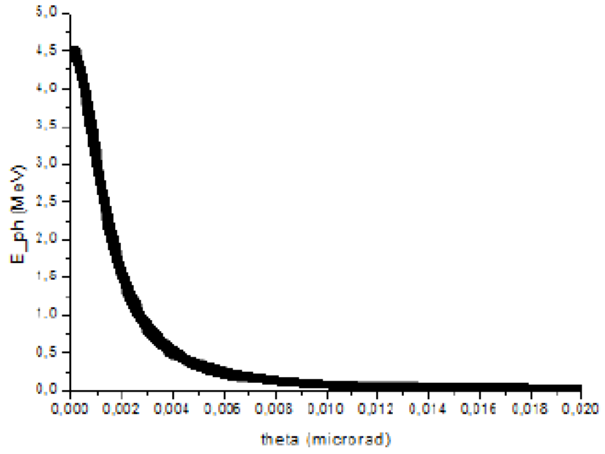

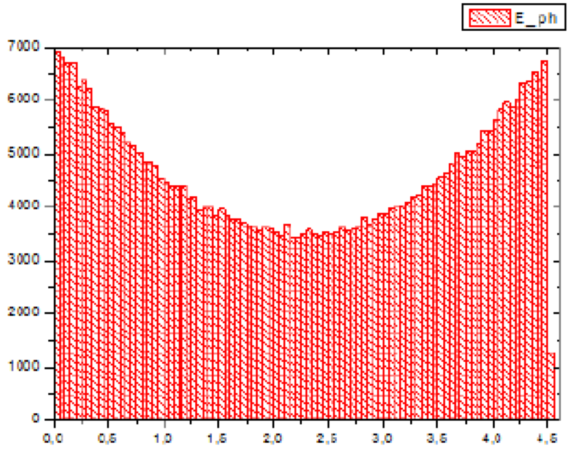

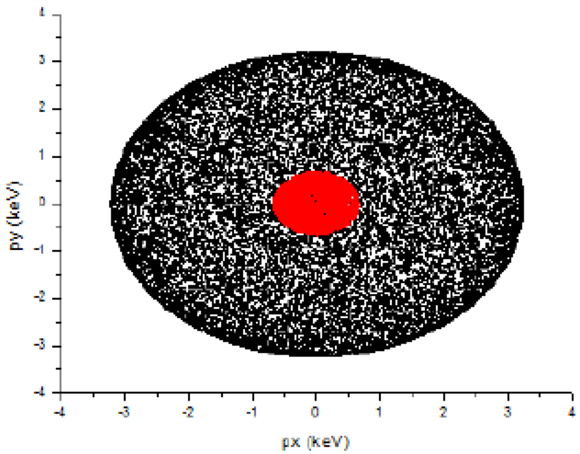

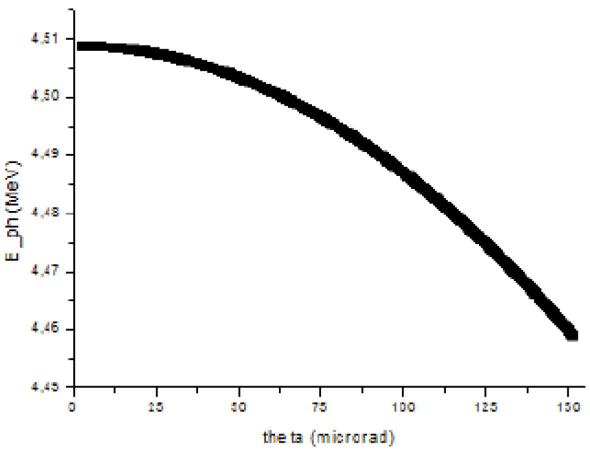

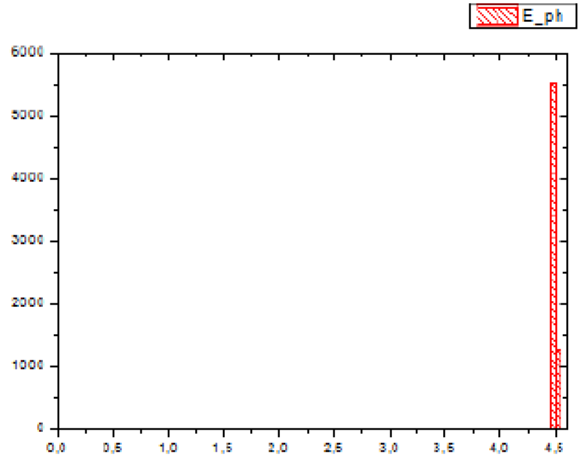

Energia elettroni 360 MeV
Energia fotoni 2.3 eV
Angolo alpha 0 gradi
Theta collimazione 151 microrad
Banda relativa 0.003

$$\gamma\vartheta = 0.11$$

What happens when we scatter beams of electron against beams of photons?

Electron beam emittance and energy spread spread out the c.m. propagation so to generate a "beam" of c.m. ref. frames

If the electron has not null transverse components respect to the z axis, the Lorentz transformations in a generic direction have to be used:

$$\begin{cases} E_{ph} = p^*_{ph}\gamma_{cm} + p^*_{phx}\gamma_{cm}\beta_x + p^*_{phy}\gamma_{cm}\beta_y + p^*_{phz}\gamma_{cm}\beta_z \\ p_{phx} = p^*_{ph}\gamma_{cm}\beta_x + p^*_{phx}\dfrac{1+\gamma^2_{cm}\beta^2_x}{1+\gamma_{cm}} + p^*_{phy}\dfrac{\gamma^2_{cm}\beta_x\beta_y}{1+\gamma_{cm}} + p^*_{phz}\dfrac{\gamma^2_{cm}\beta_x\beta_z}{1+\gamma_{cm}} \\ p_{phy} = p^*_{ph}\gamma_{cm}\beta_y + p^*_{phx}\dfrac{\gamma^2_{cm}\beta_x\beta_y}{1+\gamma_{cm}} + p^*_{phy}\dfrac{1+\gamma^2_{cm}\beta^2_y}{1+\gamma_{cm}} + p^*_{phz}\dfrac{\gamma^2_{cm}\beta_y\beta_z}{1+\gamma_{cm}} \\ p_{phz} = p^*_{ph}\gamma_{cm}\beta_z + p^*_{phx}\dfrac{\gamma^2_{cm}\beta_x\beta_z}{1+\gamma_{cm}} + p^*_{phy}\dfrac{\gamma^2_{cm}\beta_y\beta_z}{1+\gamma_{cm}} + p^*_{phz}\dfrac{1+\gamma^2_{cm}\beta^2_z}{1+\gamma_{cm}} \end{cases}$$

See C. Curatolo, PhD Thesis, Univ. of Milan, 2016 (and references therein)

Electron-photon Collider Spectra

The transverse momentum of the incoming electron beam is linked to the emittance by the relation

$$\sigma_{p_x} = \frac{\epsilon_{n,x} M_e}{\sigma_x}$$

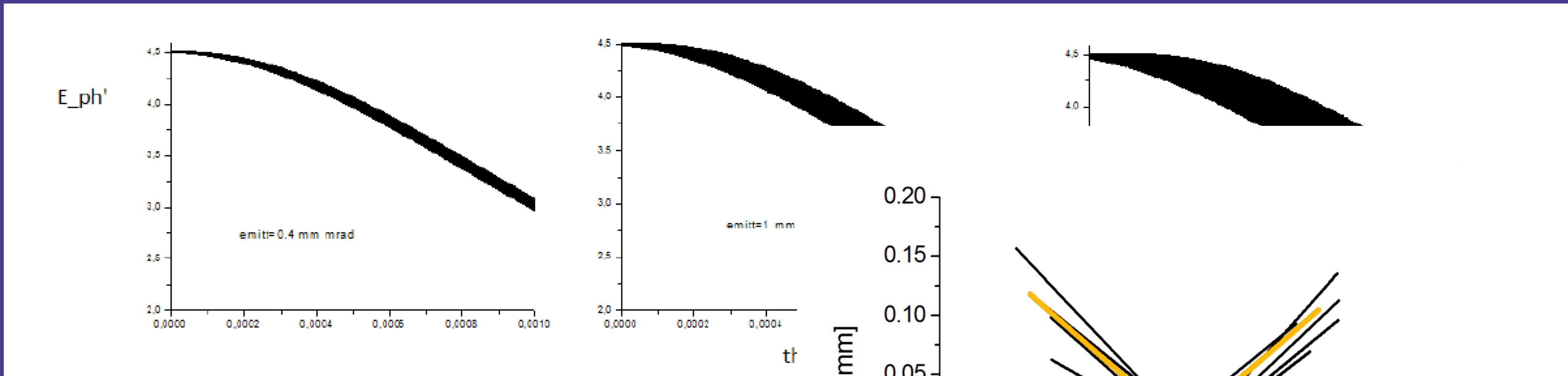

FIGURA : Energy of the emitted photons as a fun different values of the electron beam emittance.

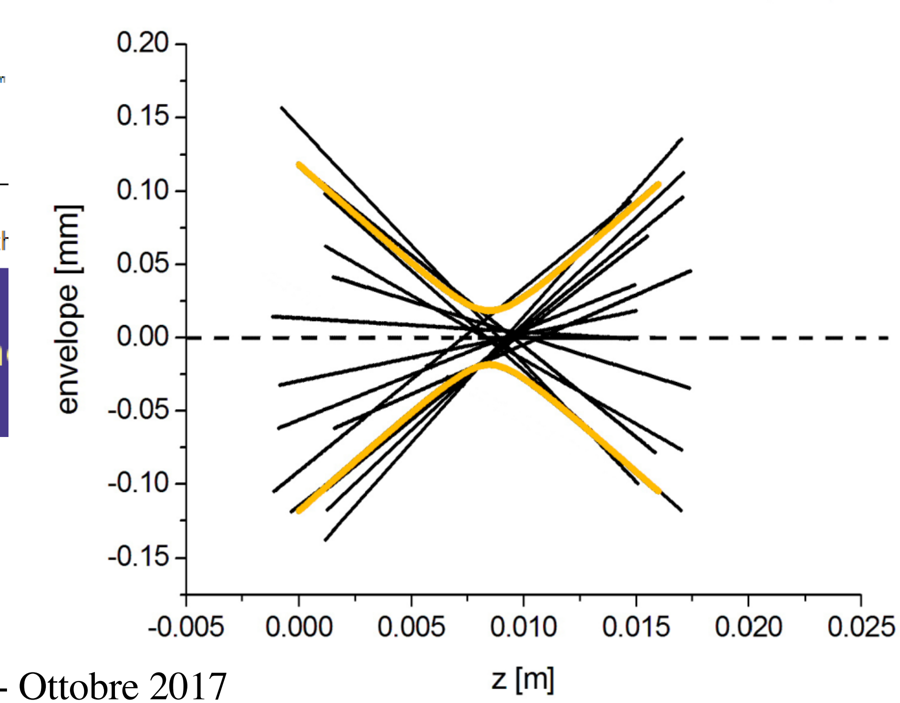

$$\nu_X = \frac{4\gamma^2\nu_L}{1+\Delta}\left(1-\frac{\gamma^2\vartheta^2}{1+\Delta}\right) + \textit{collective effects} \Rightarrow$$

$$\nu_X = \frac{4\gamma^2\nu_L}{1+\Delta}\left(1-\frac{\gamma^2\vartheta^2}{1+\Delta}-\frac{a_0^2}{2}\right)$$

$$\Delta = \frac{4\gamma h\nu_L}{m_e c^2}$$

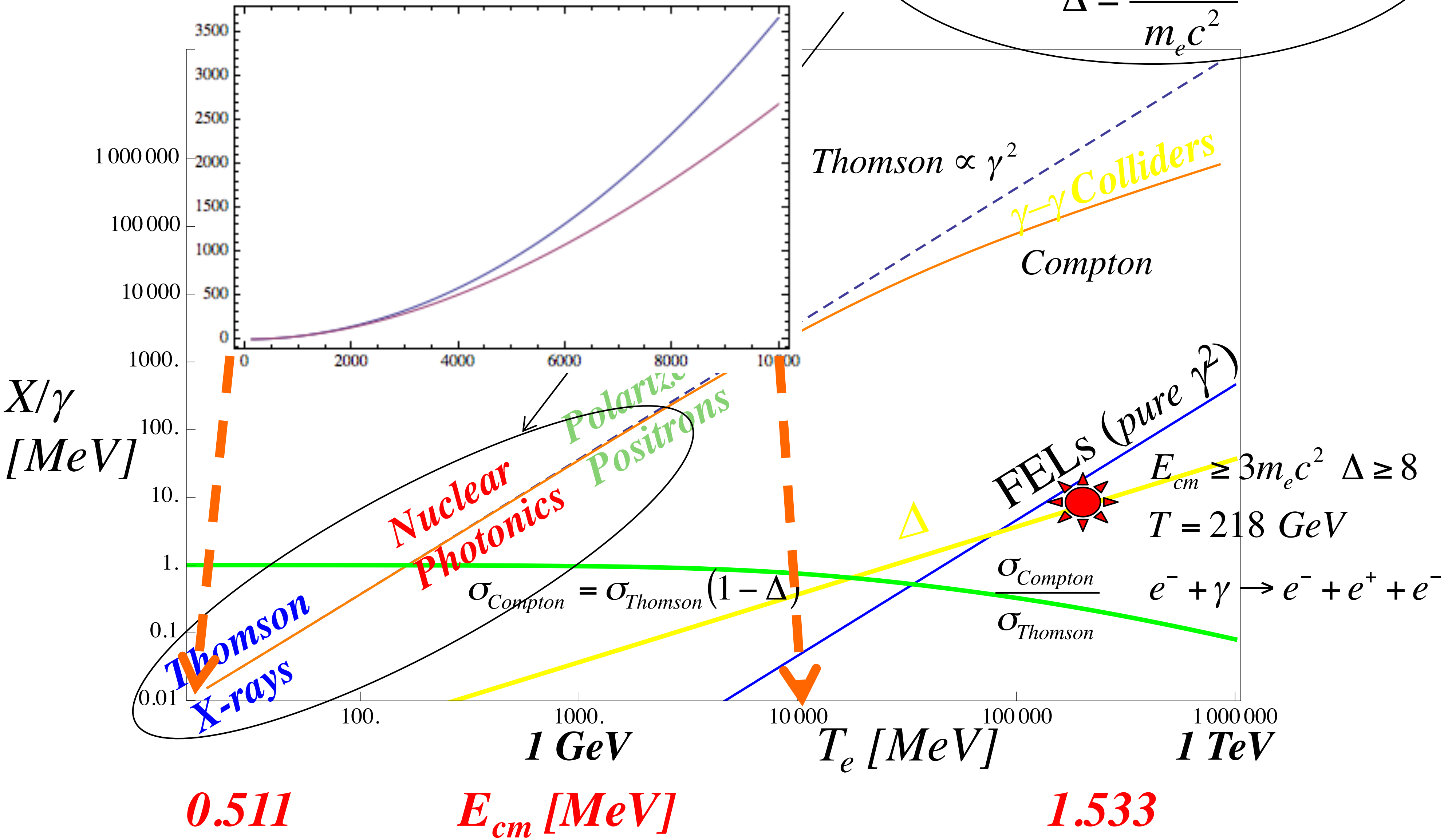

Recalling Compton differential cross-section

$$\frac{d\sigma}{d\theta' d\phi'} = r_e^2 \left(\frac{2}{2+\Delta(1-cos\theta')}\right)^2 \left(\frac{1+cos^2\theta'}{2}\right) \cdot \tag{2.11}$$

$$\left(1 + \frac{\Delta^2(1-cos\theta')^2}{2(1+cos^2\theta')(2+\Delta(1-cos\theta'))}\right) sin\theta'$$

total cross-section can be obtained from eq. (2.11) by integrating over θ' and ϕ'

$$\sigma_{tot} = 2\pi r_e^2 \frac{1}{\Delta}\left[\left(1-\frac{4}{\Delta}-\frac{8}{\Delta^2}\right)\log(1+\Delta)+\frac{1}{2}+\frac{8}{\Delta}-\frac{1}{2(1+\Delta)^2}\right] \tag{2.14}$$

and

$$\begin{cases} \lim_{\Delta\to 0}\sigma_{tot} = \frac{8\pi r_e^2}{3}(1-\Delta) = \sigma_T(1-\Delta) & \text{non-relativistic case} \quad \sigma_T = 670\ mbarn \\ \lim_{\Delta\to\infty}\sigma_{tot} = \frac{2\pi r_e^2}{\Delta}\left(\log\Delta + \frac{1}{2}\right) & \text{ultra-relativistic case.} \end{cases} \tag{2.15}$$

For example, the recoil parameter Δ associated with the head-on scattering of an electron at $E_e = 400$ MeV and a photon with $h\nu_0 = 2.4047$ eV (these energies are in LAB) is given by

$$\Delta = \frac{2h\nu_0'}{mc^2} = \frac{4\gamma_i h\nu_0}{mc^2} = 7.37 \cdot 10^{-3}$$

$$E_{cm} = m_e c^2 \sqrt{1+\Delta}$$

$$\Delta = \left(E_{cm} / m_e c^2\right)^2 - 1$$

The Physics of Compton Inverse Scattering is quite straightforward

Quantum model

What are we missing by adopting the Quantum QED treatment of Compton back-scattering?

We re-construct the beam-beam back-scattering from single electron-photon scattering events by summing over the phase space density distributions of electrons and photons (treated incoherently!)

$$mc^2(\gamma-\gamma_0)=-h(\nu-\nu_L)$$

The coherent aspect (phase) of the laser e.m. field is lost… Multi-photon absorption/scattering phenomena are not taken into account (dressed electron model in e.m. field)

Linear QED treatment is good for low intensity (a_0<1) laser pulses

3

Thomson cross-section c) Inelastic, Compton, recoil dominated

Courtesy V. Petrillo – Univ. of Milan

We ... ollider,
tha ... nosity,

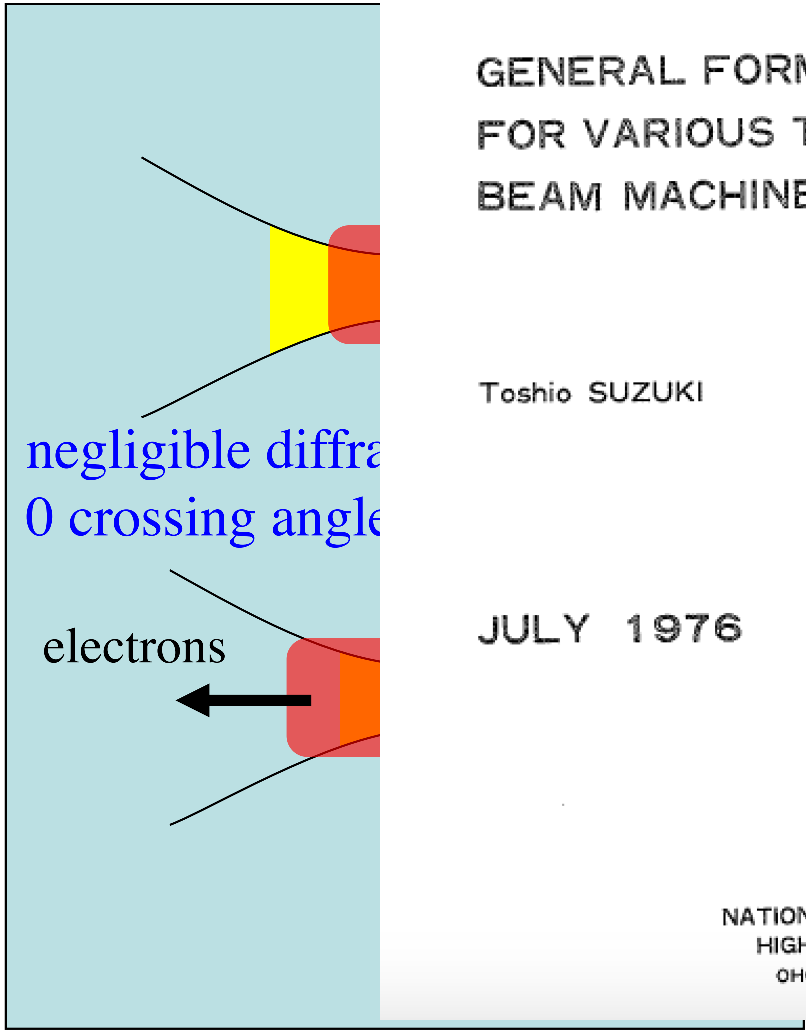

KEK-76-3

GENERAL FORMULAE OF LUMINOSITY FOR VARIOUS TYPES OF COLLIDING BEAM MACHINES

Toshio SUZUKI

JULY 1976

NATIONAL LABORATORY FOR HIGH ENERGY PHYSICS
OHO-MACHI, TSUKUBA-GUN
IBARAKI, JAPAN

$...7 \cdot 10^{-24}\, cm^2 = 0.67\ barn$

$= \mathbf{L}\sigma_T$ $\quad \sigma_T = \dfrac{8\pi}{3} r_e^2$

HEP collisions

ectrons

$= \dfrac{N_L N_{e-}}{4\pi\sigma_x^2} f$

$L_S \equiv \dfrac{L}{\Delta\nu_\gamma}$

$...) = 2.5 \cdot 10^{35}\, cm^{-2} s^{-1}$

cfr. LHC 10..., Hi-Lumi LHC 10^{35}

Matching Laser Pulse Length and Focus Size

Laser pulse length matched to focus size (Rayleigh length).

Laser pulse too long for small focus size.

Laser pulse must be short compared to Rayleigh length so that whole pulse is focused simultaneously.

Laser may be shorter than Rayleigh length, but less than 0.5 ps is not practical, and could lead to non-linear effects not included in our spectral model.

courtesy of D. Moncton

$$L = \frac{N_{el} N_{las}}{2\pi\left(\sigma_0^2 + w_0^2/4\right)} f$$

Electron Bunch Length Matched to Rayleigh Length

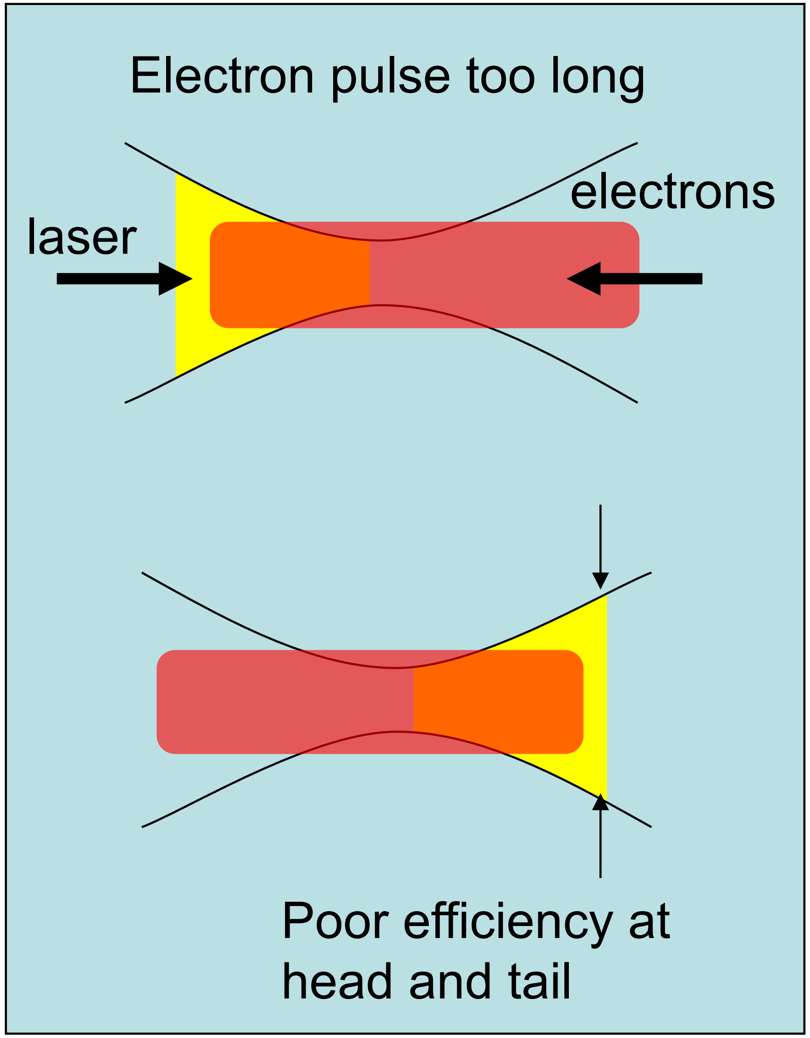

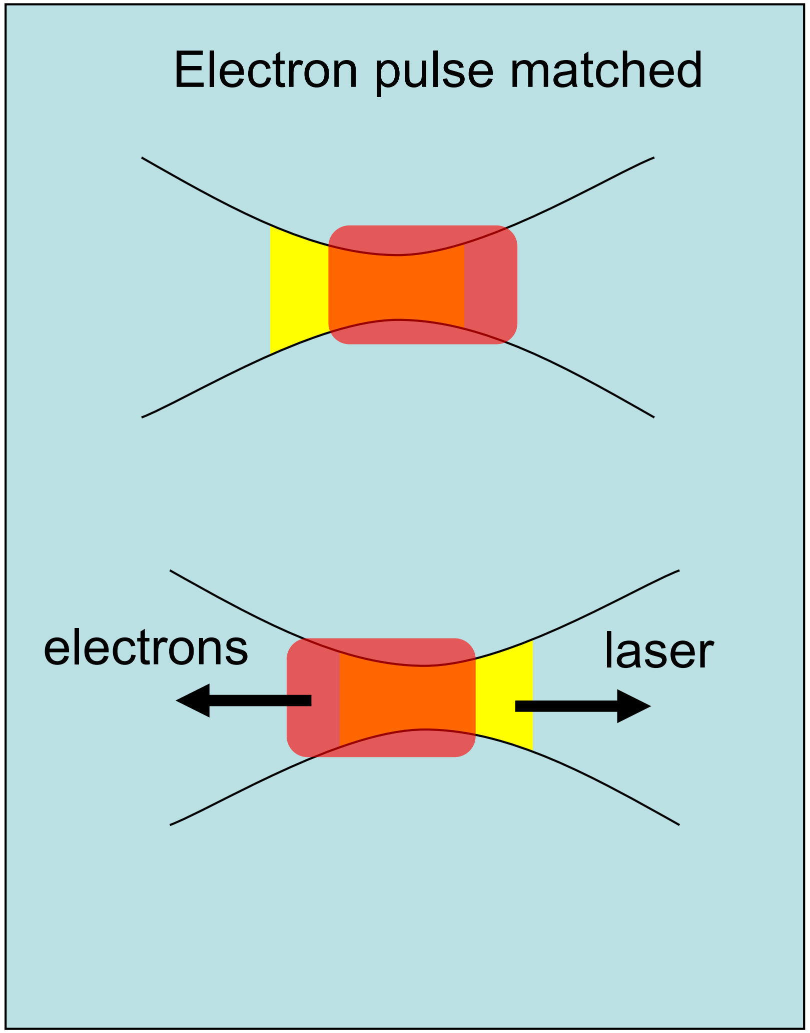

courtesy of
D. Moncton

TEM$_{00}$ Gaussian Laser mode
(circular polarization M^2=1 diffraction limited)

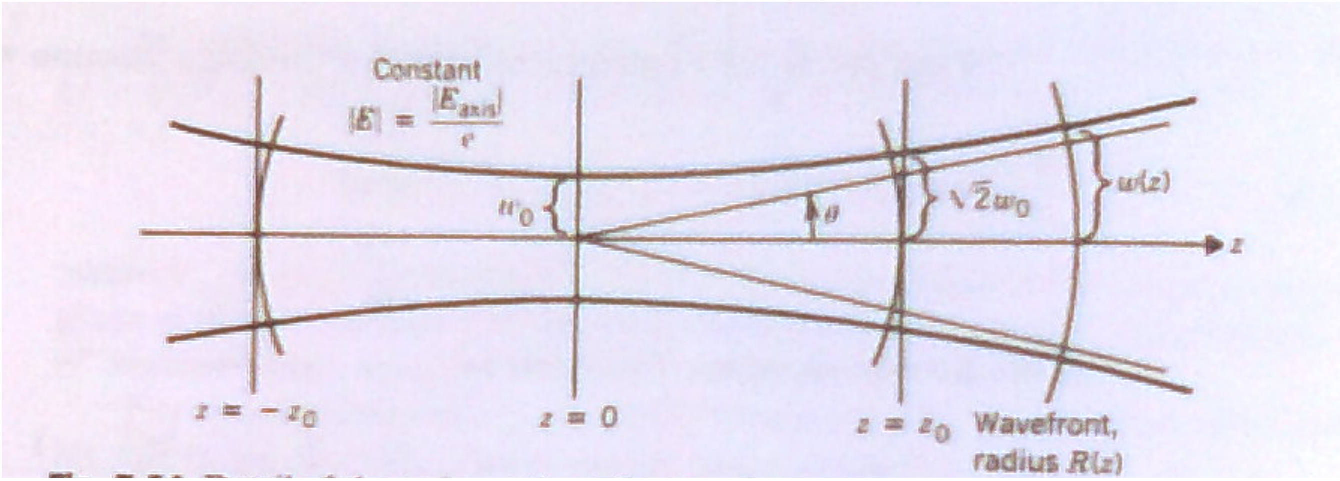

$$E_0(x,y,z,t) = A_0 e^{i\omega t} e^{-ikz} \frac{Z_0}{Z_0 - iz} \exp\left[-\frac{k\left(x^2 + y^2\right)}{2} \frac{1}{Z_0 - iz} \right] \quad k = 2\pi/\lambda$$

$$\left|E_0(x,y,z,t)\right| = E_0 \frac{w_0}{w} e^{-\frac{x^2+y^2}{w^2}}$$

$$w = w_0 \sqrt{1 + \frac{z^2}{Z_0^2}} \qquad Z_0 = \frac{\pi w_0^2}{\lambda} \qquad \vartheta = \frac{w_0}{Z_0} = \frac{\lambda}{\pi w_0}$$

$$I \propto \left|E_0(x,y,z,t)\right|^2$$

LASER

PARTICLE BEAM

$$Z_0 = \frac{4\pi\left(\frac{w_0}{2}\right)^2}{\lambda} \quad \Longleftrightarrow \quad \beta^* = \frac{\sigma_0^2}{\varepsilon_n/\gamma}$$

$$\frac{w}{2} = \frac{w_0}{2}\sqrt{1+\frac{z^2}{Z_0^2}} \quad \Longleftrightarrow \quad \sigma(z) = \sigma_0\sqrt{1+\frac{z^2}{\beta^{*2}}}$$

$$\Downarrow$$

$$\frac{\lambda}{4\pi} = \frac{\varepsilon_n}{\gamma} \quad and \quad w_0 = 2\sigma_0$$

$$\varepsilon_n \le \frac{\lambda_{FEL}\gamma}{4\pi}$$

$$w(z) = 2\sigma(z) \quad and \quad \vartheta(z) = 2\sigma'(z)$$

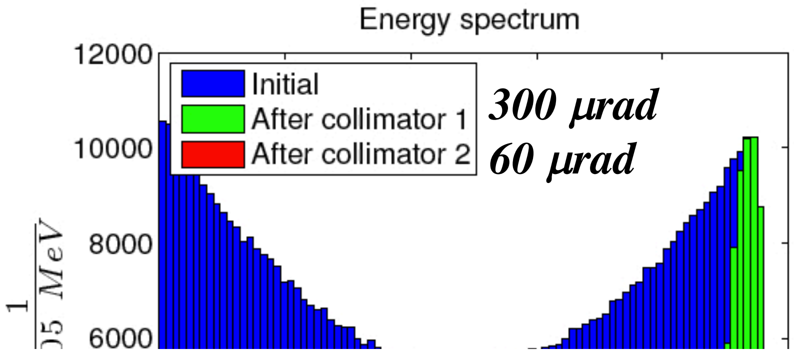

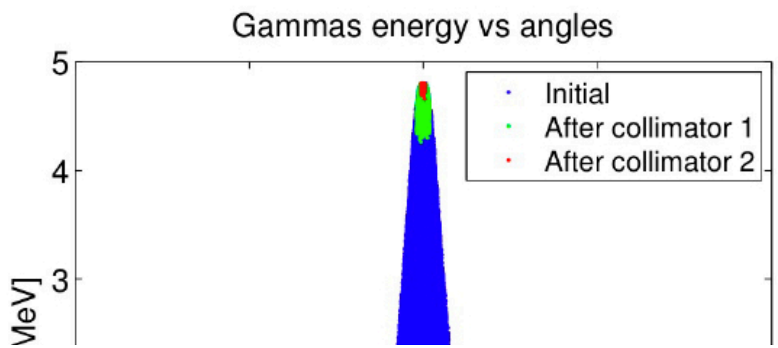

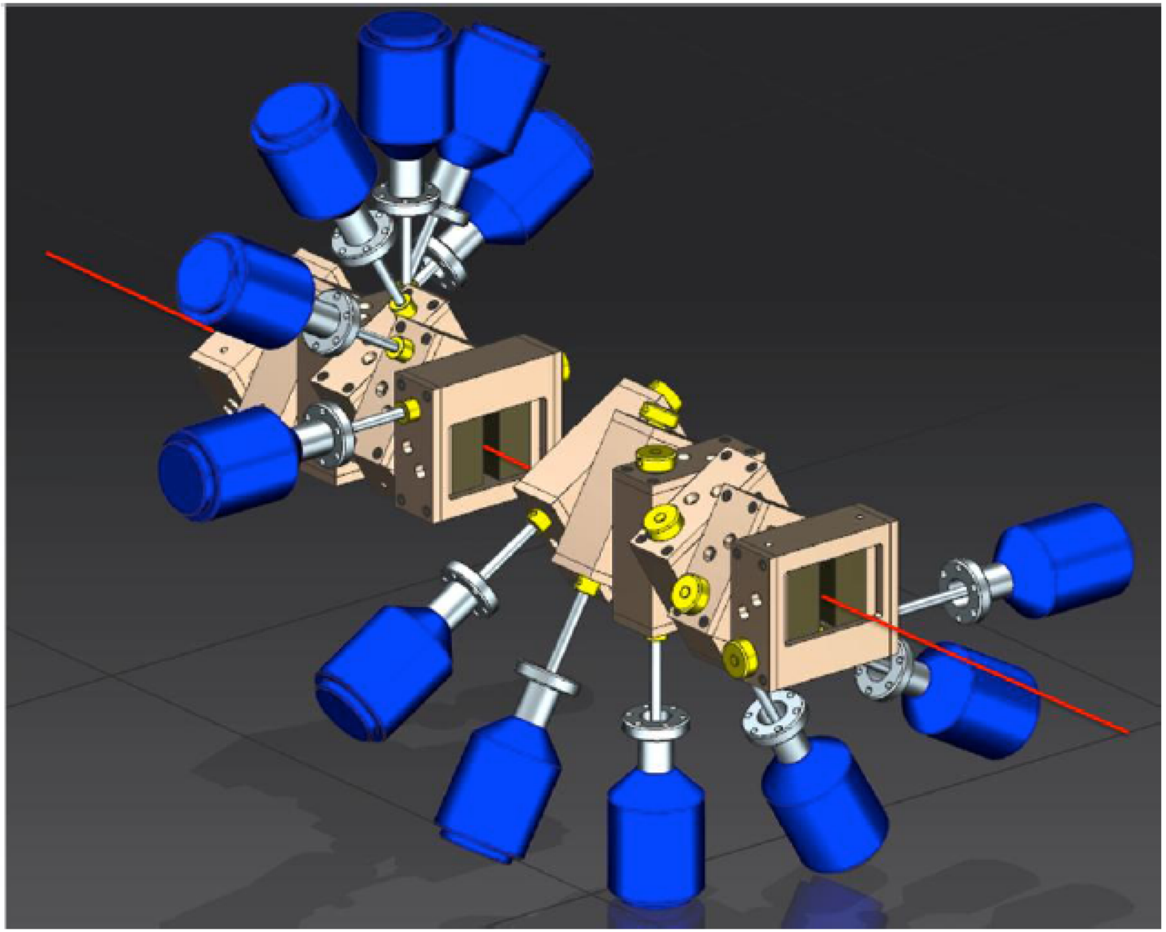

Fig. 184. Drawing of the configuration of low energy collimator made up of 12 tungsten adjustable slits with a relative 30° rotation each

Courtesy M. Gambaccini

Bandwidth due to collection angle, laser and electron beam phase space distribution

$$\nu_X = \frac{4\gamma^2\nu_L}{1+\Delta}\left(1-\frac{\gamma^2\vartheta^2}{1+\Delta}-\frac{a_0^2}{2}\right) \qquad \Delta = 4\gamma h\nu/mc^2$$

$$\left.\frac{\delta\nu_X}{\nu_X}\right|_{\nu_L} = \frac{\partial\nu_X}{\partial\nu_L}\frac{\nu_L}{\nu_X}\frac{\delta\nu_L}{\nu_L} \; ; \; \left.\frac{\delta\nu_X}{\nu_X}\right|_{\gamma} = \frac{\partial\nu_X}{\partial\gamma}\frac{\gamma}{\nu_X}\frac{\delta\gamma}{\gamma} \; ; \; \left.\frac{\delta\nu_X}{\nu_X}\right|_{\vartheta} = \frac{1}{2}\frac{\partial^2\nu_X}{\partial\vartheta^2}\frac{\delta\vartheta^2}{\nu_X} \quad etc$$

angular spread due to scattering angle and angular spread due to single electron incoming angle (emittance) are treated symmetrically

$$\left\langle\gamma^2\theta^2\right\rangle \cong \left\langle\gamma^2\vartheta^2\right\rangle + \left\langle\gamma^2\vartheta_e^2\right\rangle \cong \gamma^2\vartheta_{rms}^2 + (\sigma_{p\perp}/mc)^2 \cong \gamma^2\vartheta_{rms}^2 + 2(\varepsilon_n/\sigma_x)^2$$

$$\frac{\delta\nu_X}{\nu_X} = \sqrt{\left(\left.\frac{\delta\nu_X}{\nu_X}\right|_{\nu_L}\right)^2 + \left(\left.\frac{\delta\nu_X}{\nu_X}\right|_{\gamma}\right)^2 + \left(\left.\frac{\delta\nu_X}{\nu_X}\right|_{\vartheta}\right)^2 + \ldots\ldots}$$

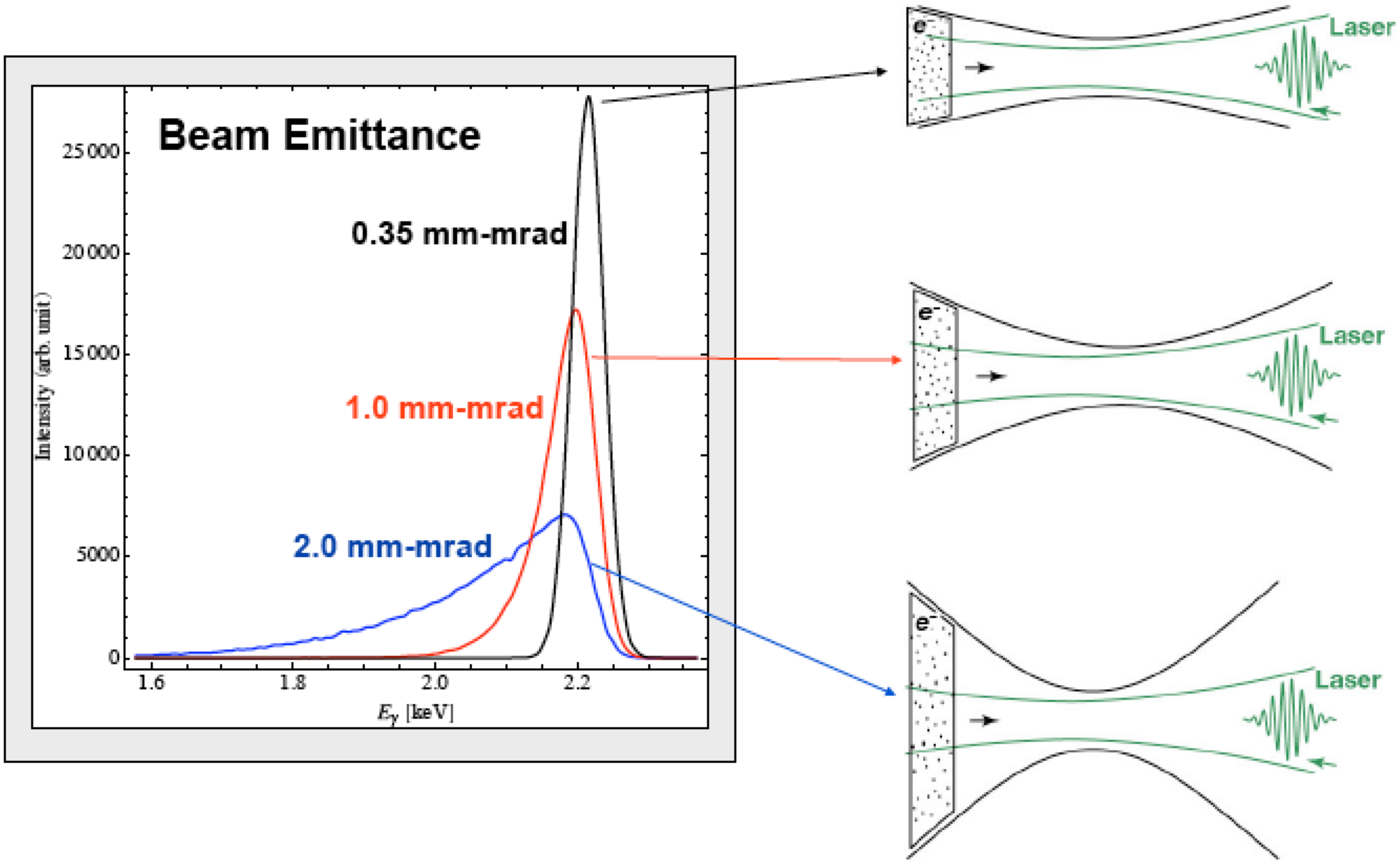

Courtesy C. Barty - LLNL

$$\Delta\theta \approx \frac{1}{\gamma} \; ; \; \Delta\nu_\gamma \approx 50\%$$

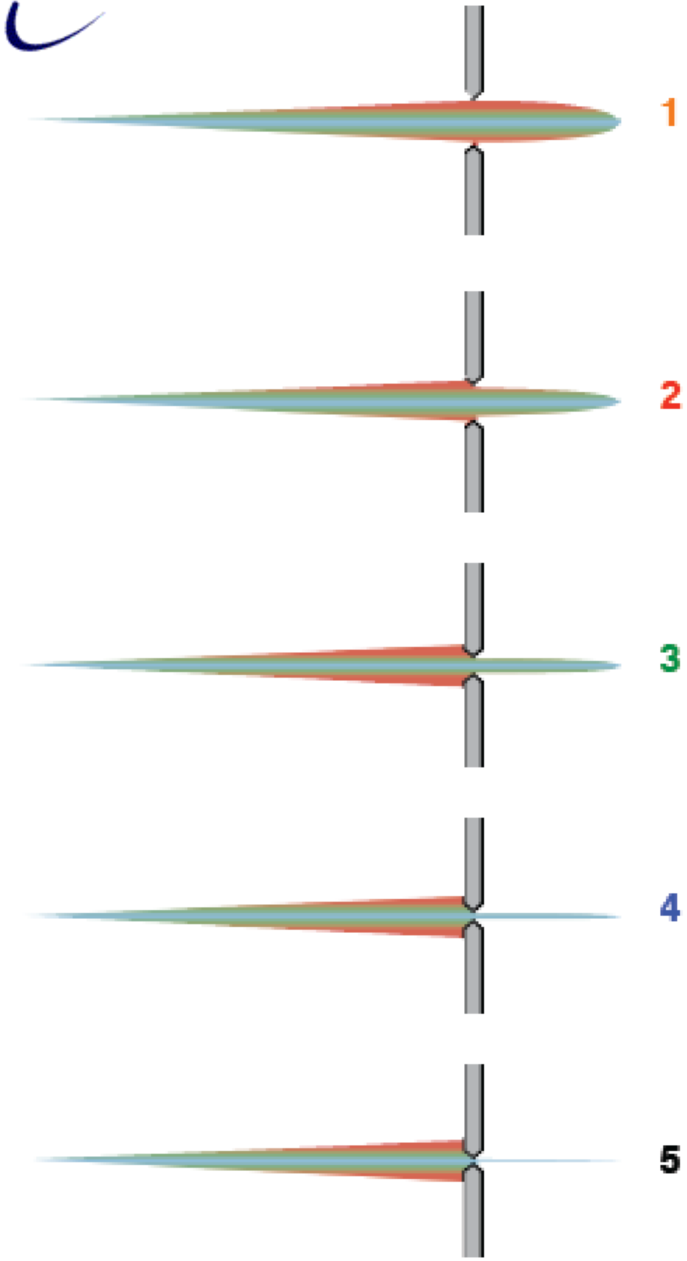

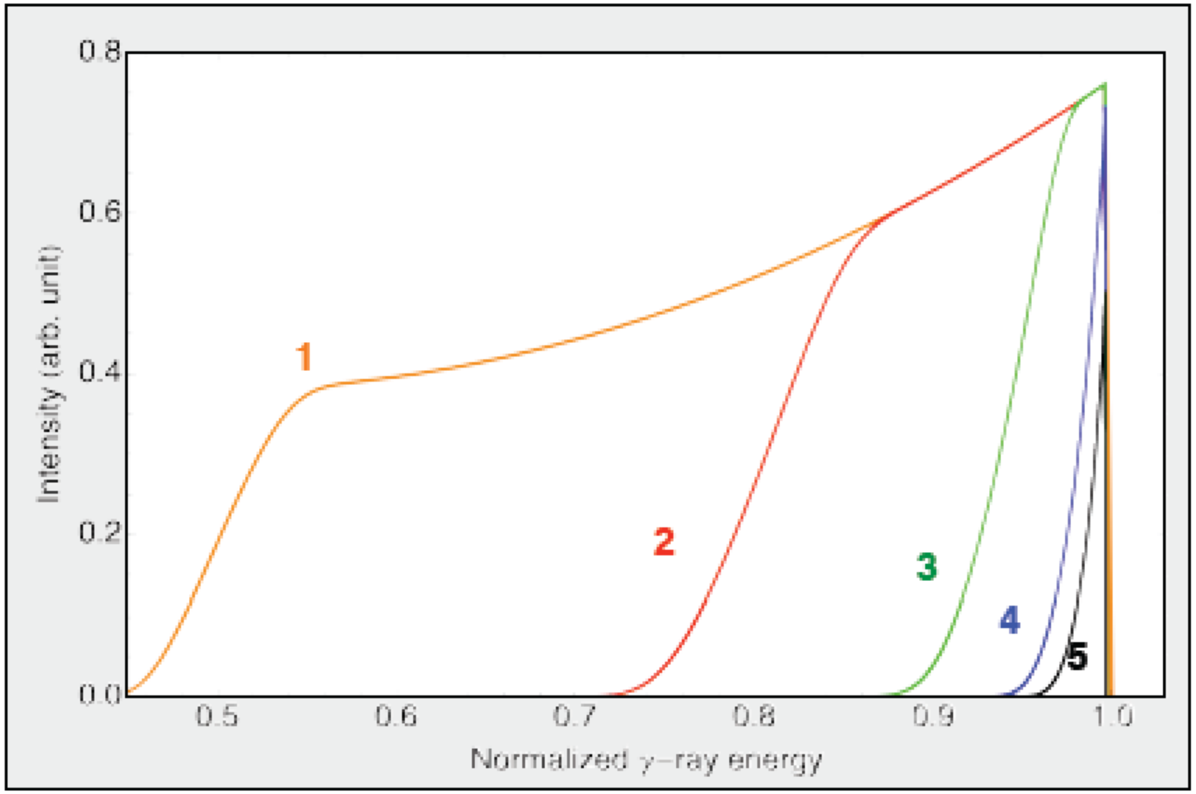

$$\Delta\theta \approx \sigma_{x'} = \frac{\varepsilon_n}{\gamma\sigma_x} \; ; \; \Delta\nu_\gamma \approx \left(\frac{\varepsilon_n^2}{\sigma_x^2}\right)$$

Courtesy C. Barty - LLNL

Petrillo-Serafini Formula* for ICS photon beam bandwidth

collimation

electron beam phase space

$$\frac{\delta\nu_\gamma}{\nu_\gamma} \cong \sqrt{\begin{array}{l}\left[\left(\frac{\gamma^2\vartheta^2/\sqrt{12}}{1+\gamma^2\vartheta^2/2}+\frac{2\varepsilon_n^2/\sigma_x^2}{1+\sqrt{12}\,\varepsilon_n^2/\sigma_x^2}\right)\frac{1}{1+\Delta}\right]^2+\left(\frac{2+\Delta}{1+\Delta}\frac{\delta\gamma}{\gamma}\right)^2+\\ +\left(\frac{1}{1+\Delta}\frac{\delta\nu}{\nu}\right)^2+\left(\frac{M^2\lambda_L}{2\pi w_0}\right)^4+\left(\frac{a_0^2/3}{1+a_0^2/2}\right)^2\end{array}}$$

laser beam phase space

laser collective effects

* *unpublished in this complete form accounting for recoil effects*

Analytical description of photon beam phase spaces in Inverse Compton Scattering sources

C. Curatolo,[1] I. Drebot,[1] V. Petrillo,[1,2] and L. Serafini[1]

[1] *INFN-Milan, via Celoria 16, 20133 Milano, Italy*
[2] *Università degli Studi di Milano, via Celoria 16, 20133 Milano, Italy*

(Dated: 22 May 2017)

We revisit the description of inverse Compton scattering sources and the photon beams generated therein, emphasizing the behavior of their phase space density distributions and how they depend upon those of the two colliding beams of electrons and photons. Main objective is to provide practical formulas for bandwidth, spectral density, brilliance, which are valid in general for any value of the recoil factor, i.e. both in the Thomson regime of negligible electron recoil, and in the deep Compton recoil dominated region, which is of interest for gamma-gamma colliders and Compton Sources for the production of multi-GeV photon beams. We adopt a description based on the center of mass reference system of the electron-photon collision, in order to underline the role of the electron recoil and how it controls the relativistic Doppler/boost effect in various regimes. Using the center of mass reference frame greatly simplifies the treatment, allowing to derive simple formulas expressed in terms of rms momenta of the two colliding beams (emittance, energy spread, etc.) and the collimation angle in the laboratory system. Comparisons with Monte Carlo simulations of inverse Compton scattering in various scenarios are presented, showing very good agreement with the analytical formulas: in particular we find that the bandwidth dependence on the electron beam emittance, of paramount importance in Thomson regime, as it limits the amount of focusing imparted to the electron beam, becomes much less sensitive in deep Compton regime, allowing a stronger focusing of the electron beam to enhance luminosity without loss of mono-chromaticity. A similar effect occurs concerning the bandwidth dependence on the frequency spread of the incident photons: in deep recoil regime the bandwidth comes out to be much less dependent on the frequency spread. The set of formulas here derived are very helpful in designing inverse Compton sources in diverse regimes, giving a quite accurate first estimate in typical operational conditions for number of photons, bandwidth, spectral density and brilliance values - the typical figures of merit of such radiation sources.

I. INTRODUCTION

Inverse Compton Scattering sources (ICSs) are becoming increasingly attractive as radiation sources in photon energy regions either not covered by other high brilliance sources (FEL's, synchrotron light sources) or where compactness becomes an important figure of merit, like for advanced X-ray imaging applications to be implemented in university campus, hospitals, museums, etc., i.e. outside of research centers or large scale laboratories [1]. ICSs are becoming the γ-ray sources of reference in nuclear photonics, photo-nuclear [2, 3] and fundamental physics [4], thanks to superior performances in spectral densities achievable. Eventually they will be considered for very high energy photon generation (in the GeV to TeV range) since there are no other competing techniques at present, neither on the horizon, based on artificial tools at this high photon energy [5]. As a consequence, a flourishing of design activities is presently occurring in several laboratories [6–15] and companies [16–19], where ICSs are being conceived, designed and built to enable several domains of applications, and ranging from a few keV photon energy up to GeV's and beyond. Designs of ICSs are carried out considering several diverse schemes, ranging from high gradient room temperature pulsed RF Linacs [3, 20, 21] to CW ERL Super-conducting Linacs [22, 23] or storage rings [2, 24–27], as far as the electron beam generation is concerned, and from single pulse J-class amplified laser systems running at 100 Hz to optical cavities (e.g. Fabry-Perot) running at 100 MHz acting as photon storage rings for the optical photon beams, not to mention schemes based on FEL's to provide the colliding photon beam [22, 28, 29].

In order to assess the performances of a specific ICSs under design, detailed simulations of the electron-photon beam collision are typically carried out using Monte Carlo codes [30–32] able to model the linear and nonlinear electron-photon quantum interaction leading to Compton back-scattering events, taking into account in a complete fashion the space-time propagation of the two colliding beams through the interaction point region, including possible multiple scattering events occurring during the overlap of the two pulses. Only in case of negligible electron recoil, i.e. in the so called Thomson regime typical of low energy X-ray ICSs, classical electromagnetic numerical codes (e.g. TSST [33]), modelling the equivalent undulator radiation emitted by electrons wiggling in the electromagnetic field of the incoming laser pulse, allow to analyze particular situations such as the use of chirped [34], tilted [35] and twisted [36] lasers.

In the recent past some efforts have been developed to carry out analytical treatments of the beam-beam collision physics, embedding the single electron-photon collision from a quantum point of view within a rms distribution of the scattered photon beam [27, 37–43], or,

$\Delta E_{ph}/E_{ph}$ from the laser and the electron beam parameters, which are: γ the Lorentz factor, $\Delta\gamma/\gamma$ the relative energy spread, ϵ_n the normalized emittance and σ_x the rms spot size at interaction point of the electron beam, $\Delta E_L/E_L$ the laser bandwidth, λ_0 the laser wavelength, w_0 the laser focal spot size, M^2 the beam quality factor and the laser parameter a_0. We improve and generalize the formula described in Refs. [3, 36, 41, 45] by taking into to account the effect given by the electron recoil on the emitted radiation: the use of γ_{CM} instead then γ extends the validity of the equation to any recoil regime.
As in the above mentioned references, we consider a Gaussian phase space distribution for the electron beam and for the laser pulse while the resulting shape of the photon spectrum is determined by the energy-angle correlation described by Eqs. (6) and (11).
We define the acceptance angle as

$$\Psi = \gamma_{CM}\theta_{max} \tag{12}$$

and the term

$$\overline{P} = \gamma_{CM}\frac{\sqrt{2}\epsilon_x}{\sigma_x} = \frac{\sqrt{2}\epsilon_n}{\sigma_x\sqrt{1+X}} \tag{13}$$

where $\sqrt{2}\epsilon_n/\sigma_x$ represents the normalized rms transverse momentum of the electron beam which coincides with $\overline{P}$ at low recoil. Instead $\overline{P}$ is reduced by a factor $\gamma_{CM}/\gamma \simeq \sqrt{X}$ when the recoil is large. The relative bandwidth of the emitted radiation is given by

$$\frac{\Delta E_{ph}}{E_{ph}} \simeq \sqrt{\left[\frac{\Psi^2/\sqrt{12}}{1+\Psi^2} + \frac{\overline{P}^2}{1+\sqrt{12}\,\overline{P}^2}\right]^2 + \left[\left(\frac{2+X}{1+X}\right)\frac{\Delta\gamma}{\gamma}\right]^2 + \left(\frac{1}{1+X}\frac{\Delta E_L}{E_L}\right)^2 + \left(\frac{M^2\lambda_0}{2\pi w_0}\right)^4 + \left(\frac{a_0^2/3}{1+a_0^2/2}\right)^2} \tag{14}$$

length.
We note that Eq. (14) is based on a fourth order expansion in the acceptence angle Ψ: this approach limits the validity of the formula to angles $\Psi < 1$.
The number of scattered photons per second is given by

$$\mathcal{N} = \mathcal{L}\sigma = \frac{N_e N_L r}{2\pi\,(\sigma_x^2 + \sigma_L^2)}\,\sigma \tag{16}$$

where $\mathcal{L}$ is the luminosity,

$$\sigma = \frac{2\pi r_e^2}{X}\left[\frac{1}{2} + \frac{8}{X} - \frac{1}{2(1+X)^2} + \left(1 - \frac{4}{X} - \frac{8}{X^2}\right)\log(1+X)\right] \tag{17}$$

is the total unpolarized Compton cross section [49], N_e, N_L are the number of incoming electrons and photons, r is the repetition rate of the collisions, and σ_x, $\sigma_L = w_0/2$ are the rms spot size radius at the interaction point of the electron and photon beams respectively. The value of σ varies between the classical limit $X \to 0$ and the ultra-relativistic limit $X \to \infty$ as presented in Eq. (18) where $\sigma_T = 0.67$ barn represents the total Thomson cross section [50].

$$\mathcal{N} = 4.2 \cdot 10^8 \frac{\sigma\, U_L(J)\, Q(pC)\, r}{\sigma_T\, E_L(eV)\, (\sigma_x^2(\mu m) + \sigma_L^2(\mu m))}. \tag{19}$$

By using the Compton differential cross section [49] in the approximation $\Psi < 1$, we obtain the analytical expression to estimate $\mathcal{N}^\Psi$, the number of photons in acceptance angle Ψ, and the spectral density S:

$$\mathcal{N}^\Psi = 6.25 \cdot 10^8 \frac{U_L(J)\, Q(pC)\, r}{E_L(eV)\, (\sigma_x^2(\mu m) + \sigma_L^2(\mu m))} \cdot \frac{\left(1 + \sqrt[3]{X}\,\Psi^2/3\right)\Psi^2}{(1 + (1 + X/2)\Psi^2)\,(1 + \Psi^2)}, \tag{20}$$

$$S = \frac{\mathcal{N}^\Psi}{\sqrt{2\pi}\, 4\, E_L \gamma_{CM}^2\, \frac{\Delta E_{ph}}{E_{ph}}}. \tag{21}$$

The rms source spot size is

$$\sigma_s = \frac{\sigma_x\, \sigma_L}{\sqrt{\sigma_x^2 + \sigma_L^2}} \tag{22}$$

and the emittance of the emitted radiation is

$$\epsilon_\gamma = \sigma_s \frac{\theta_{max}}{\sqrt[4]{12}\,\sqrt[9]{1+X}}. \tag{23}$$

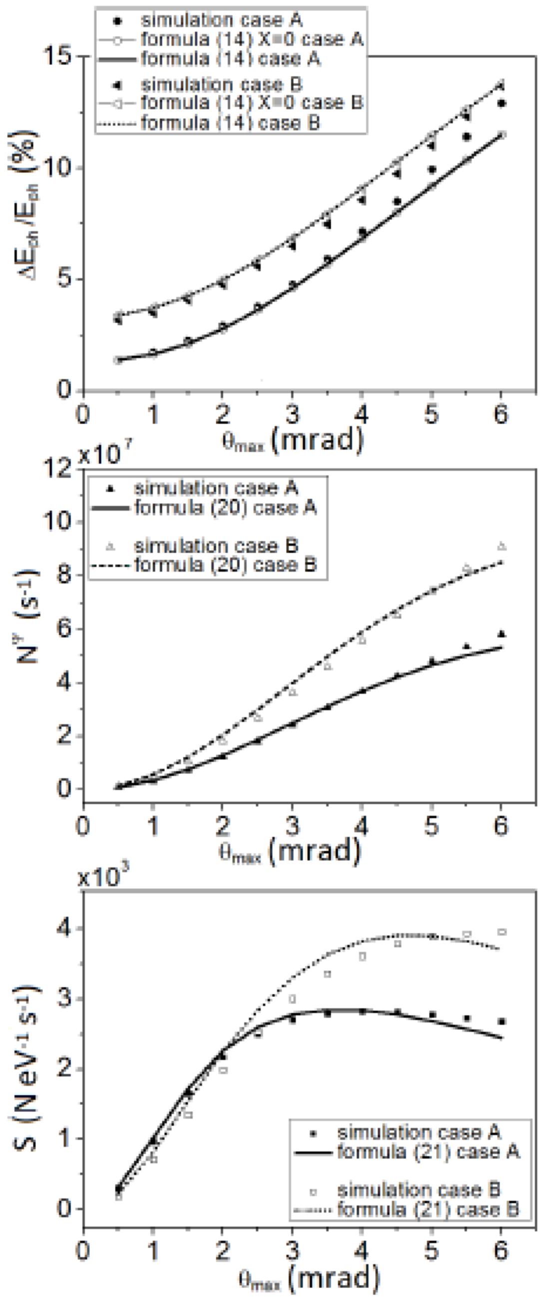

Figure 1. Cases A and B: $\Delta E_{ph}/E_{ph}$ (%) from CAIN simulation vs formula (14) without and with X correction, N^{Ψ} (s^{-1}) number of photons from CAIN simulation vs formula (20), S (N eV^{-1} s^{-1}) spectral density per shot ($r = 1$) from CAIN simulation vs formula (21) as a function of θ_{max} (mrad).

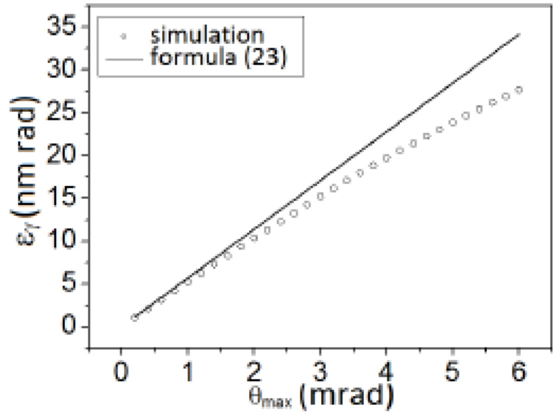

Figure 2. Case A: ϵ_{γ} (nm rad) value from CAIN simulation vs formula (23) as a function of θ_{max} (mrad).

Efficiency of Compton Sources in converting electron beam energy into radiation beam energy

energy of photons in collimation angle

number of photons per shot in collimation angle

electron beam total energy

$$\eta^{\Psi} \simeq \frac{4\gamma_{CM}^2 E_L}{N_e E_e}\frac{N^{\Psi}}{r} \simeq \frac{4\gamma_{CM}^2 E_L}{N_e E_e}\left(\frac{6.25\cdot 10^8 U_L(J)Q(pC)}{E_L(eV)\left(\sigma_x^2(\mu m)+\sigma_L^2(\mu m)\right)}\frac{\left(1+\sqrt[3]{X}\Psi^2/3\right)\Psi^2}{\left(1+(1+X/2)\Psi^2\right)\left(1+\Psi^2\right)}\right)$$

$$= \frac{7.82\cdot 10^{-4}\,\gamma U_L(J)}{\left(\sigma_x^2(\mu m)+\sigma_L^2(\mu m)\right)}\frac{\Psi^2}{(1+\Psi^2)^2} = \frac{3.38\cdot 10^{-5}\gamma\ a_0^2\ \sigma_t(ps)}{\lambda_0^2(\mu m)}\frac{\Psi^2}{(1+\Psi^2)^2}$$

$$\boxed{\begin{array}{l}\text{if } X \ll 1 \Rightarrow \\ \gamma_{CM} \simeq \gamma,\ \Psi \simeq \gamma\theta_{max}\end{array}}$$

$$\boxed{\begin{array}{l}\sigma_x = \sigma_L,\ w_0 = 2\sigma_L \\ a_0 = 6.8\,\frac{\lambda_0}{w_0}\sqrt{\frac{U_L(J)}{\sigma_t(ps)}}\end{array}}$$

Ex: TABLE I. Interaction parameters for STAR. $\sigma_L = 15\ \mu$m, $\sigma_t = 1$ ps and σ_{p_x} electron beam rms transverse momentum (keV).

Case	Q (nC)	E_e (MeV)	$\Delta\gamma/\gamma$ (10^{-3})	ϵ_n (μm rad)	σ_{p_x} (keV)	σ_x (μm)	λ_0 (μm)	U_L (J)
A	1	65	5	1	34	15	1	0.2
				$X = 0.00123$				

ELI-NP-GBS eta-psi=1.2*10^-5

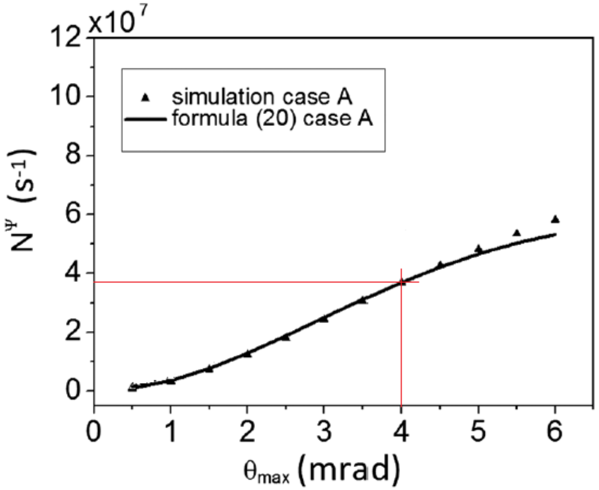

$$\eta^{\Psi\,SIM} \simeq \frac{3.67\cdot 10^7\cdot 4\cdot 127.2^2\cdot 1.239}{6.24\cdot 10^9\cdot 65\cdot 10^6} = 7.25\cdot 10^{-6}$$

$$\eta^{\Psi\,FOR} \simeq \frac{7.82\cdot 10^{-4}\cdot 0.2\cdot 127.2^3\cdot 16\cdot 10^{-6}}{2\cdot 15^2\cdot (1+127.2^2\cdot 16\cdot 10^{-6})^2} = 7.22\cdot 10^{-6}$$

Inverse Compton Sources, Overview, Theory, Main Technological Challenges – Photonic Colliders

Luca Serafini – *INFN-Milan and University of Milan*

4 Lecture Outline

- **Overview of Projects/Proposal for ICS' and Applications**
- **Classical e.m. and Linear Quantum Theory of Inverse Compton Sources (ICS) and paradigms for ICS**
- **Photon-Photon Colliders at low energy for Breit-Wheeler and photon-photon scattering experiments**
- **Hadron-Photon Colliders as muon photo-cathodes for TeV photons, neutrino and pion/muon low emittance beam generation**

Presently there are 3 main Paradigms for high performance ICS:

A) RF Photo-injector producing a high charge 1-2 nC electron bunch against a J-class laser pulse delivered by an amplified *Yb:Yag* laser system, tightly focused down to 10-20 μm, running collisions at 100 Hz. Best example of this model is STAR [9] (Southern europe Thomson source for Applied Research), in construction as a dedicated user facility at the University of Calabria (Italy) by a collaboration INFN-ST-CNISM-UniCal. Maximum achievable fluxes in excess of $3 \cdot 10^{11}$ with maximum photon energy 200 keV.

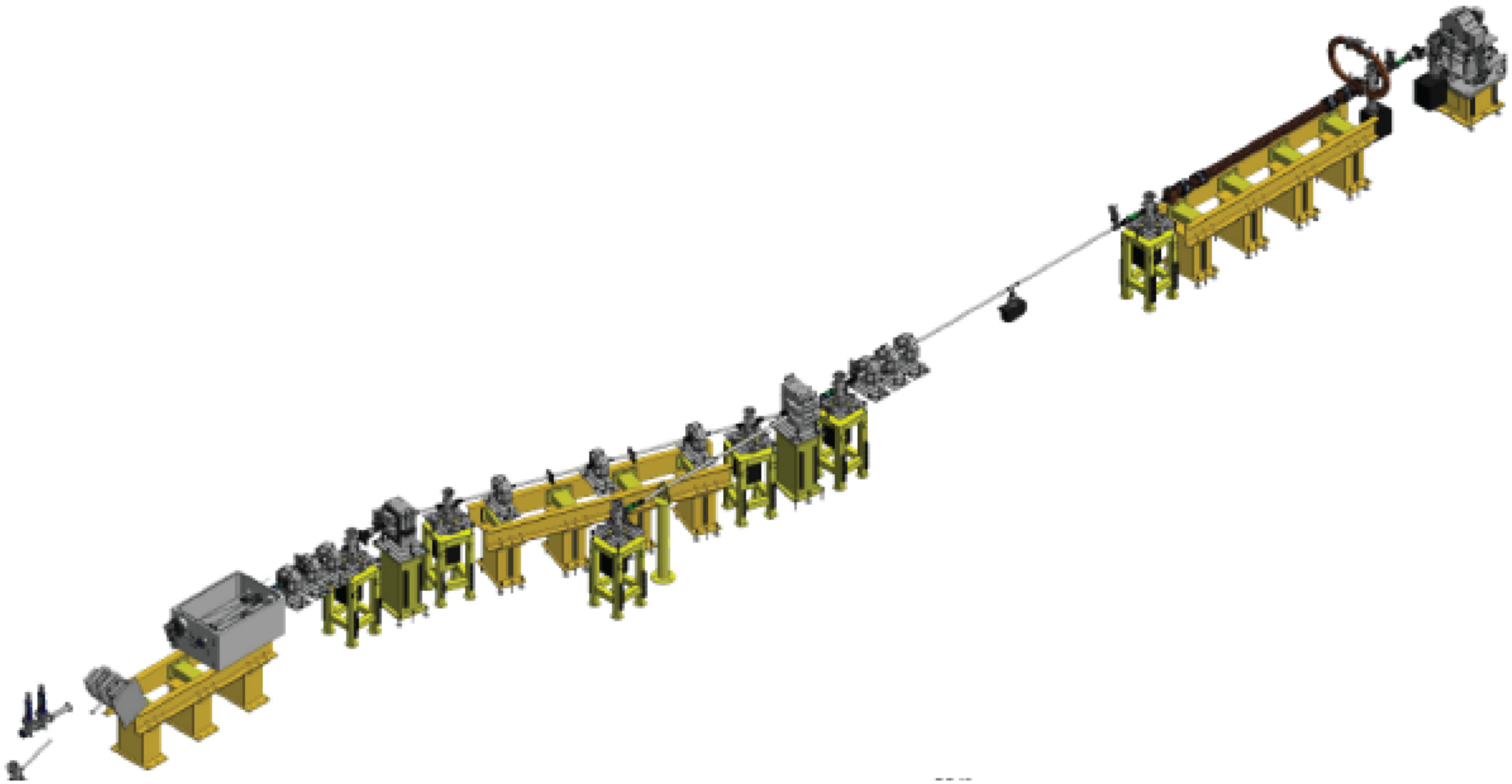

***Fig.2** – STAR machine as an example of Paradigm A. Overall length about 12 m.*

B) Compact Storage Ring for the electron beam, colliding at a high repetititon rate (up to 25 MHz, *i.e.* an average beam current of 15 mA) a moderately high charge electron bunch with a mJ-class laser pulse stored in an optical Fabry-Perot Cavity [17], focused to 70 μm spot size at collision. Best example of this category is ThomX, in construction at Orsay-LAL by

a cc ... $\cdot 10^{12}$.
Ma ... ype is
curı ... es are
a n ... . The
uno

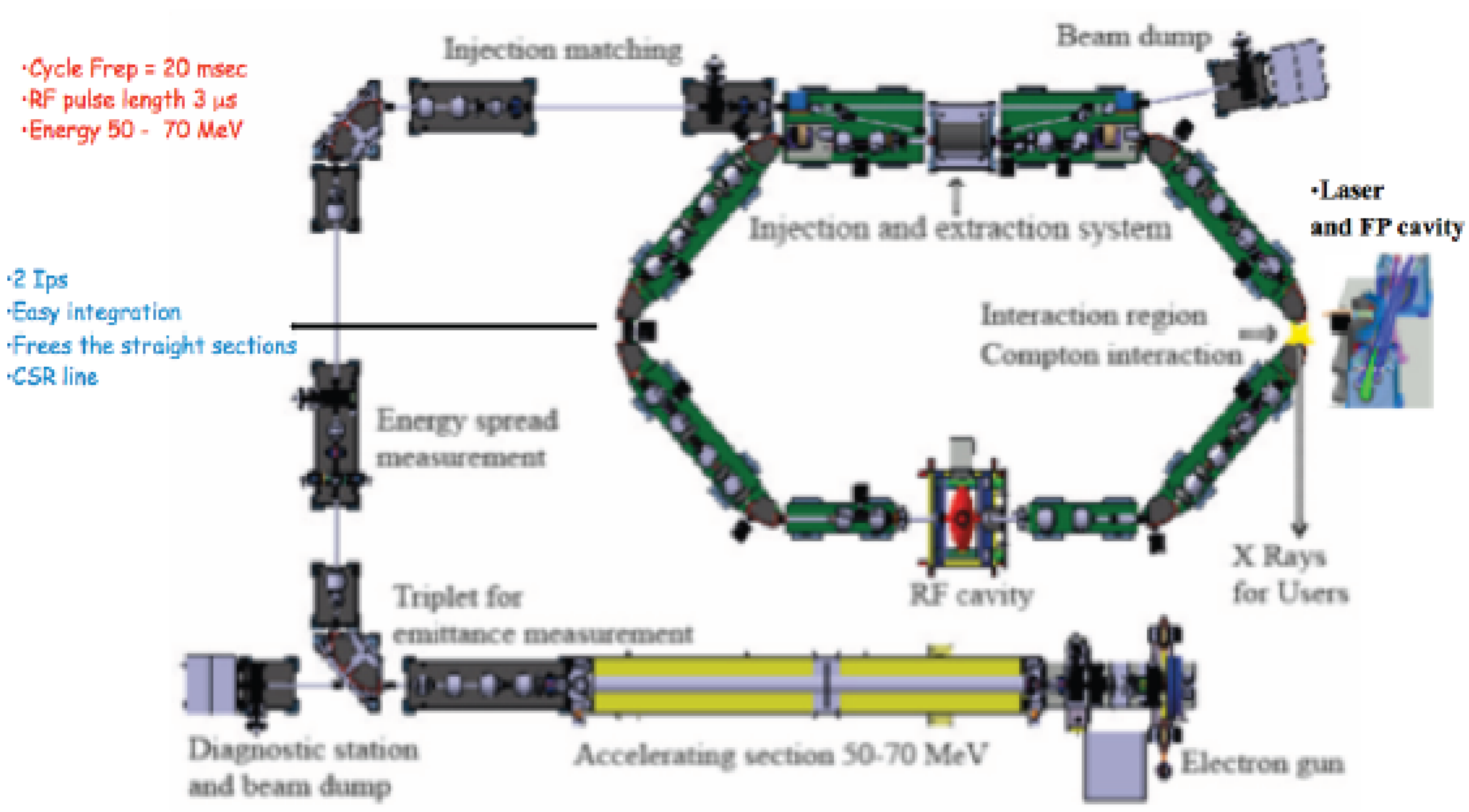

Fig.3 – ThomX as an example of Paradigm B. Size is about 10x10 m^2.

C) Super-Conducting RF Photo-Injector delivering a low charge (tens of pC) electron bunch at a very high rep. rate (up to 100 MHz), colliding with a mJ-class laser pulse stored in an optical Fabry-Perot Cavity (up to 1 MW stored laser power), focused to 20-30 μm spot size at collision. Maximum achievable fluxes about $3.5 \cdot 10^{12}$ without energy recovery (average electron beam current 1 mA) while in excess of an impressive 10^{15} with energy recovery at an average electron current of 100 mA. Maximum photon energy 200 keV. BriXS would belong to this type of ICS, together with UH-FLUX, a similar project [11] in development in UK (with energy recovery) and CUBIX, an ongoing project [12] at MIT (without energy recovery).

BriXS: BRIght and compact X-ray Source - Proposal at INFN-Milan and Univ. of Milan (post EXPO-2015 initiative submitted to regional and metropolitan area governments)

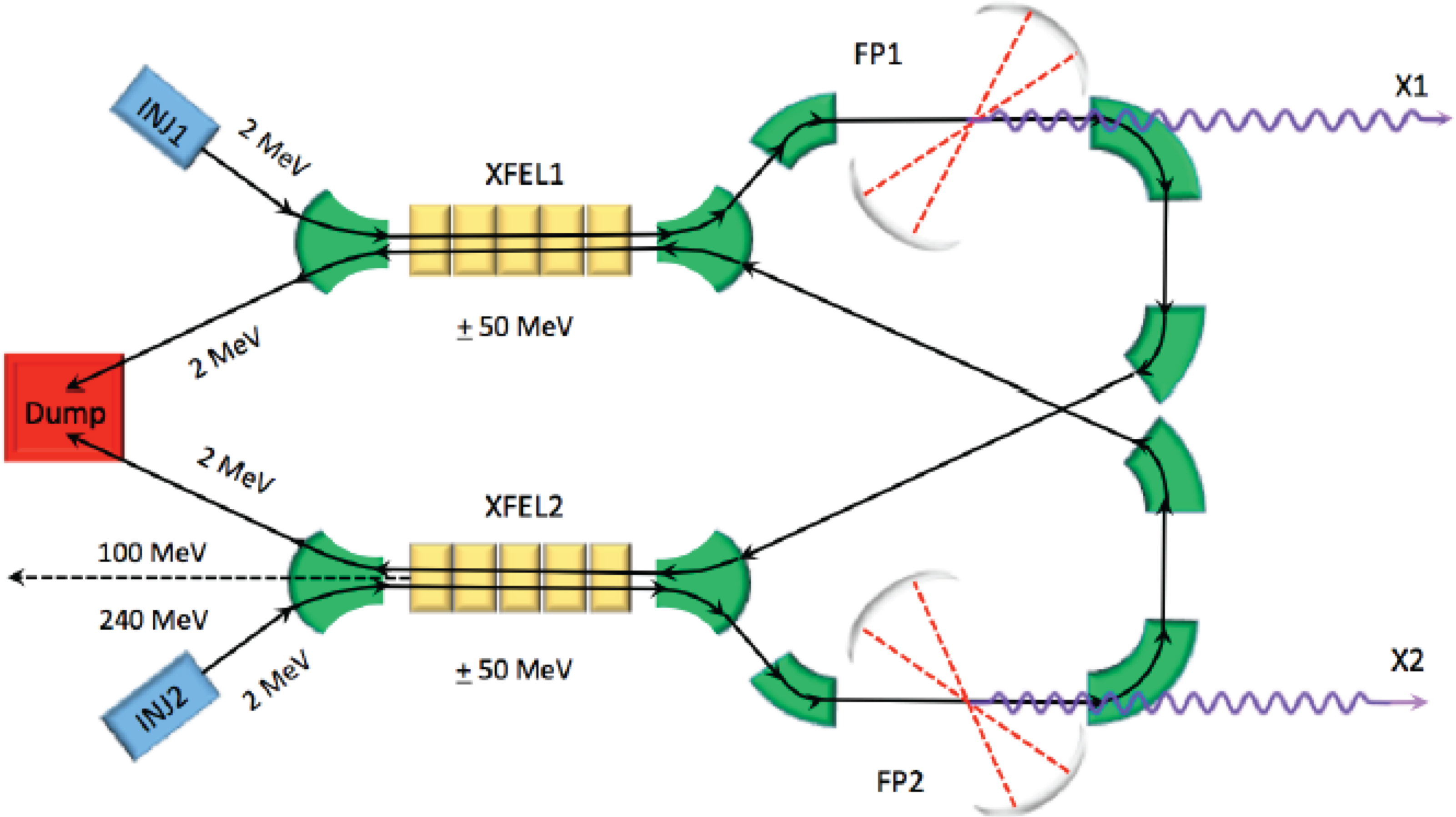

Fig.6 – BriXS conceptual lay-out, based on a wrapped push-and-pull modified Tigner-Variola scheme.

X-ray flux N_X^{bw} in photons/sec within rms bandwidth *bw*

Case A: head-on collision STAR-like

U_L energy of colliding laser pulse, Q electron bunch charge, f_{RF} rep rate of electron bunches, σ_x electron beam spot size at collision

$$N_X^{bw} = 5.8 \cdot 10^8 \frac{U_L[J]Q[pC]f_{RF}}{\sigma_x^2[\mu m^2]} bw$$

$$U_L = 1\ J, Q = 1\ nC, f_{RF} = 100\ Hz, \sigma_x = 15\ \mu m, bw = 0.1 \Rightarrow N_X^{bw} = 2.6 \cdot 10^{10}$$

$$U_L = 0.4\ J, Q = 1\ nC, f_{RF} = 3.2\ kHz, \sigma_x = 15\ \mu m, bw = 0.1 \Rightarrow N_X^{bw} = 3.3 \cdot 10^{11}$$

Case B: BriXS-like with F-P optical cavity

P_{FP} power stored in Fabry-Perot cavity, $\langle I_e \rangle$ average electron beam current

$$N_X^{bw} = 1.4 \cdot 10^{17} \frac{P_{FP}[MW]\langle I_e \rangle[mA]}{f_{FP}[MHz]\sigma_x^2[\mu m^2]} bw$$

$$P_{FP} = 1\ MW, \langle I_e \rangle = 1\ mA, f_{FP} = 100\ MHz, \sigma_x = 20\ \mu m, bw = 0.1 \Rightarrow N_X^{bw} = 3.5 \cdot 10^{12}$$

$$P_{FP} = 1\ MW, \langle I_e \rangle = 100\ mA, f_{FP} = 100\ MHz, \sigma_x = 12\ \mu m, bw = 0.1 \Rightarrow N_X^{bw} = 10^{15}$$

Table 0 – BriXS commissioning phase performances

Electron beam energy (MeV)	Electron beam average current (μA)	Stored laser power in FP cavity (MW)	X-ray photon energy range (keV)	X-ray flux (photons/s) @ 10% bdw
70	**300**	**0.15**	**20-90**	**10^{11}**

Table 1 – BriXS first phase performances

Electron beam energy (MeV)	Electron beam average current (mA)	Stored laser power in FP cavity (MW)	X-ray photon energy range (keV)	X-ray flux (photons/s *) @ 10% bdw
70	**1**	**0.3**	**20-90**	**10^{12}**

Table 2 – BriXS second phase performances

Electron beam energy (MeV)	Electron beam average current (mA)	Stored laser power in FP cavity (MW)	X-ray photon energy range (keV)	X-ray flux (photons/s *) @ 10% bdw
100	**100**	**1**	**20-200**	**10^{15}**

* effective collision repetition rate 100 MHz and collision spot size 12 μm

Existing and planned Thomson sources

	Type	Energy [KeV]	Flux (@ 10% bandwidth)	Source size (μm)
*PLEIADES (LLNL) [11,12]	Linac	10-100	10^7 (10 Hz)	18
*Vanderbilt [13,14]	Linac	15-50	10^8 (few Hz)	30
*SLAC [15]	Linac	20-85		
*Waseda University [16,17]	Linac	0.25-0.5	$2.5\ 10^4$ (5 Hz)	
*AIST, Japan [18]	Linac	10-40	10^6	30
*Tsinguha University [19]	Linac	4.6	$1.7\ 10^4$	
*LUCX (KEK) [20]	Linac	33	$5\ 10^4$ (12.5 Hz)	80
+ UTNL, Japan [21,22]	Linac	10-40	10^9	
MIT project [23]	Linac	3-30	$3\ 10^{12}$ (100 MHz)	2
MXI systems [24]	Linac	8-100	10^9 (10Hz)	
SPARC –PLASMONX [25]	Linac	20-380	$2\ 10^8$ -$2\ 10^{10}$	0.5-13
Quantum Beam (KEK) [26,27]	Linac		10^{13}	3
*TERAS (AIST) [28]	Storage ring	1-40	$5\ 10^4$	2
*Lyncean Tech [29,30,31]	Storage ring	7-35	~ 10^{12}	30
Kharkov (SNC KIPT) [32]	Storage ring	10-500	$2.6\ 10^{13}$ (25 MHz)	35
TTX (THU China) [33,34]	Storage ring	20-80	$2\ 10^{12}$	35
ThomX France [35]	Storage ring	50	10^{13} (25 MHz)	70

Table 3: Compact Compton X ray sources. Symbols * and + refers respectively to machines in operation and to machines in construction.

STAR (Calabria) Linac 20-100 10^{11} (100 Hz) 18

From **THOMX** Conceptual Design Report, A.Variola, A.Loulergue, F.Zomer, LAL RT 09/28, SOLEIL/SOU-RA-2678, 2010

Rivaling with Synchr. Light Sources for energies above 50 keV

ICS vs. other sources

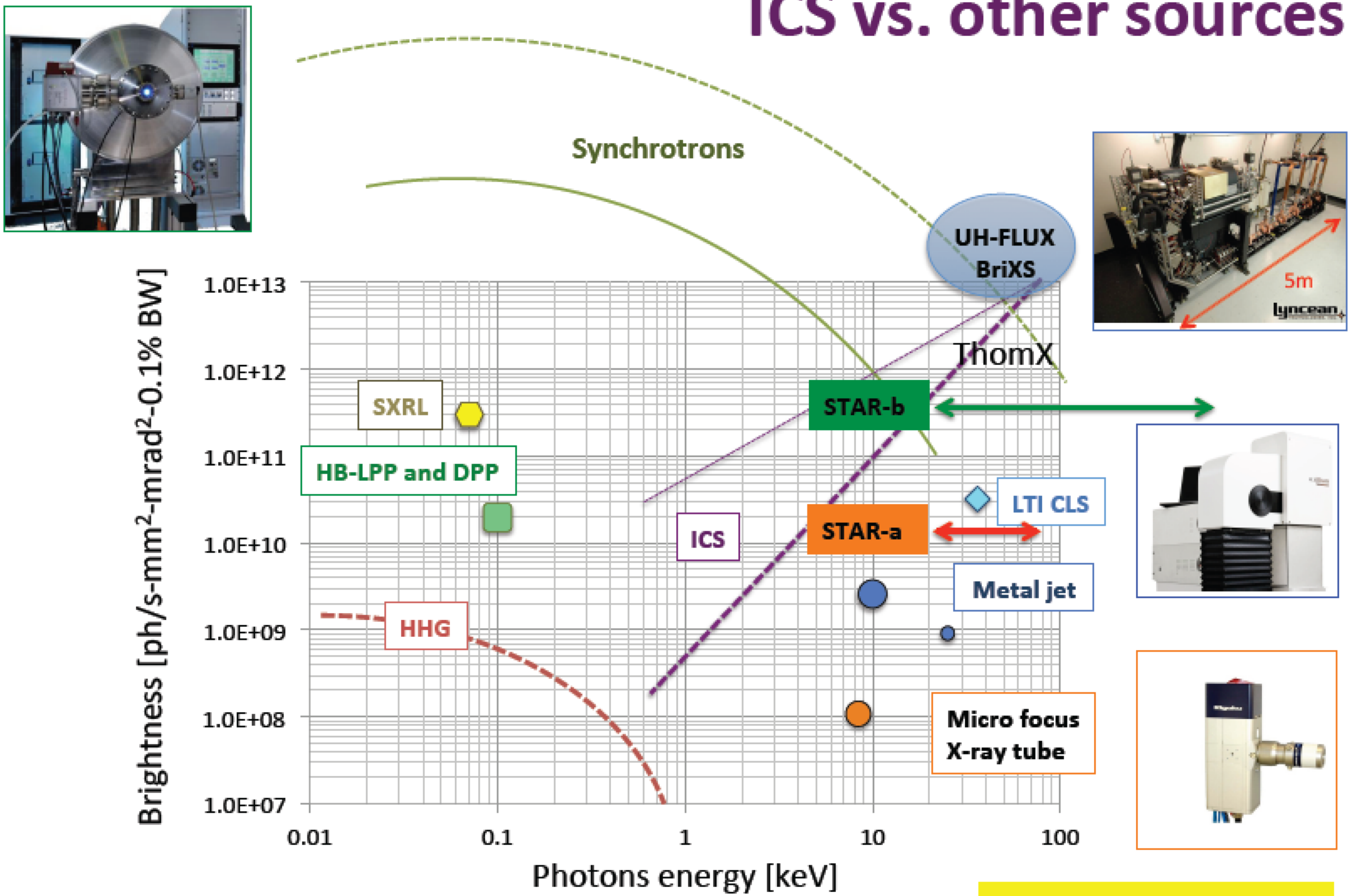

Courtesy of A. Murokh
RadiaBeamTechnology

31 Mar 2016 High Brightness Beams, Havana, Cuba

$$Peak\ \ Brilliance\ \ B_\gamma \equiv \frac{N_\gamma^{bw}}{\varepsilon_\gamma^2 \dfrac{\Delta\nu_\gamma}{\nu_\gamma}\sigma_t}$$

(10)

$$B_\gamma = 5.6 \cdot 10^{19} \frac{\gamma^2 U_L[J]Q[pC]}{h\nu[eV]\dfrac{\Delta\nu_\gamma}{\nu_\gamma}\sigma_0^2 w_0^2 \sigma_t}$$

$$correction\ \ factor\ \ for\ \ collision\ \ angle\ \ \phi$$

(11)

$$\delta_\phi = \frac{1}{\sqrt{1+\dfrac{\phi^2\left(\sigma_{z-el}^2 + c^2\sigma_t^2\right)}{4\left(\sigma_0^2+\dfrac{w_0^2}{4}\right)}}}$$

Brilliance of Lasers and X-ray sources

ELI

BELLA

$$N_{ph} = 10^{19} - 10^{20}$$
$$\sigma_t = 10 - 20 \quad fs$$

$$B = \frac{N_{ph}}{\sqrt{2\pi}\sigma_t \left(M^2 \lambda\right)^2 \frac{\Delta\lambda}{\lambda}}$$

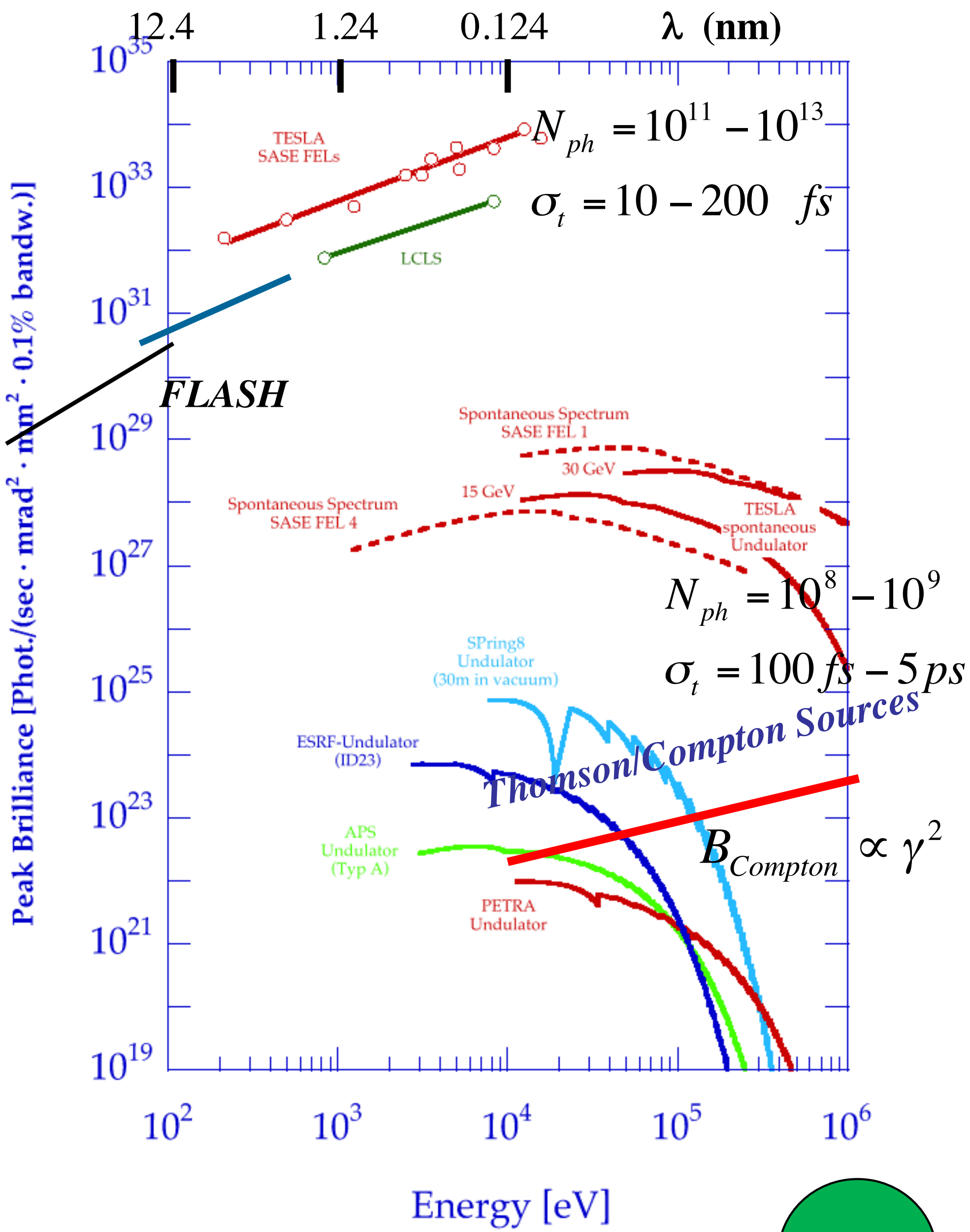

Outstanding X/γ photon beams for Exotic Colliders

Unsurpassable by any other technology/source for energies > 1 MeV

The peak brilliance of an optimized MEGa-ray source is both revolutionary and transformative

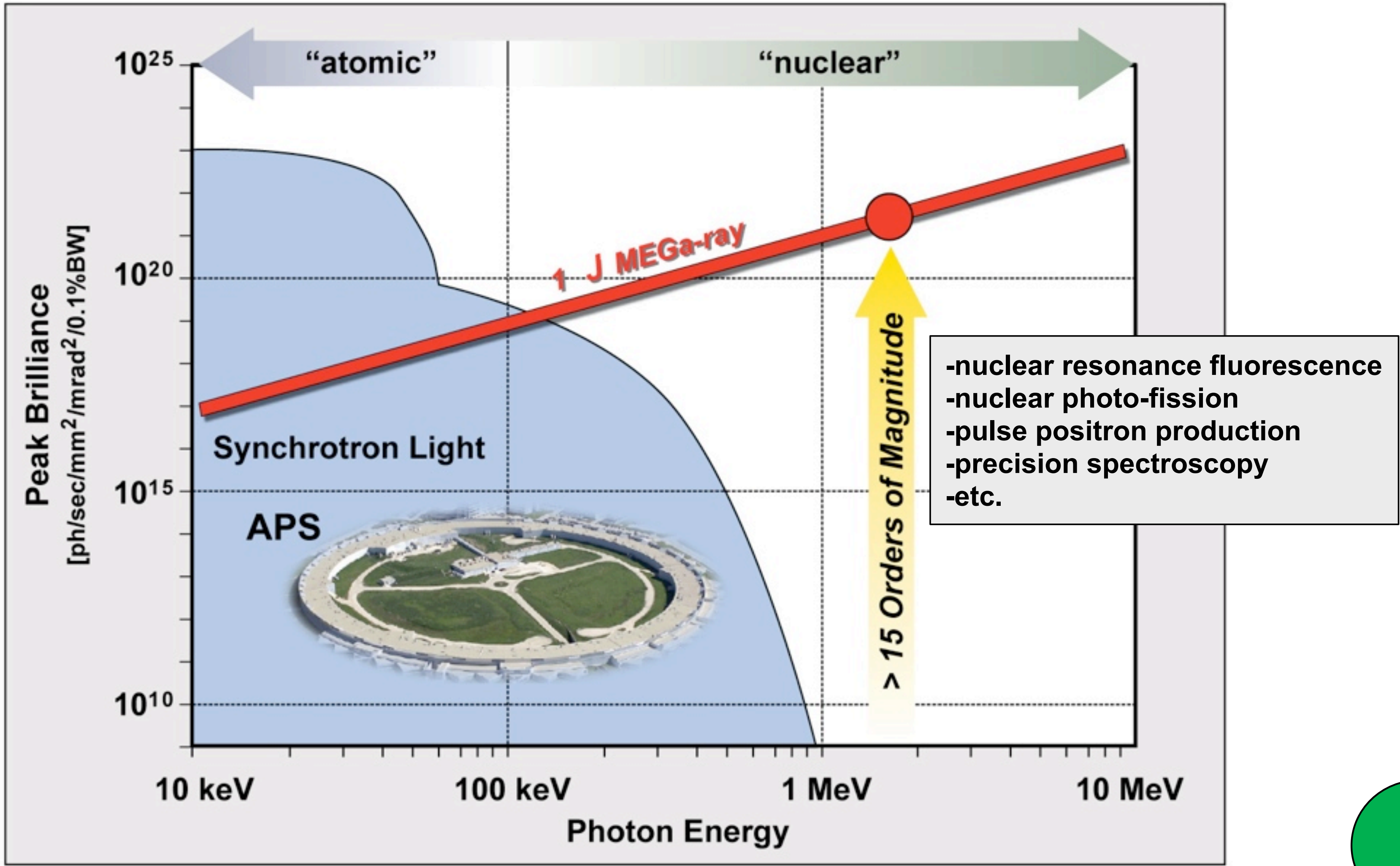

Courtesy C. Barty - LLNL

ELI-NP γ beam: the quest for narrow bandwidths (from 10^{-2} down to 10^{-3})

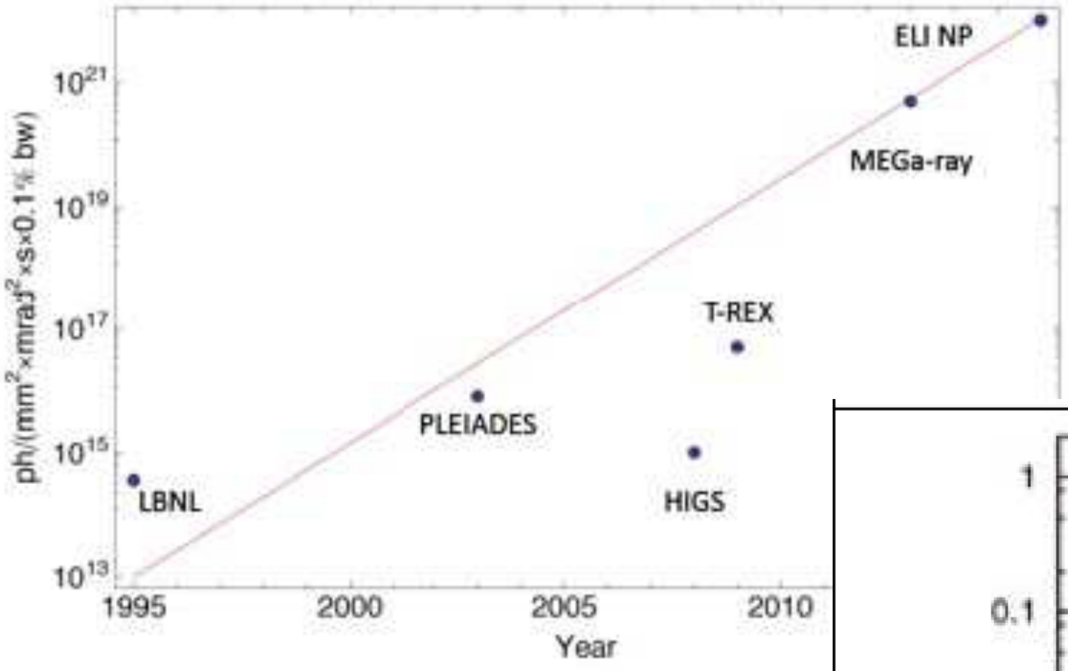

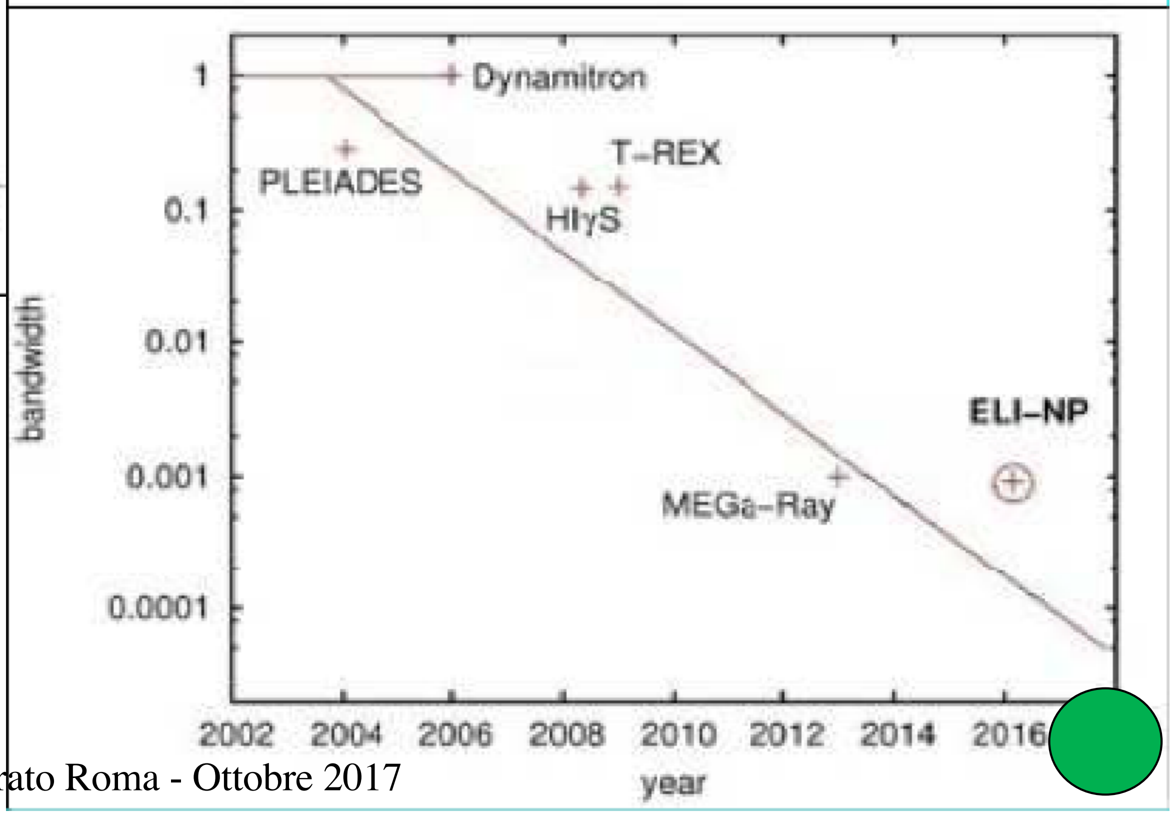

Courtesy V. Zamfir – ELI-NP

ELI-NP GBS (Extreme Light Infrastrucutre Gamma Beam System) Main Parameters

$$\gamma - ray \quad 1-20 \quad MeV \ ; \ rms \ \ Bandwidth \ \ 3.-5.\ 10^{-3}$$

$$Spectral \ \ Density: \quad 10^{3}-10^{4} \quad photons/s\cdot eV$$

$$needs \ \ 3.10^{5} \quad photons/pulse \ @ \ 3 \ \ kHz \ \ rep \ \ rate$$

$$rms \ \ divergence \ \ 30 < \ 300 \ \ \mu rad$$

$$linear \ \ or \ \ circular \ \ polarization \ \ > \ 9[illegible]\%$$

outstanding electron beam @ 750 MeV with high phase space density
(all values are projected, not slice! cmp. FEL's)

$$Q = 250\,pC \ ; \ \varepsilon_n = 4.10^{-7} m\cdot rad \ ; \ \Delta\gamma/\gamma = 5\cdot 10^{-4}$$

Back-scattering a high quality *J-class* ps laser pulse

$$U_L = 400 \ \ mJ \ ; \ M^2 = 1.2 \ ; \ \frac{\Delta\nu}{\nu} = 5\cdot 10^{-4}$$

not sustainable by RF, Laser!

New generation of Gamma Beam Source (GBS)

Gamma ray beam specifications table

Photon energy	$0.2 - 19.5$	MeV
Bandwidth (RMS)	$\lesssim 0.5\%$	-
Spectral density (TASD)	$0.8 - 4 \times 10^4$	ph/(s eV)
ph/s within BW	$\sim 10^9$	-
source size (RMS)	$10 - 30$	μm
source divergence (RMS)	$25 - 250$	μrad
Peak Brilliance	$10^{20} - 10^{23}$	ph/(s·mm^2·mrad^2 $\cdot$ 0.1%BW
γ pulse length (RMS)	$0.7 - 1.5$	ps
polarization (linear, circular)	$> 95\%$	-
macro pulse rep. rate	100	Hz
pulses / macropulse	$30 - 40$	-
pulse period	$15 - 20$	ns

- Bright / monochromatic beam ➠ High spectral flux
- Tunable
- Linear polarization ➠ possible update to any state.

Gamma Beam Source : electron-photon collider approach

Leading with GBS machine parameters to a :

$$\mathcal{L} = \frac{N_l N_e \delta\Phi}{2\pi(\sigma_r^2 + w_0^2/4)} \times f \cdot n_{RF}$$

- green laser pulse energy : $h\nu_l = 2.4\,\mathrm{eV}$, $U_l = 0.4\,\mathrm{J}$,
- electron bunch charge : $Q_b = 250\,\mathrm{pC}$
- effective collision rate $n_{RF} \times f = 100 \times 32\,\mathrm{Hz}$
- optimization of electron - laser beams space time overlap :
  time : $c\Delta\tau < 2Z_r$ and $\sigma_z < \gamma\sigma_r^2/\epsilon_{n,x}$ ➠ $\Delta\tau \approx 3.5ps$ and $\sigma_z \approx 300\,\mu\mathrm{m}$
  space : $w_0 \approx 2\sigma_r$ ➠ $w_0 \approx 28\,\mu\mathrm{m}$, $\sigma_r \approx 15\,\mu\mathrm{m}$

the total gamma ray flux in the whole solid angle is :

$$N_\gamma = \sigma_{th} \cdot \mathcal{L} > 10^{10}\,\mathrm{ph.s}^{-1}$$

src: A. Bacci et al. J. Appl. Phys. 113, 194508 (2013)

New generation of Gamma Beam Source (GBS)

Gamma ray beam specifications table

Photon energy	$0.2 - 19.5$	MeV
Bandwidth (RMS)	$\lesssim 0.5\%$	-
Spectral density (TASD)	$0.8 - 4 \times 10^4$	ph/(s eV)
ph/s within BW	$\sim 10^9$	-
source size (RMS)	$10 - 30$	μm
source divergence (RMS)	$25 - 250$	μrad
Peak Brilliance	$10^{20} - 10^{23}$	ph/(s·mm^2·mrad$^2 \cdot 0.1\% BW$
γ pulse length (RMS)	$0.7 - 1.5$	ps
polarization (linear, circular)	$> 95\%$	-
macro pulse rep. rate	100	Hz
pulses / macropulse	$30 - 40$	-
pulse period	$15 - 20$	ns

- Bright / monochromatic beam ➠ High spectral flux
- Tunable
- Linear polarization ➠ possible update to any state.

Electron beam is transparent to the laser (only 10^9 photons are back-scattered at each collision out of the 10^{18} carried by the laser pulse)

CIRCULATOR PRINCIPLE

- 2 high-grade quality parabolic mirrors
  - Aberration free
- Mirror-pair system (MPS) per pass
  - Synchronization
  - Optical plan switching
    - ⇒ Constant incident angle = small bandwidth

PARAMETERS = OPTIMIZED ON THE GAMMA-RAY FLUX

- Laser power = state of the art
- Angle of incidence ($\varphi = 7.54°$)
- Waist size ($\omega_0 = 28.3\mu m$)
- Number of passes = 32 passes

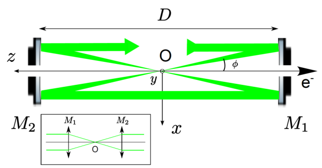

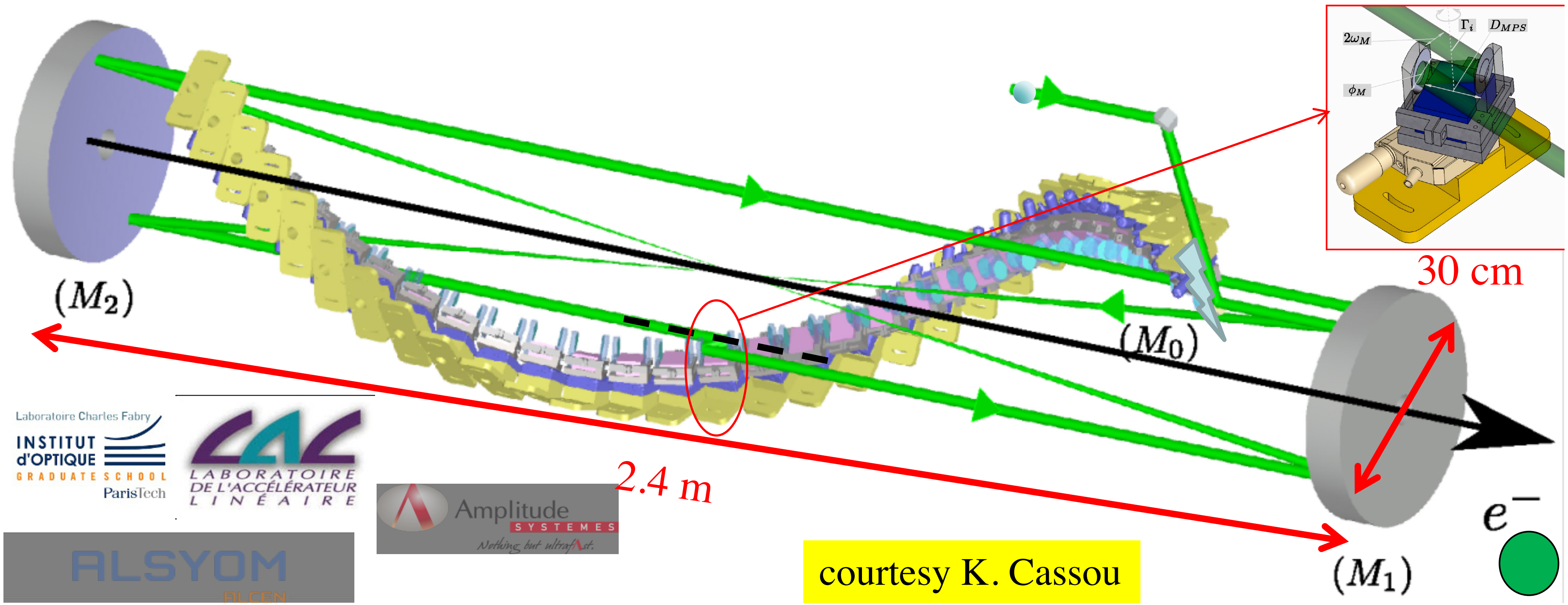

Laboratoire Charles Fabry INSTITUT d'OPTIQUE GRADUATE SCHOOL ParisTech
LABORATOIRE DE L'ACCÉLÉRATEUR LINÉAIRE
Amplitude SYSTEMES
ALSYOM

courtesy K. Cassou

PHYSICAL REVIEW SPECIAL TOPICS - ACCELERATORS AND BEAMS 17, 033501 (2014)

Design and optimization of a highly efficient optical multipass system for γ-ray beam production from electron laser beam Compton scattering

K. Dupraz,* K. Cassou, N. Delerue, P. Fichot, A. Martens, A. Stocchi, A. Variola, and F. Zomer
LAL, Université Paris-Sud, CNRS/IN2P3, Orsay, Bâtiment 200, BP 34, 91898 Orsay cedex, France

A. Courjaud and E. Mottay
Amplitude Systèmes, 6 allée du Doyen Georges Brus, 33600 Pessac, France

F. Druon
Laboratoire Charles Fabry de l'Institut d'Optique, UMR 8501 CNRS, Université Paris Sud, 91127 Palaiseau, France

G. Gatti and A. Ghigo
INFN-LNF, Via Enrico Fermi 40, 00044 Frascati Rome, Italy

T. Hovsepian, J. Y. Riou, and F. Wang
Alsyom, Parc des Algorithmes, Bâtiment Aristote, 9 Avenue du Marais, 95100 Argenteuil, France

A. C. Mueller
National Institute for Nuclear and Particle Physics, CNRS, 3 rue Michel-Ange, 75016 Paris, France

L. Palumbo
Universita di Roma La Sapienza, Dipartimento Energetica, Via Antonio Scarpa, 14-00161 Rome, Italy

L. Serafini and P. Tomassini
INFN-MI, Via Celoria 16, 20133 Milano, Italy
(Received 31 December 2013; published 26 March 2014)

A new kind of nonresonant optical recirculator, dedicated to the production of γ rays by means of Compton backscattering, is described. This novel instrument, inspired by optical multipass systems, has its design focused on high flux and very small spectral bandwidth of the γ-ray beam. It has been developed to fulfill the project specifications of the European Extreme Light Infrastructure "Nuclear Pillar," i.e., the Gamma Beam System. Our system allows a single high power laser pulse to recirculate 32 times synchronized on the radio frequency driving accelerating cavities for the electron beam. Namely, the polarization of the laser beam and crossing angle between laser and electrons are preserved all along the 32 passes. Moreover, optical aberrations are kept at a negligible level. The general tools developed for designing, optimizing, and aligning the system are described. A detailed simulation demonstrates the high efficiency of the device.

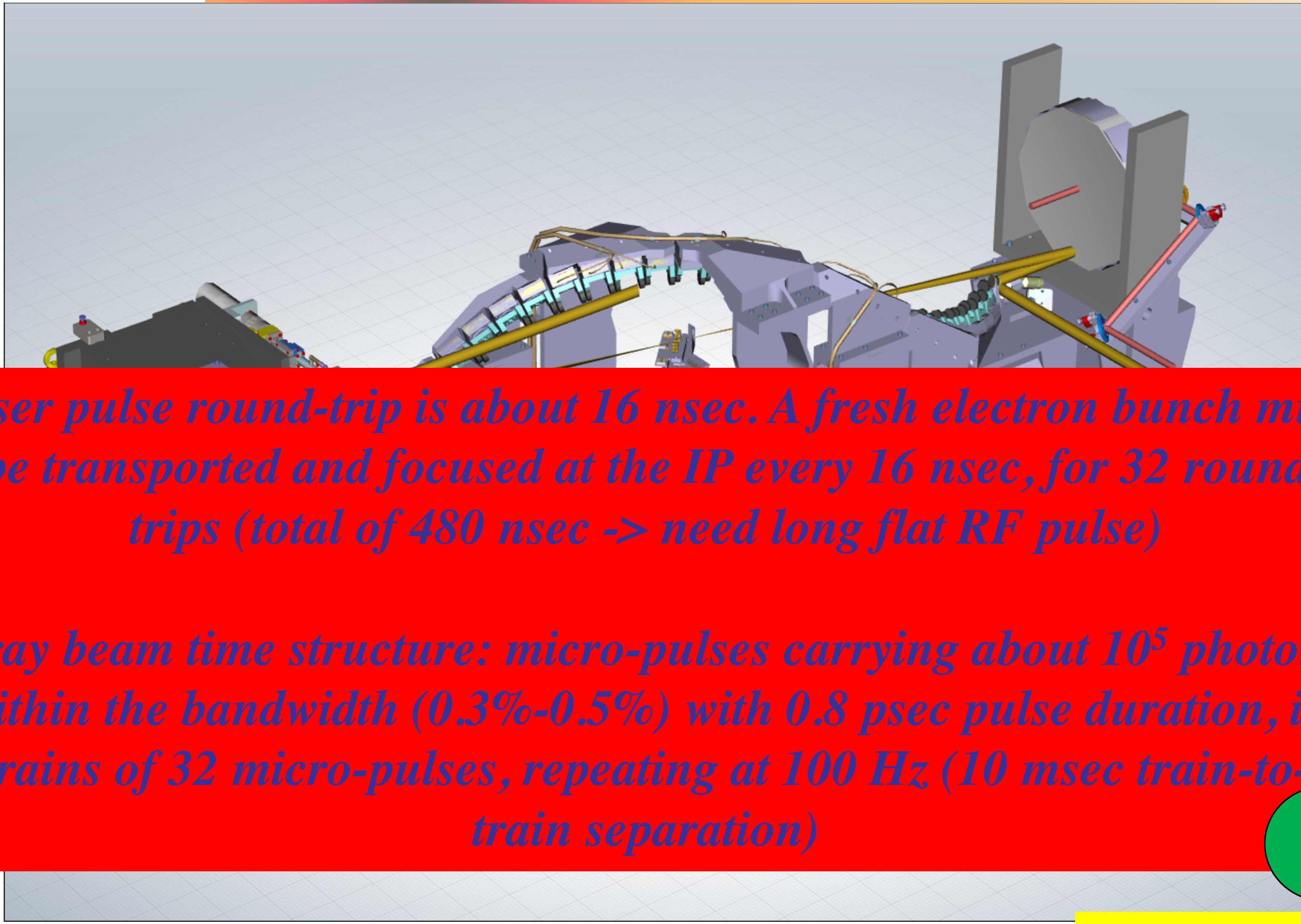

Laser pulse round-trip is about 16 nsec. A fresh electron bunch must be transported and focused at the IP every 16 nsec, for 32 round trips (total of 480 nsec -> need long flat RF pulse)

γ-ray beam time structure: micro-pulses carrying about 10^5 photons within the bandwidth (0.3%-0.5%) with 0.8 psec pulse duration, in trains of 32 micro-pulses, repeating at 100 Hz (10 msec train-to-train separation)

courtesy K. Cassou

ELI-NP-GBS High Order mode Damped RF structure

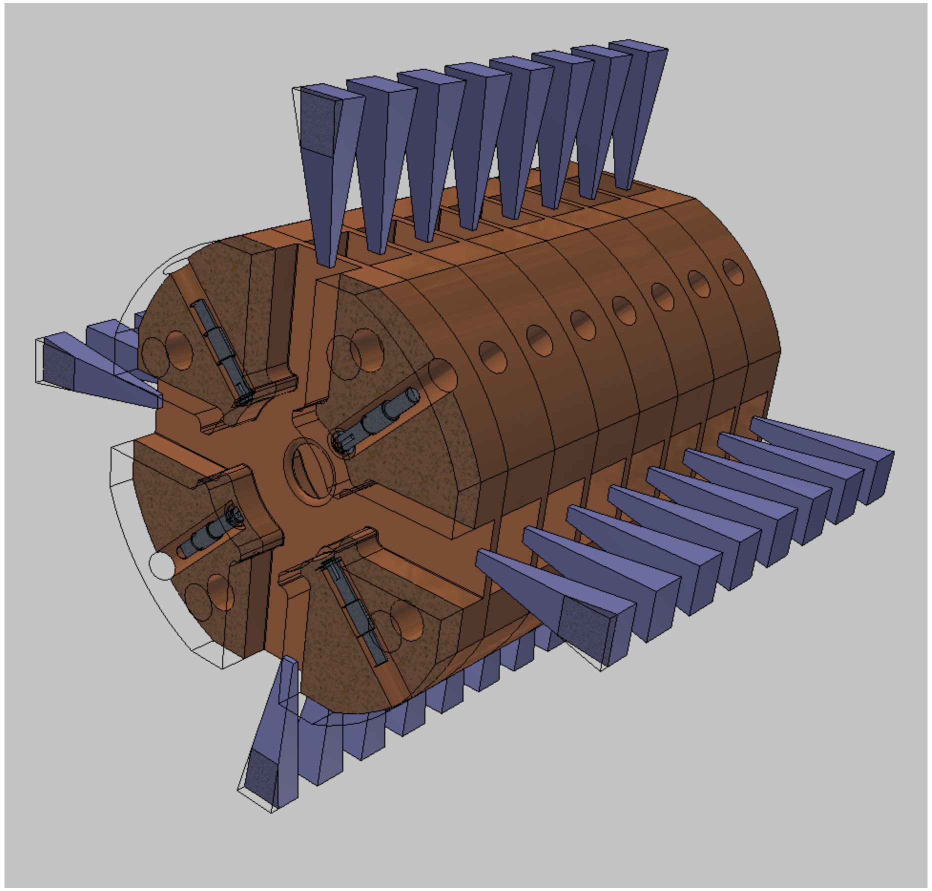

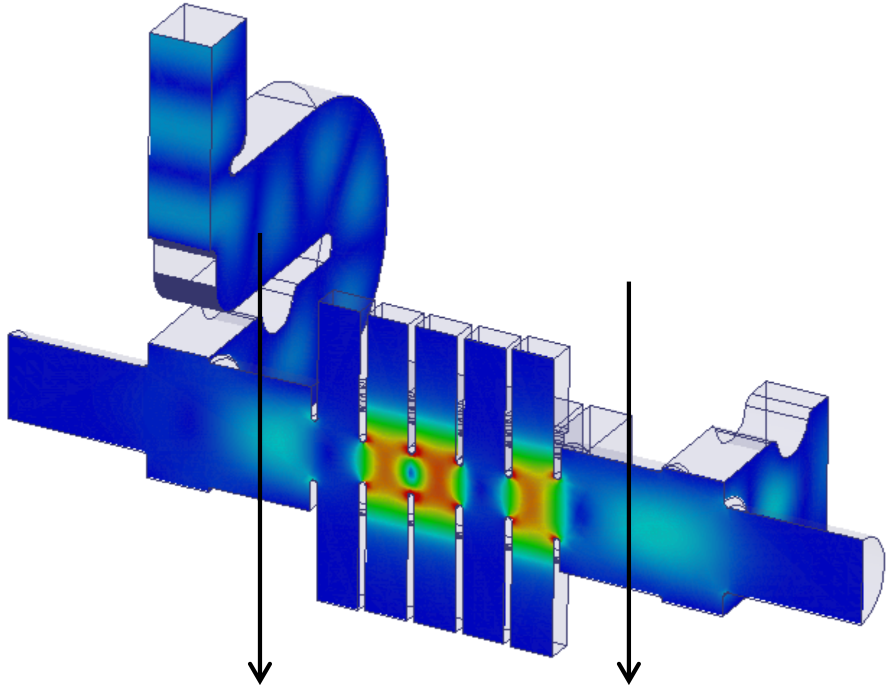

Unlike FEL’s Linacs, ELI-NP-GBS is a multi-bunch accelerator, therefore we need to control the Beam-Break-Up Instability to avoid complete deterioration of the electron beam emittance, i.e. of its brightness and phase space density

courtesy David Alesini

C-BAND STRUCTURES: HIGH POWER TEST SETUP

The structure has been tested at **high power at the Bonn University under RI responsibility**.

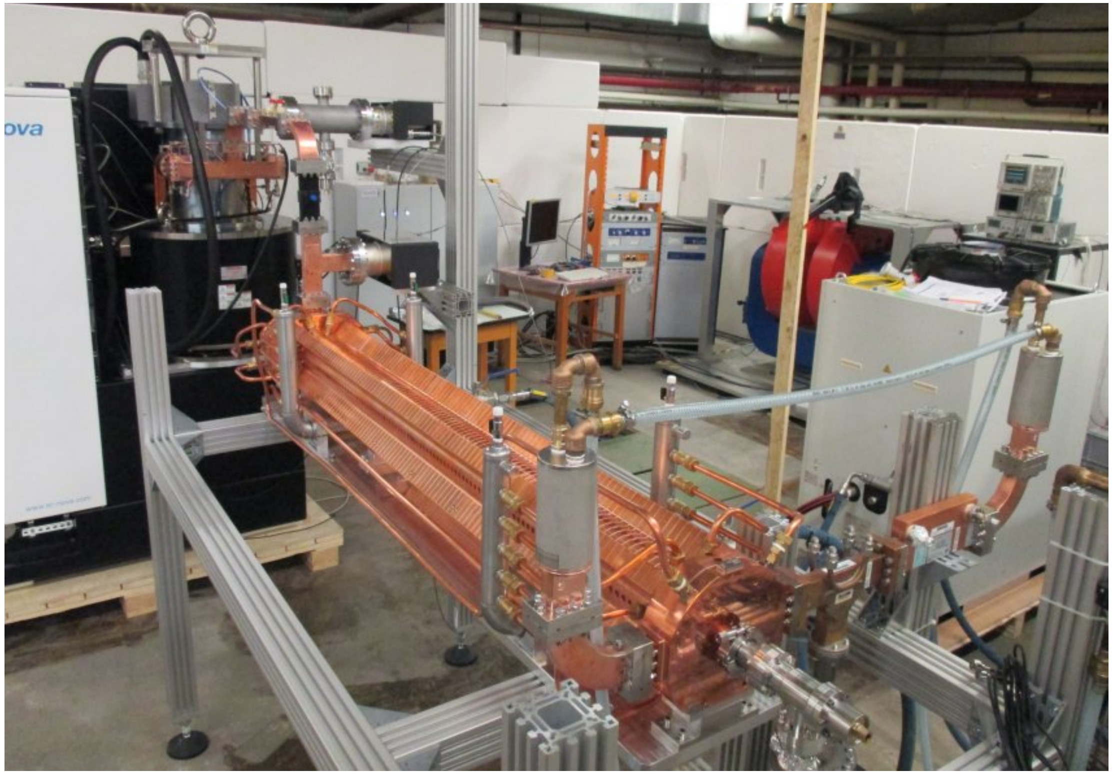

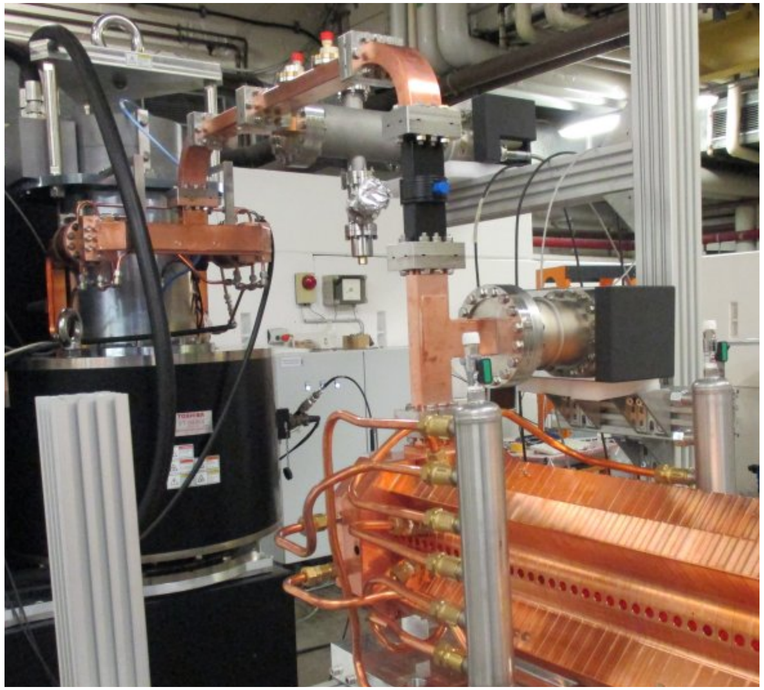

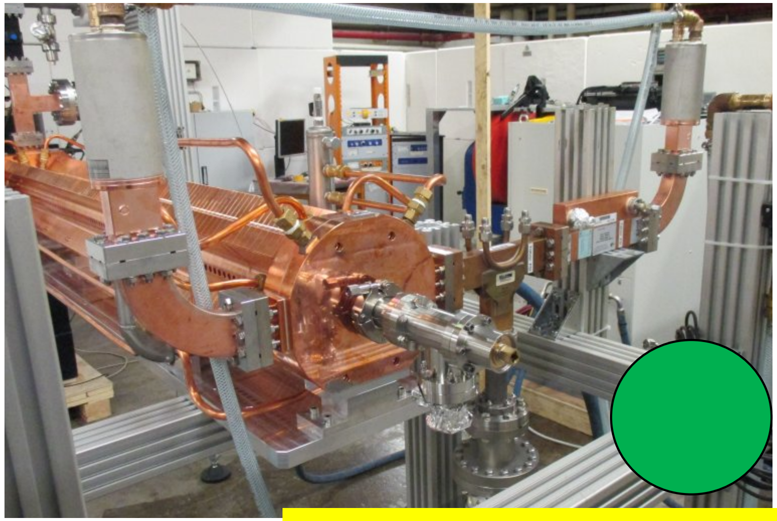

Successfully tested at full power (40 MW)

courtesy David Alesini

Inverse Compton Sources, Overview, Theory, Main Technological Challenges – Photonic Colliders

Luca Serafini – INFN-Milan and University of Milan

4 Lecture Outline

- **Overview of Projects/Proposal for ICS' and Applications**
- **Classical e.m. and Linear Quantum Theory of Inverse Compton Sources (ICS) and paradigms for ICS**
- **Photon-Photon Colliders at low energy for Breit-Wheeler and photon-photon scattering experiments**
- **Hadron-Photon Colliders as muon photo-cathodes for TeV photons, neutrino and pion/muon low emittance beam generation**

Total cross section of various γ–γ or e-γ interactions

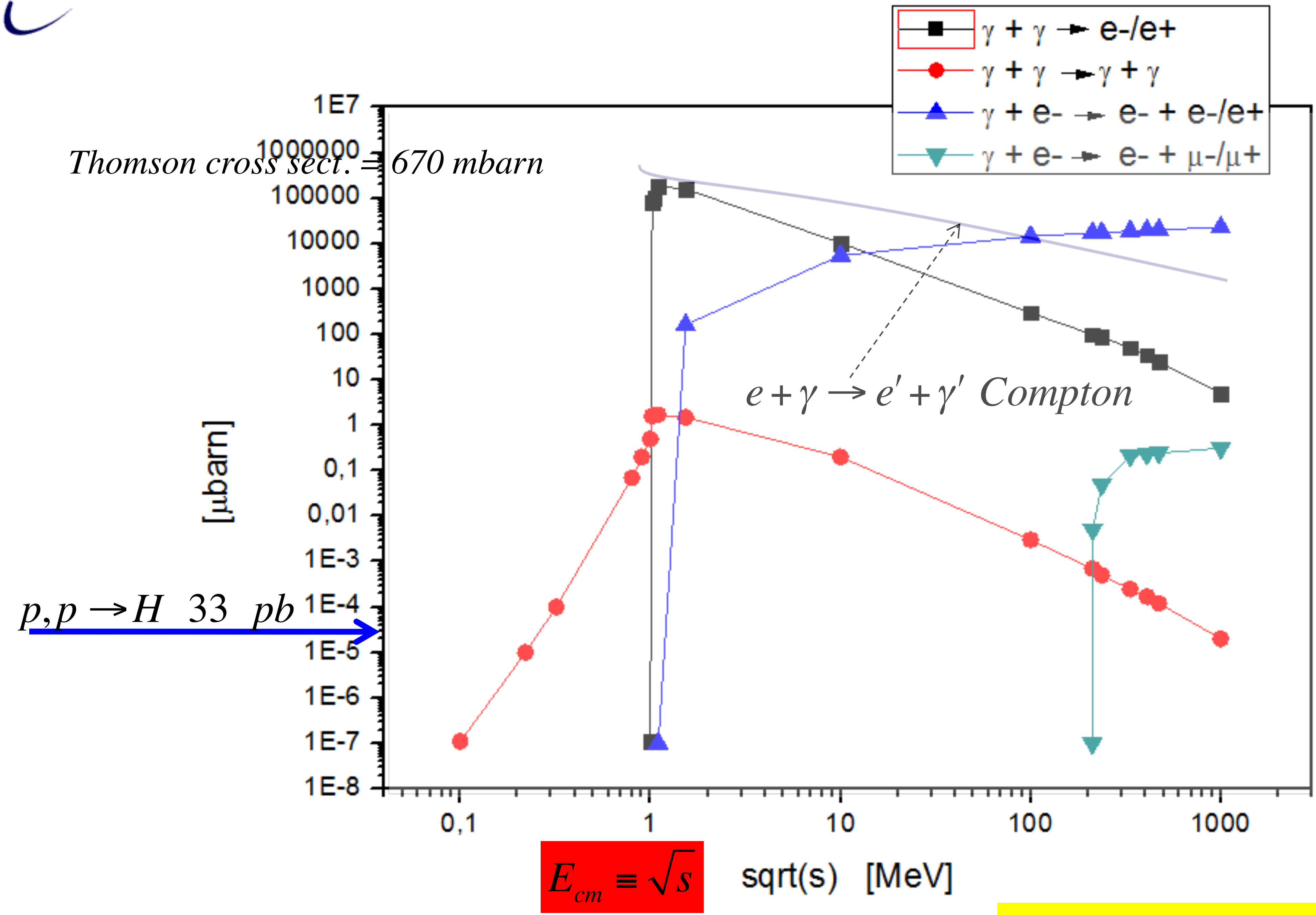

Courtesy C. Curatolo

The cosmological constant problem is related to the zero-point energy, i.e., to the fluctuations of quantum vacuum, and therefore also to the renormalization procedure in QFT.

Photon-photon scattering directly probes the fluctuations of quantum vacuum.

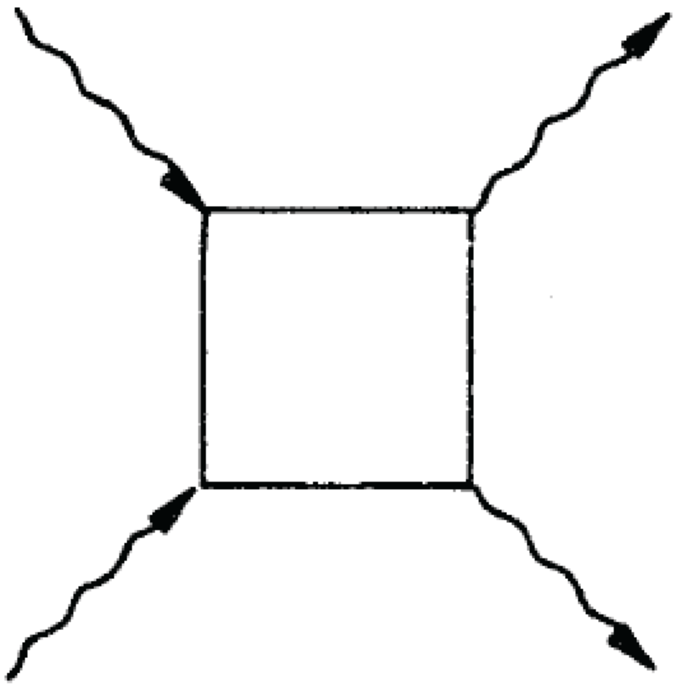

This is the first nonvanishing diagram: there are no tree-level diagrams

All the involved photons are real particles

courtesy E. Milotti

$$\sigma \approx 0.13\left(\frac{\hbar\omega}{m_e c^2}\right)^6 \mu\text{barn}$$

peak cross-section, $\approx 1.6\,\mu$barn at $\hbar\omega \approx 1.5 m_e c^2$

$$\sigma \approx 20\left(\frac{m_e c^2}{\hbar\omega}\right)^2 \mu\text{barn}$$

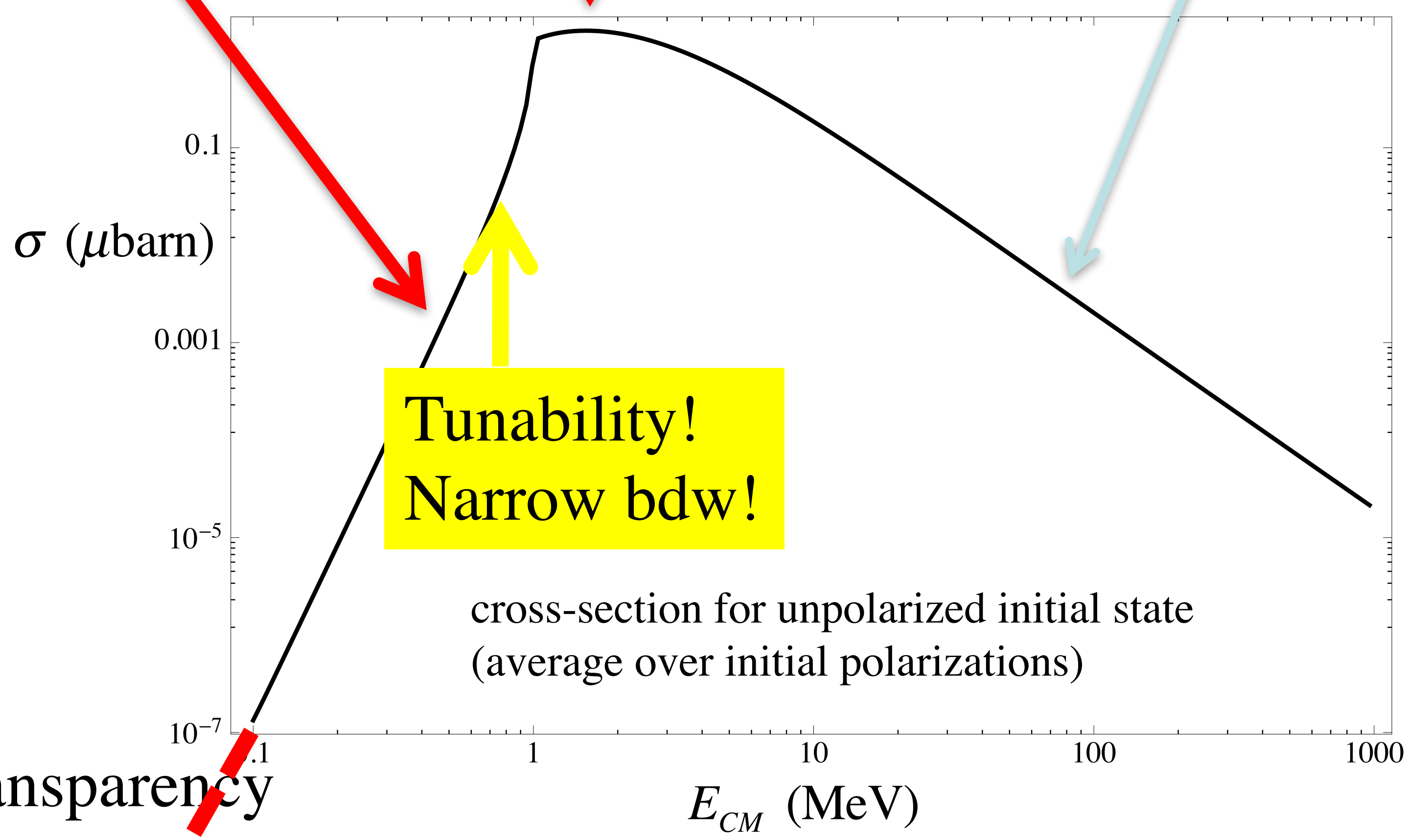

optical transparency
of the Universe

courtesy E. Milotti

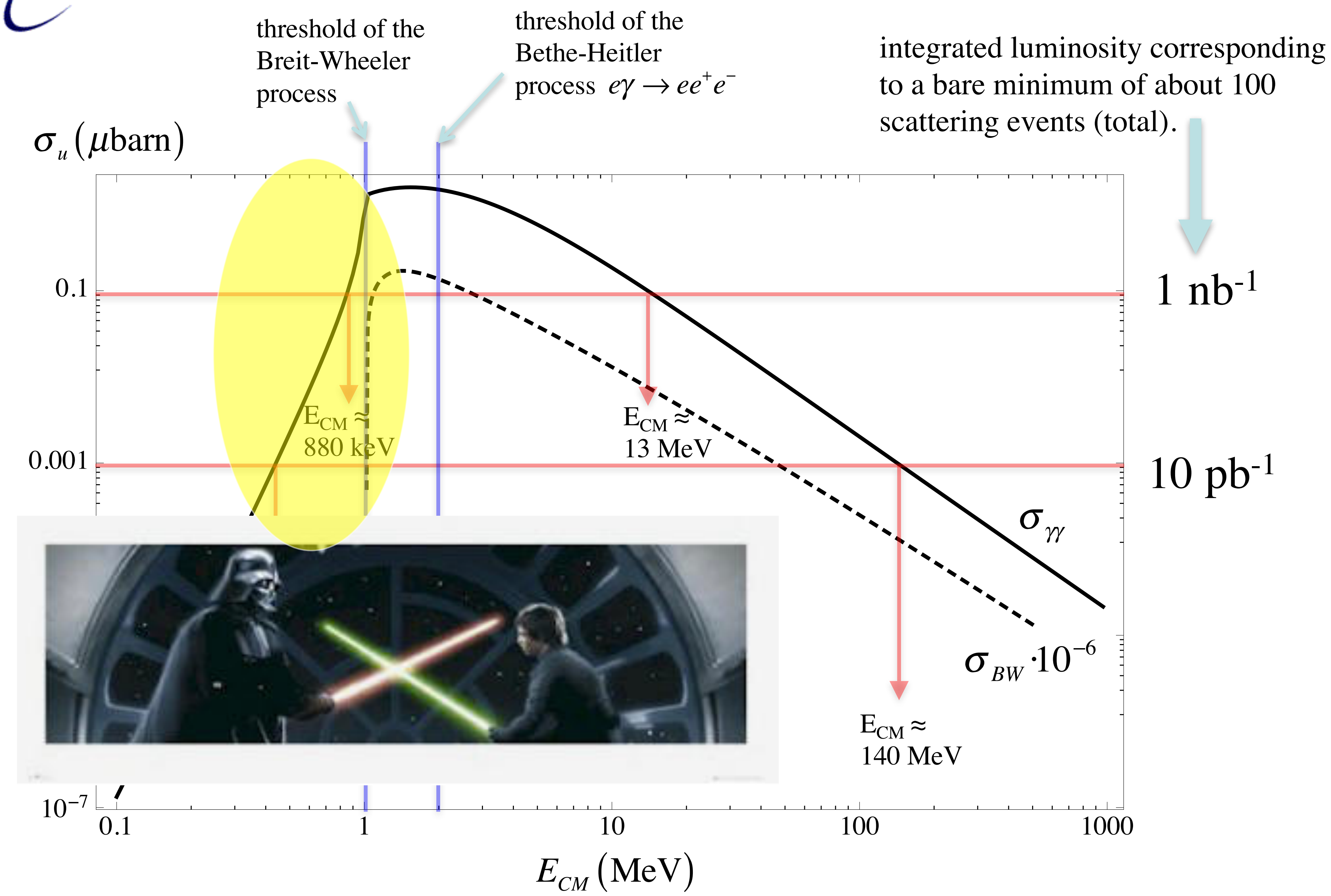

courtesy E. Milotti

PHYSICAL REVIEW ACCELERATORS AND BEAMS **19,** 093401 (2016)

Compton sources for the observation of elastic photon-photon scattering events

D. Micieli,[1] I. Drebot,[2] A. Bacci,[2] E. Milotti,[3] V. Petrillo,[2,4,*] M. Rossetti Conti,[2,4] A. R. Rossi,[2] E. Tassi,[1] and L. Serafini[2]

[1]*Universitá degli Studi della Calabria, via Pietro Bucci, 87036 Arcavacata di Rende (Cosenza) Italy*
[2]*INFN-Sezione di Milano, via Celoria 16, 20133 Milano, Italy*
[3]*Universitá di Trieste and INFN-Sezione di Trieste, Via Valerio 2, 34127 Trieste, Italy*
[4]*Universitá degli Studi di Milano, via Celoria 16, 20133 Milano, Italy*

(Received 13 May 2016; published 1 September 2016)

We present the design of a photon-photon collider based on conventional Compton gamma sources for the observation of elastic $\gamma\gamma$ scattering. Two symmetric electron beams, generated by photocathodes and accelerated in linacs, produce two primary gamma rays through Compton backscattering with two high energy lasers. The elastic photon-photon scattering is analyzed by start-to-end simulations from the photocathodes to the detector. A new Monte Carlo code has been developed *ad hoc* for the counting of the QED events. Realistic numbers of the secondary gamma yield, obtained by using the
or approved Compton devices, a discussion of the feasibility of the experiment an
background are presented.

DOI: 10.1103/PhysRevAccelBeams.19.093401

D. MICIELI *et al.*

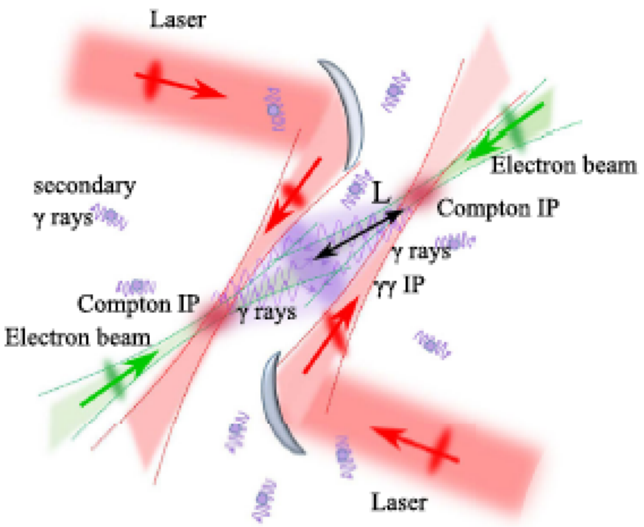

FIG. 1. Scheme of the $\gamma\gamma$ interaction. Two lasers (in red) impinge on two electron beams (in green) in two interaction points (Compton IP), generating primary gamma rays (in violet). The primary gamma rays interact in the $\gamma\gamma$ IP, generating secondary gammas.

Nuclear Instruments and Methods in Physics Research A ■ (■■■■) ■■■–■■■

Contents lists available at ScienceDirect

Nuclear Instruments and Methods in Physics Research A

journal homepage: www.elsevier.com/locate/nima

Q2 Study of photon–photon scattering events

I. Drebot [a], A. Bacci [a], D. Micieli [b], E. Milotti [c], V. Petrillo [a,d,*], M. Rossetti Conti [a,d], A.R. Rossi [a], Q1 E. Tassi [b], L. Serafini [a]

[a] INFN-Sezione di Milano, via Celoria 16, 20133 Milano, Italy
[b] Università degli Studi della Calabria, Arcavacata di Rende (Cosenza), Italy
[c] Università di Trieste and INFN-Sezione di Trieste, Via Valerio 2, 34127 Trieste, Italy
[d] Università degli Studi di Milano, via Celoria 16, 20133 Milano, Italy

ARTICLE INFO

Article history:
Received 25 May 2016
Received in revised form
24 June 2016
Accepted 19 July 2016

Keywords:
Compton
Gamma
Sources

ABSTRACT

We present the design of a photon–photon collider based on conventional Compton gamma sources for the observation of secondary $\gamma\gamma$ production. Two symmetric electron beams, generated by photocathodes and accelerated in linacs, produce two primary gamma rays through Compton back scattering with two high energy lasers. Tuning the system energy to the energy of the photon–photon cross section maximum, a flux of secondary gamma photons is generated. The process is analyzed by start-to-end simulations from the photocathodes to the propagation of the QED photons towards the detector. The new Monte Carlo code 'Rate Of Scattering Events' (ROSE) has been developed *ad hoc* for the counting of the QED events. Realistic numbers of the secondary gamma yield, referring to existing or approved set-ups and a discussion of the feasibility of the experiment are presented. Q3

PHYSICAL REVIEW ACCELERATORS AND BEAMS **20,** 043402 (2017)

Matter from light-light scattering via Breit-Wheeler events produced by two interacting Compton sources

Illya Drebot,[1] D. Micieli,[2,3] E. Milotti,[4] V. Petrillo,[5,1] E. Tassi,[2,3] and L. Serafini[1]

[1] *INFN-Sezione di Milano, via Celoria 16, 20133 Milano, Italy*
[2] *Università degli Studi della Calabria, Arcavacata di Rende (Cosenza), Italy*
[3] *INFN-Sezione di Cosenza, Arcavacata di Rende (Cosenza), Italy*
[4] *Università di Trieste and INFN-Sezione di Trieste, Via Valerio 2, 34127 Trieste, Italy*
[5] *Università degli Studi di Milano, via Celoria 16, 20133, Milano, Italy*

(Received 24 December 2016; published 26 April 2017)

We present the dimensioning of a photon-photon collider based on Compton gamma sources for the observation of Breit-Wheeler pair production and QED $\gamma\gamma$ events. Two symmetric electron beams, generated by photocathodes and accelerated in linacs, produce two gamma ray beams through Compton back scattering with two J-class lasers. Tuning the system energy above the Breit-Wheeler cross section threshold, a flux of electron-positron pairs is generated out of light-light interaction. The process is analyzed by start-to-end simulations. Realistic numbers of the secondary particle yield, referring to existing state-of-the-art set-ups and a discussion of the feasibility of the experiment taking into account the background signal are presented.

DOI: 10.1103/PhysRevAccelBeams.20.043402

I. INTRODUCTION

The recent development of high-energy, high-brilliance

observed to this date as well. Several different experimental schemes have been proposed [6–11], but not a single one has

A MeV-class Photon-Photon Scattering Machine based on twin Photo-Injectors and Compton Sources

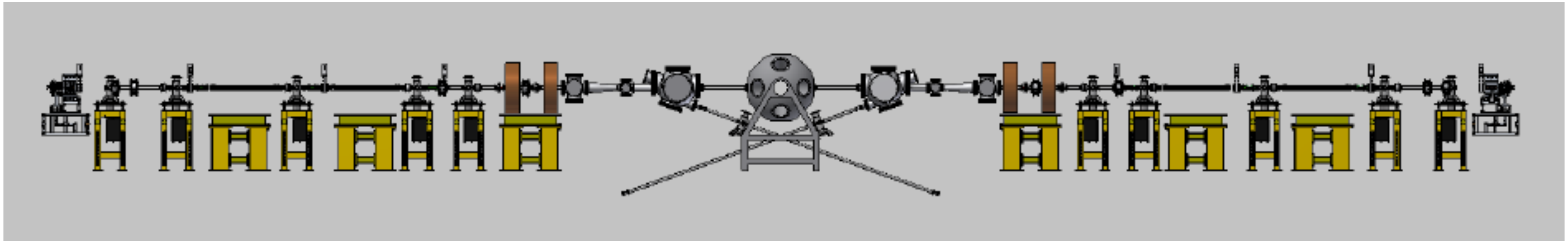

- *γ*-ray beams similar to those generated by Compton Sources for Nuclear Physics/Photonics
- issue with photon beam diffraction at low energy!
- Best option: twin system of high gradient *X-band* 200 *MeV* photo-injectors with *J-class ps* lasers (ELI-NP-GBS)

We evaluated the event production rate of several schemes for photon-photon scattering, based on *ultra-intense lasers*, *bremsstralhung machines*, *Nuclear Photonics gamma-ray machines*, etc, in all possible combinations: collision of 0.5 MeV photon beams is the only viable solution to achieve 1 $nbarn^{-1}$ in a reasonable measurement time.

1)Colliding 2 ELI-NP 10 PW lasers under construction (ready in 2018), $h\nu=1.2\ eV$, $f=1/60\ Hz$, we achieve (E_{cm}=3 eV): $L_{SC}=6.10^{45}$, cross section= 6.10^{-64}, events/sec=10^{-19}
2)Colliding 1 ELI-NP 10 PW laser with the 20 MeV gamma-ray beam of ELI-NP-GBS we achieve (E_{cm}=5.5 keV): $L_{SC}=6.10^{33}$, cross section=10^{-41}, events/sec = 10^{-8}

3)Colliding a high power Bremsstralhung 50 keV X-ray beam (unpolarized, 100 kW on a mm spot size) with ELI-NP-GBS 20 MeV gamma-ray beam (E_{cm}=2 MeV) we achieve: $L_{SC}=6.10^{22}$, cross section=1 μbarn, events/s = 10^{-8}

4) **Colliding 2 gamma-ray 0.5 MeV beams, carrying 10^{9} photons per pulse at 100 Hz rep rate, with focal spot size at the collision point of about 2 *μm*, we achieve: $L_{SC}=2.10^{26}$, cross section = 1 *μbarn*, events/s=2.10^{-4}, events/day=18, 1 *nanobarn*$^{-1}$ accumulated after 3 months of machine running.**

Nuclear Instruments and Methods in Physics Research B 402 (2017) 343–348

Contents lists available at ScienceDirect

Nuclear Instruments and Methods in Physics Research B

journal homepage: www.elsevier.com/locate/nimb

Production of TeV-class photons via Compton back-scattering on proton beams of a keV high brilliance FEL

L. Serafini, F. Broggi, C. Curatolo *

INFN-Milan and Universitá degli Studi di Milano, via Celoria 16, 20133 Milano, Italy

A R T I C L E   I N F O

Article history:
Received 6 December 2016
Received in revised form 25 January 2017
Accepted 2 March 2017
Available online 10 March 2017

Keywords:
Inverse Compton scattering off protons
Hadron-Photon collision

A B S T R A C T

Present availability of high brilliance photon beams as those produced by X-ray Free Electron Lasers in combination with intense TeV proton beams like those available at SPS, LHC or in the future at FCC, makes possible to conceive the production of TeV-class photons by Compton back-scattering of keV photons carried by the FEL radiation pulse. We present here the study of spectra and fluxes of the TeV-class photons, which are collimated in the typical $1/\gamma$ forward angle with respect to the propagation of the proton beam (γ is the proton beam relativistic factor). Using a room-temperature Linac based X-ray FEL delivering radiation pulses at 100 Hz up to 6 keV photon energy (implying a Linac electron beam energy in the 5–8 GeV range), fluxes of tens photons/s are achievable. It is also shown that a proper control of proton beam emittance and focusing at the interaction point is crucial to assure a reasonable energy spread of the photons emitted within an angle smaller than $1/\gamma$. Moreover, due to the reasonably small proton recoil, the back-

Study of Hadron-Photon Colliders for Secondary Beam Generation

Camilla Curatolo*[1], Francesco Broggi[1], Luca Serafini[1]
[1] INFN Milan, via Celoria 16, Milan, Italy
*camilla.curatolo@mi.infn.it

INFN Istituto Nazionale di Fisica Nucleare

IPAC17

INTRODUCTION

We summarize the potentialities of combining the hadron colliders for high energy physics and the FELs for applied and fundamental science with light, towards the generation of secondary beams with unprecedented characteristics.

The collision between their typical pulses of high energy protons and X-ray photons opens a **collider scenario with potentials for luminosities in excess of 10^{38} s^{-1}cm^{-2}, adequate to generate TeV-class pion, muon, neutrino and photon beams with very high phase space densities**.

SCHEME & PARAMETERS

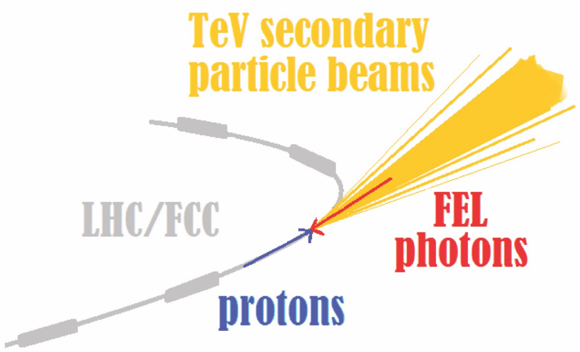

Table 1: Collider performances in various scenarios.

Proton source	E_{pr}	N_{pr}	spot size σ_0	Photon source	E_{ph}	N_{ph}
LHC	7 TeV	$2 \cdot 10^{11}$	7 μm	FEL	$10 - 20$ keV	10^{13}
FCC	50 TeV	10^{11}	1.6 μm	FEL	$1.43 - 12$ keV	10^{14}

ADVANTAGES

- Assuming head-on collision and $E_{ph} \ll E_{pr}$, the photon energy in proton rest frame is given by

$$E'_{ph} = (1 - \underline{\beta} \cdot \underline{e}_k)\, \gamma\, E_{ph} \simeq 2\, \gamma\, E_{ph}$$

  where $\gamma = E_{pr}/M_{pr}$, E_{pr}, $\underline{\beta}$ and M_{pr} are Lorentz factor, energy, velocity, mass of the proton and E_{pr}, $\underline{e}_k$ are energy, direction of propagation of the photon.

- The asymmetric collision of hadrons and FEL keV photons imparts a strong Lorentz boost to the secondary particles which are emitted at hundreds GeV energy in a small angle around the hadron beam propagation axis.

RELEVANT REACTIONS

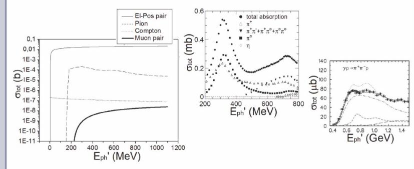

Figure 1: Total cross section σ_{tot} as a function of the photon energy E'_{ph} for different reactions: pion, double pion, electron/positron, muon pair photoproduction and inverse Compton scattering.

SECONDARY BEAMS: FLUXES, SPECTRA AND PHASE SPACES

Number of a certain kind of particle:

$$\mathcal{N} = \mathcal{L} \cdot \sigma_{tot} = \frac{N_{pr} N_{ph} r}{4\pi\sigma_0^2} \cdot \sigma_{tot}$$

with σ_{tot} total cross section, N_{pr}, N_{ph} number of protons, photons and r repetition rate.
Ex: FCC beam of $E_p = 50$ TeV, $N_{pr} = 10^{11}$ and $\sigma_0 = 1.6$ μm, $N_{ph} = 10^{14}$ and $r = 10$ MHz. $\mathcal{L} = 3.1 \cdot 10^{38}$ cm^{-2}s^{-1} and expected number of events per second specified in Table 2. Electron/positron pair production is the dominant reaction, but the proton beam is not affected since the e^-e^+ energy is low (see Fig. 2). Inverse Compton scattering does not substantially perturb the proton beam due to its very small cross section. Dominant proton beam loss rate given by the pion production: at FCC it is of about $\sim 1.3 \cdot 10^{11}$ protons/s, twenty times higher than loss rate $\sim 6.8 \cdot 10^9$ protons/s foreseen for p-p operation. With an expected number of circulating proton bunches of about 3000, the proton beam life-time would be of about 1/2 hour, nearly equivalent to the one set by beam dynamics and instabilities in FCC ring.

Table 2: Rate of events per second for $E_p = 50$ TeV, $\mathcal{L} = 3.1 \cdot 10^{38}$ cm^{-2}s^{-1} and various photon beam energies.

E_{ph} (keV)	$\mathcal{N}_{\pi^+}$ (s^{-1})	$\mathcal{N}_{\mu^-/\mu^+}$ (s^{-1})	$\mathcal{N}_{e^-/e^+}$ (s^{-1})
3	$6.8 \cdot 10^{10}$	$4 \cdot 10^5$	$5.4 \cdot 10^{12}$
5	$3.2 \cdot 10^{10}$	$1.2 \cdot 10^6$	$5.6 \cdot 10^{12}$
10	$3.1 \cdot 10^{10}$	$4.8 \cdot 10^6$	$6.5 \cdot 10^{12}$
12	$2.5 \cdot 10^{10}$	$5.6 \cdot 10^6$	$6.8 \cdot 10^{12}$

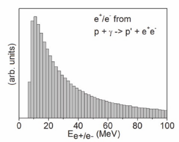

Figure 2: e^-/e^+ energy spectrum (MeV) for FCC protons at $E_{pr} = 50$ TeV and photons at $E_{ph} = 10$ keV colliding head-on. Homemade simulation code based on Geant4 differential cross sections.

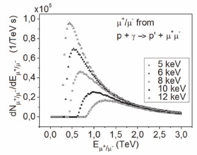

Figure 3: Number of muons from $p + \gamma \rightarrow p' + \mu^+\mu^-$ per second in 10 GeV bins produced by FCC protons at $E_{pr} = 50$ TeV and photons $E_{ph} = 5$, 10, 12 keV colliding head-on. Homemade simulation code based on Geant4 differential cross sections.

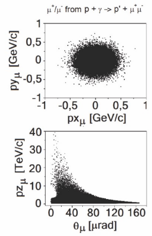

Figure 4: Phase spaces of muons from $p + \gamma \rightarrow p' + \mu^+\mu^-$ for $E_p = 50$ TeV and $h\nu = 10$ keV. Here $\epsilon^{\mu}_{n-cath} = 0.83$ mm·mrad.

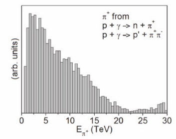

Figure 5: Spectrum of π^+ produced by FCC protons at $E_{pr} = 50$ TeV and photons at $E_{ph} = 6.566$ keV colliding head-on. Particles generated by Fluka and boosted to the laboratory frame.

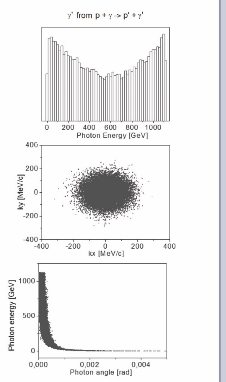

Figure 6: Scattered photons from LHC beam with $\epsilon_{n_x} = 2.5$ mm· mrad and photons at $E_{ph} = 6$ keV with $\sigma_0 = 5$ μm. Energy spectrum (GeV), transverse phase space (k_y vs k_x (MeV/c)) at the IP and energy (GeV) as a function of the emission angle θ (rad). Assuming $\mathcal{L} = 6.36 \cdot 10^{31}$ cm^{-2}s^{-1}: total number of photons per second $\mathcal{N} = 10.62$.

CONCLUSION

- Combined operation of LHC/FCC with a X-ray Free Electron Laser: opportunity of conceiving a hybrid **Hadron-Photon Collider at a luminosity exceeding 10^{38} s^{-1}cm^{-2}**.
- Hadron-Photon Collider to generate secondary beams of unique characteristics, via a highly boosted Lorentz frame corresponding to a very relativistic moving center of mass reference frame: **TeV-class secondary beams are produced with outstanding properties of low transverse emittance and collimation within very narrow forward angles**.
- Muon beams obtained by direct muon pair production or pion production and decay: quite low flux but outstanding phase space properties. The long life of the high energy generated muons (in excess of 10 ms) may offer the opportunity to accumulate them in a storage ring so to achieve muon collider requested bunch intensities.

REFERENCES

L. Serafini, C. Curatolo and V.Petrillo, *Low emittance pion beams generation from bright photons and relativistic protons*, arXiv:1507.06626v2, (2015)
C. Curatolo, *PhD Thesis: High brilliance photon pulses interacting with relativistic electron and proton beams*, https://air.unimi.it/handle/2434/358227, (2016)
C. Curatolo, F. Broggi and L. Serafini, *Phase space analysis of secondary beams generated in hadron-photon collisions*, in press on Nucl. Instr. Meth. Phys. Res. A
L. Serafini, F. Broggi and C. Curatolo, *Production of TeV-class photons via Compton back scattering on proton beams of a keV high brilliance FEL*, in press on Nucl. Instr. Meth. Phys. Res. B

Courtesy C. Curatolo

Reaction: $p+\gamma \to p' + \gamma'$

Total number of scattered photons per second

$$\mathcal{N} = \mathcal{L} \cdot \Sigma_p = \frac{N_p N_{ph} r}{4\pi\sigma_0^2} \cdot \Sigma_p$$

with

$$\Sigma_p = \left(\frac{M_e}{M_p}\right)^2 \Sigma_C = \left(\frac{0.511}{938}\right)^2 2\pi r_e^2 \frac{1}{\Delta}\left[\left(1-\frac{4}{\Delta}-\frac{8}{\Delta^2}\right)\log(1+\Delta)+\frac{1}{2}+\frac{8}{\Delta}-\frac{1}{2(1+\Delta)^2}\right]$$

total cross section and $\Delta \equiv 4\gamma h\nu/M_p$.

$$\begin{cases} \lim_{\Delta\to 0} \Sigma_p = \left(\frac{M_e}{M_p}\right)^2 \frac{8\pi r_e^2}{3}(1-\Delta) = \left(\frac{M_e}{M_p}\right)^2 \sigma_T(1-\Delta) = 2\cdot 10^{-7}(1-\Delta) \\ \lim_{\Delta\to\infty} \Sigma_p = \left(\frac{M_e}{M_p}\right)^2 \frac{2\pi r_e^2}{\Delta}\left(\log\Delta+\frac{1}{2}\right) = \frac{1.491\cdot 10^{-7}}{\Delta}\left(\log\Delta+\frac{1}{2}\right) \end{cases}$$

Table 1: Collider performances: $N_{ph} = 10^{13}$ photons at $h\nu = 6$ keV from FEL.

Proton source (case)	E_p	N_{pr}	spot size σ_0	Δ	$h\nu'$ [MeV]	$1/\gamma$ [μrad]
SPS	400 GeV	10^{12}	7 μm	0.01	5.117	2345
LHC	7 TeV	$2\cdot 10^{11}$	5 μm	0.19	89.55	134
FCC	50 TeV	10^{11}	1 μm	1.36	639.65	18.76

Table 2: Total cross section, luminosity, total number of photons per second, Mandelstam invariant s and energy range of the interaction for the 3 cases.

Case	Σ_p [barn]	$\mathcal{L}$ [cm^{-2}s^{-1}]	$\mathcal{N}$ [s^{-1}]	s [GeV^2]	Energy range
SPS	$1.944\cdot 10^{-7}$	$1.62\cdot 10^{32}$	31.57	0.889	Low
LHC	$1.66\cdot 10^{-7}$	$6.36\cdot 10^{31}$	10.62	1.047	Low
FCC	$0.98\cdot 10^{-7}$	$7.95\cdot 10^{32}$	78.54	2.079	Medium

f=100 Hz

SPS: 400 GeV 6 keV

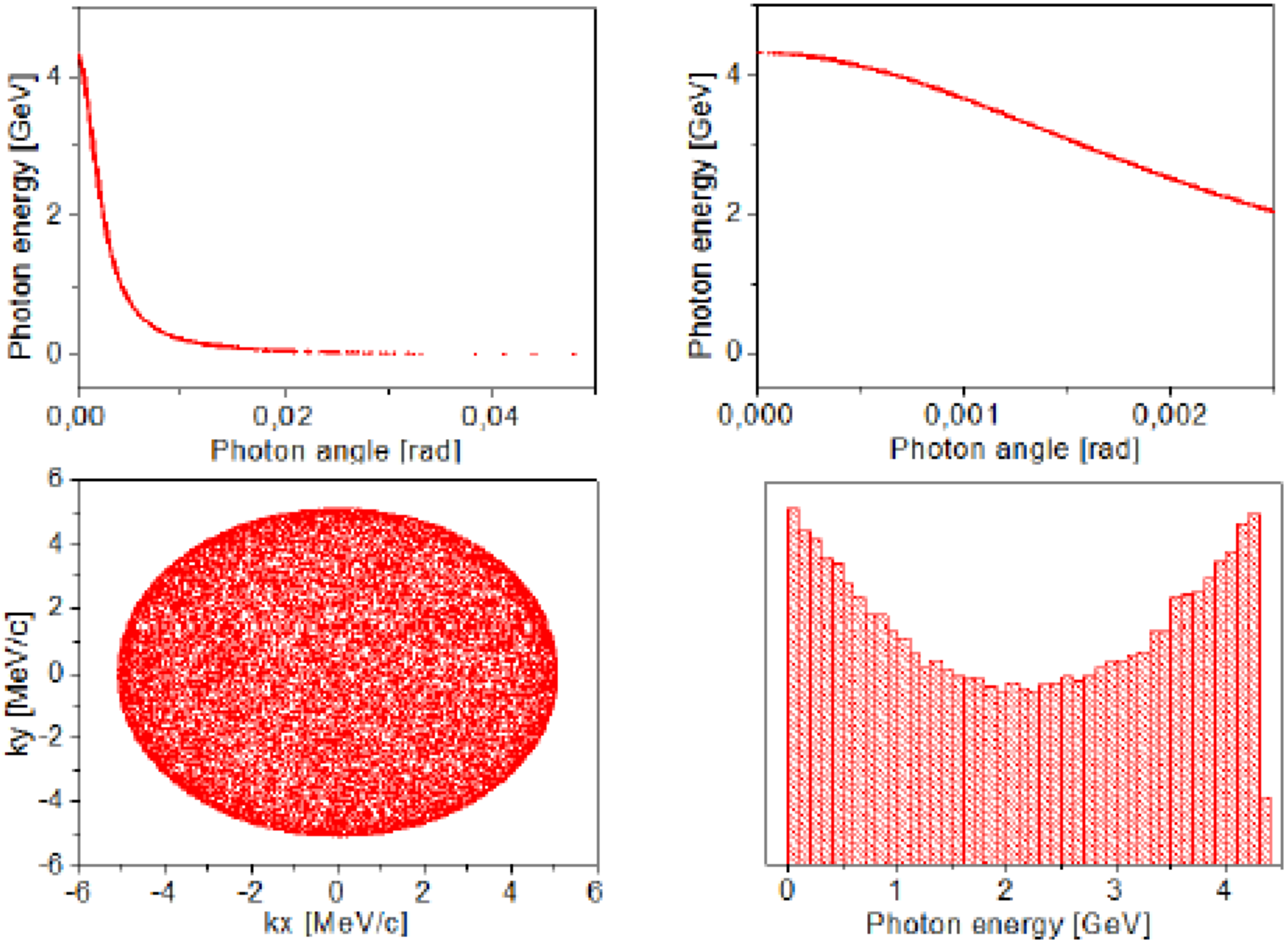

Figure 2: Analysis of the scattered photons in SPS case.

LHC: 7 TeV 6 keV

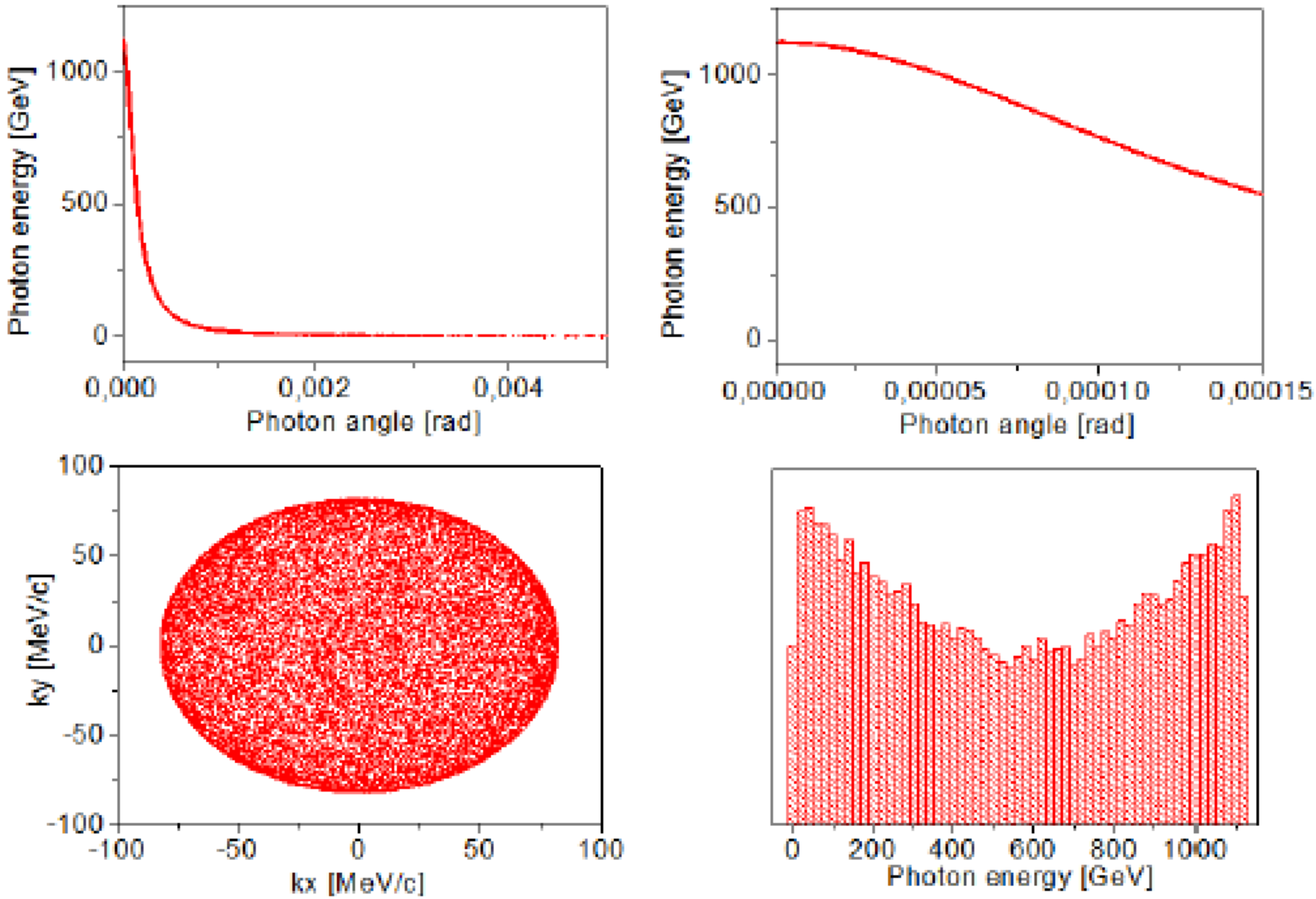

Figure 4: Analysis of the scattered photons in LHC case.

FCC: 50 TeV 6 keV

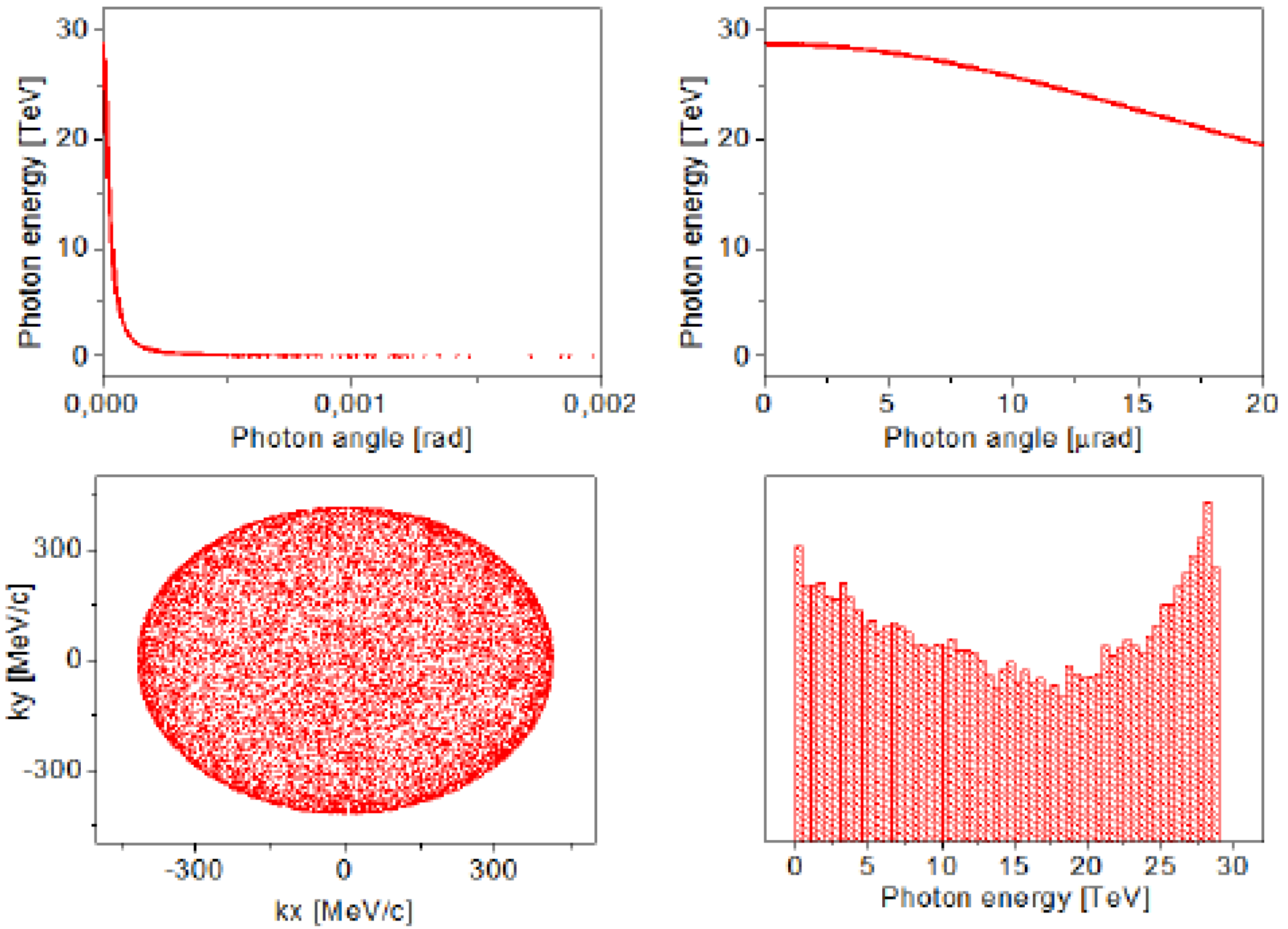

Figure 6: Analysis of the scattered photons in FCC case.

CONCLUSIONS on e-gamma colliders

- Compton Sources are opening an era of high brilliance photon beams spanning from keV to TeV energy with unprecedented phase space density features
- Medical Applications are being enabled by compact Thomson Sources that can be located and operated inside Hospitals
- Nuclear Photonics is beginning an era of research and discovery enabled by MeV-class Compton back-scattered photon beams
- MeV-class invariant mass photon-photon colliders are now conceivable by exploiting the potentialities of advanced Compton Sources – basic energy physics oriented

CONCLUSIONS on Hadron-Photon Colliders

- Several advantages of exploiting the "formidable" portfolio of hadron beams available at CERN to generate very high energy photons by Compton back-scattering: high intensity beams -> high luminosity collisions, combined to low recoil regime, assuring very high photon polarization
- Hadron beam life time not perturbed by hadron-FEL collisions
- Scientific motivation… nobody produced so far TeV photons tunable, polarized, nsec synchronized, highly collimated
- The cost – a 2 Angstrom FEL, FEL radiation beam-lines, interaction region, etc

C. Curatolo, *PhD Thesis: High brilliance photon pulses interacting with relativistic electron and proton beams*, `https://air.unimi.it/handle/2434/358227`, (2016)

Iniziativa MariX – UniMi/INFN

Multi-Disciplinary advanced research infrastructure with X-rays

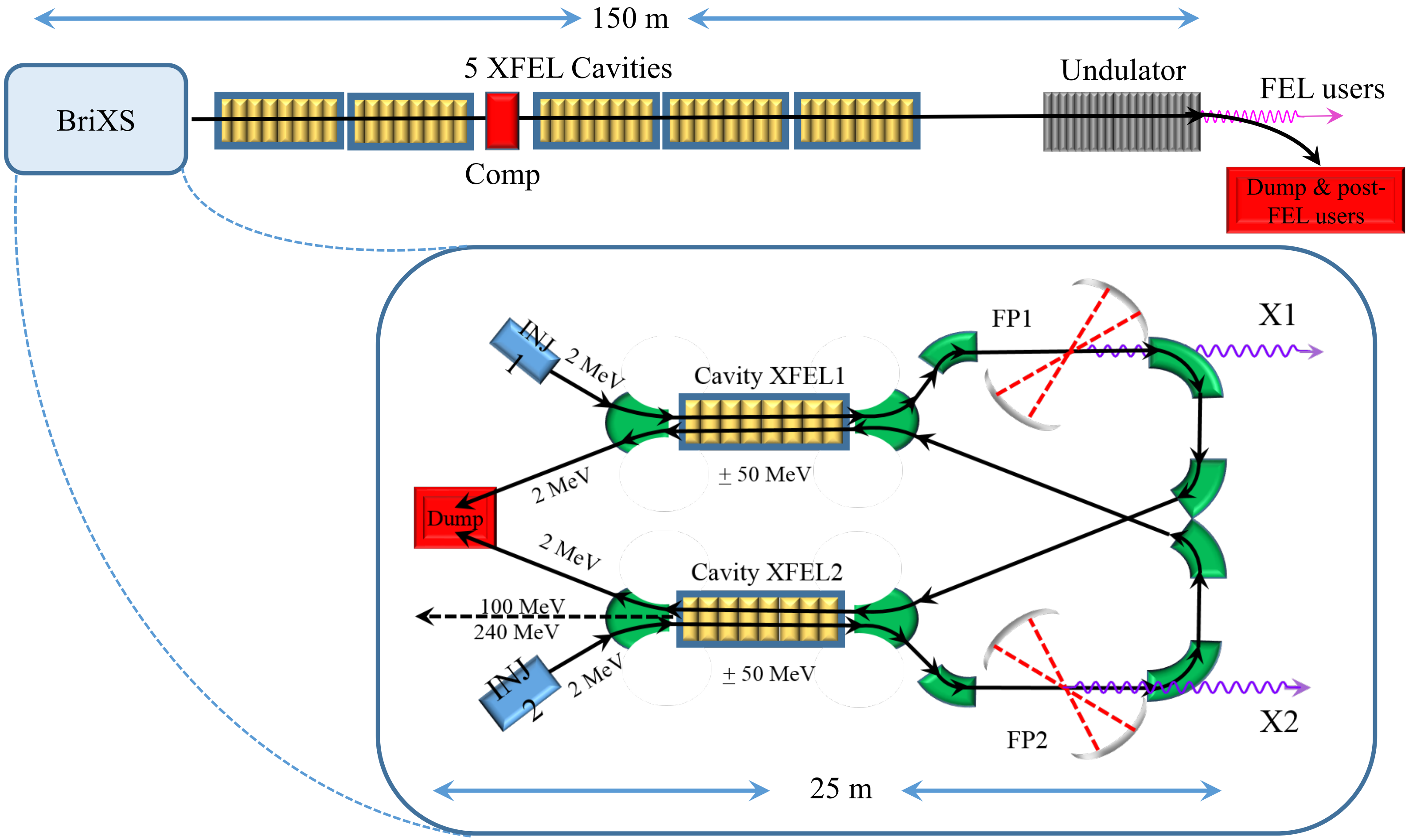

http://www.fisica.unimi.it/ecm/home/aggiornamenti-e-archivi/tutte-le-notizie/content/marix-un-progetto-interdipartimentale-per-il-nuovo-campus-di-unimi.0000.UNIMIDIRE-58782

Courtesy V. Petrillo

Extra-Slides (optional) after this one
(all green dot)

Low emittance pion beams generation from bright photons and relativistic protons

L. Serafini, C. Curatolo and V. Petrillo
INFN-Milan and Università degli Studi di Milano, via Celoria 16, 20133 Milano, Italy
(Dated: July 11th, 2015)

Present availability of high brilliance photon beams as those produced by X-ray Free Electron Lasers in combination with intense TeV proton beams typical of the Large Hadron Collider makes it possible to conceive the generation of pion beams via photo-production in a highly relativistic Lorentz boosted frame: the main advantage is the low emittance attainable and a TeV-class energy for the generated pions, that may be an interesting option for the production of low emittance muon and neutrino beams. We will describe the kinematics of the two classes of dominant events, i.e. the pion photo-production and the electron/positron pair production, neglecting other small cross-section possible events like Compton and muon pair production. Based on the phase space distributions of the pion and muon beams we will analyze the pion beam brightness achievable in three examples, based on advanced high efficiency high repetition rate FELs coupled to *LHC* or Future Circular Collider (*FCC*) proton beams, together with the study of a possible small scale demonstrator based on a Compton Source coupled to a Super Proton Synchrotron (*SPS*) proton beam.

I. INTRODUCTION

One of the main challenges of present muon collider design studies is the capture/cooling stage of muons after generation by intense GeV-class proton beams impinging on solid targets: this mechanism produces pions further decaying into muons and neutrinos. As extensively analyzed in Ref. [1, 2], the large emittance of the generated pion beams, which is mapped into the muon beam, is mainly given by the mm-size beam source at the target (i.e. the proton beam focal spot size) and by Coulomb scattering of protons and pions propagating through the target itself, inducing large transverse momenta which in

Their combined capability of producing ultra-high phase space density particle beams is the base of our strategy for generating low emittance pion, muon and neutrino beams, using collisions between two counter-propagating beams of highly relativistic protons and ultra-high intensity photons. The extremely high luminosity achievable by such a collider (10^{38} cm^{-2}s^{-1}) can compensate for the low efficiency of the pion photo-production which has a total cross section of $\simeq$ 220 μbarn with 300 MeV photons, much smaller than GeV-proton based pion production ($\simeq$ 20 mbarn).

There are two crucial aspects in such a collision scheme. The first is the much higher energy of the X-ray

Download PDF   Export   Search ScienceDirect   Advanced search

Article outline   Show full outline

Figures and tables

Table 1

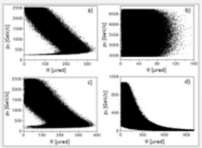

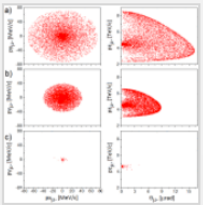

Nuclear Instruments and Methods in Physics Research Section A: Accelerators, Spectrometers, Detectors and Associated Equipment

Available online 2 September 2016

In Press, Accepted Manuscript — Note to users

Phase space analysis of secondary beams generated in hadron-photon collisions

C. Curatolo, F. Broggi, L. Serafini

Show more

http://dx.doi.org/10.1016/j.nima.2016.09.002

Abstract

Present availability of high brilliance photon beams in combination with intense TeV hadron beams makes it possible to conceive the generation of low emittance TeV-class energy pion/muon beams via photoproduction in a highly relativistic Lorentz boosted frame. We analyze the secondary beams brightness achievable by the coupling of

RELEVANT REACTIONS

$\mathbf{p} + \mathbf{h}\nu \to \mathbf{p}' + \mu^-\mu^+$	Best way to produce both signs muons. Threshold energy: $h\nu'^{th} = 235$ MeV.

$$p + h\nu \to n + \pi^+ \to n + \mu^+ + \nu_\mu$$

$$\left.\begin{array}{l} p + h\nu \to p' + e^-e^+ \\ p + h\nu \to p' + h\nu' \end{array}\right\} \text{ side effects}$$

- Photon energy in proton rest frame is

$$h\nu' = h\nu\gamma(1 - \underline{\beta} \cdot \underline{e}_k) \simeq 2\gamma h\nu$$

where $\underline{\beta}$ is the velocity of the proton, $\underline{e}_k$ is the direction of propagation of the photon and $\gamma = E_p/M_p$.

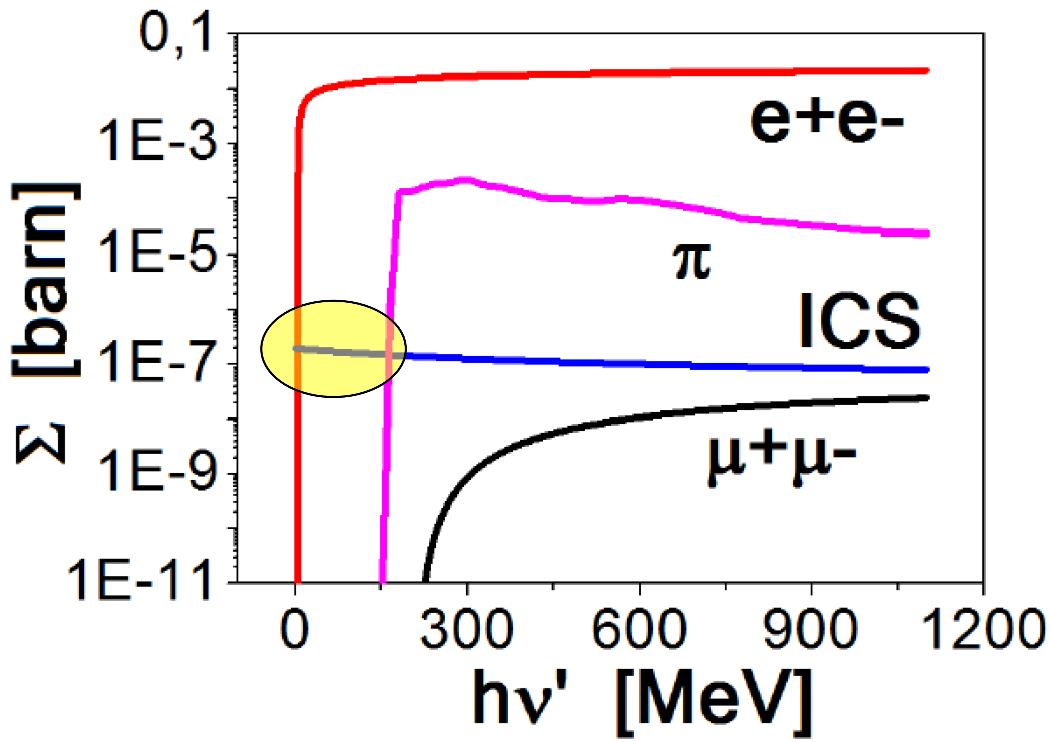

Figure 4: Total cross sections of relevant reactions.

Table 3: Transverse normalized emittance, spot size and total number of photons per second for the 3 cases.

Case	ϵ_T^N [mm·mrad]	σ_0 [μ]	p_T^{RMS} [MeV/c]	$\mathcal{N}$ [s^{-1}]
SPS	2.5	15	156.33	6.88
LHC	2.5	10	234.5	2.65
FCC	2.5	5	469	3.14

$$bw \propto \gamma^2 \left\langle \sigma'^2 \right\rangle = 2\frac{\varepsilon_n^2}{\sigma_x^2}$$

SPS with emittance

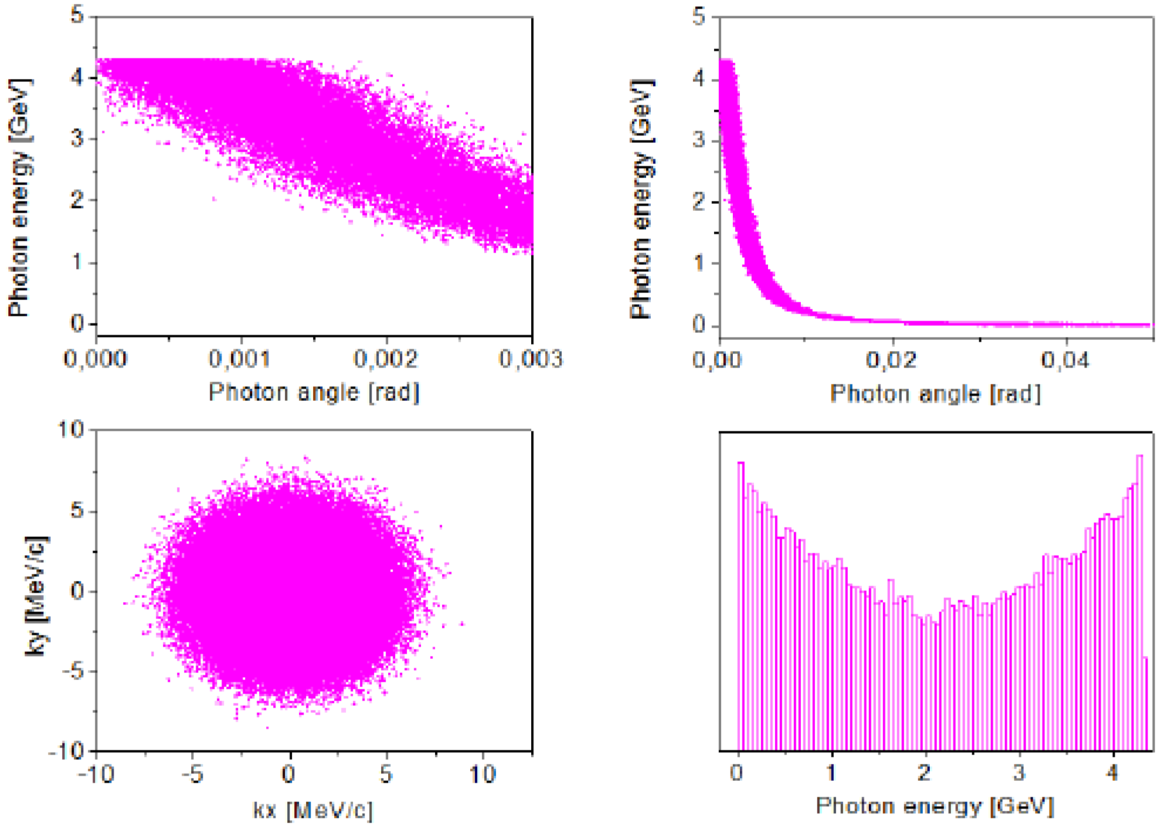

Figure 8: Analysis of the scattered photons in SPS case with $\sigma_0 = 15$ μrad and $\epsilon_T^N = 2.5$ mm·mrad.

LHC with emittance

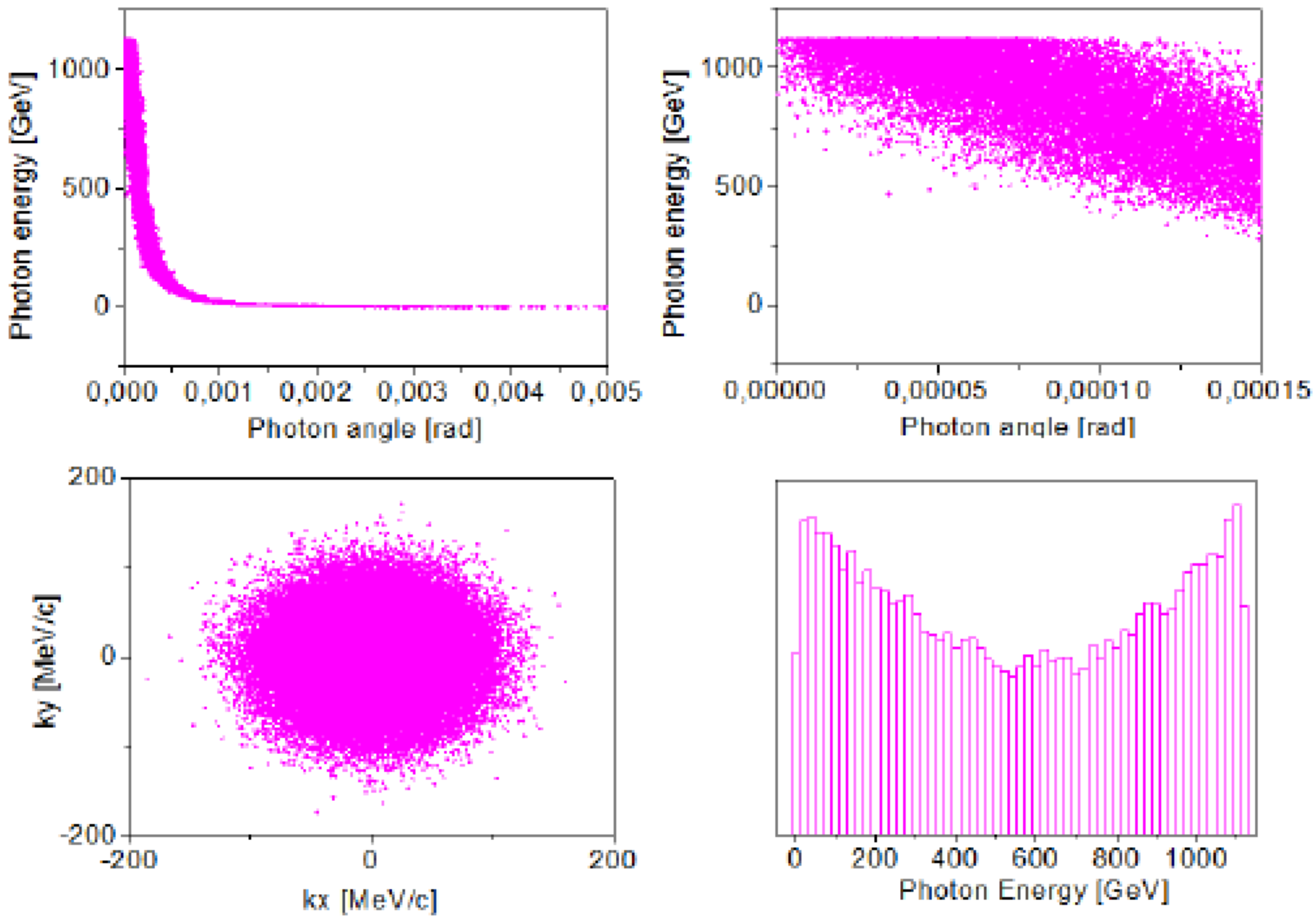

Figure 9: Analysis of the scattered photons in LHC case with $\sigma_0 = 10\ \mu$rad and $\epsilon_T^N = 2.5$ mm·mrad.

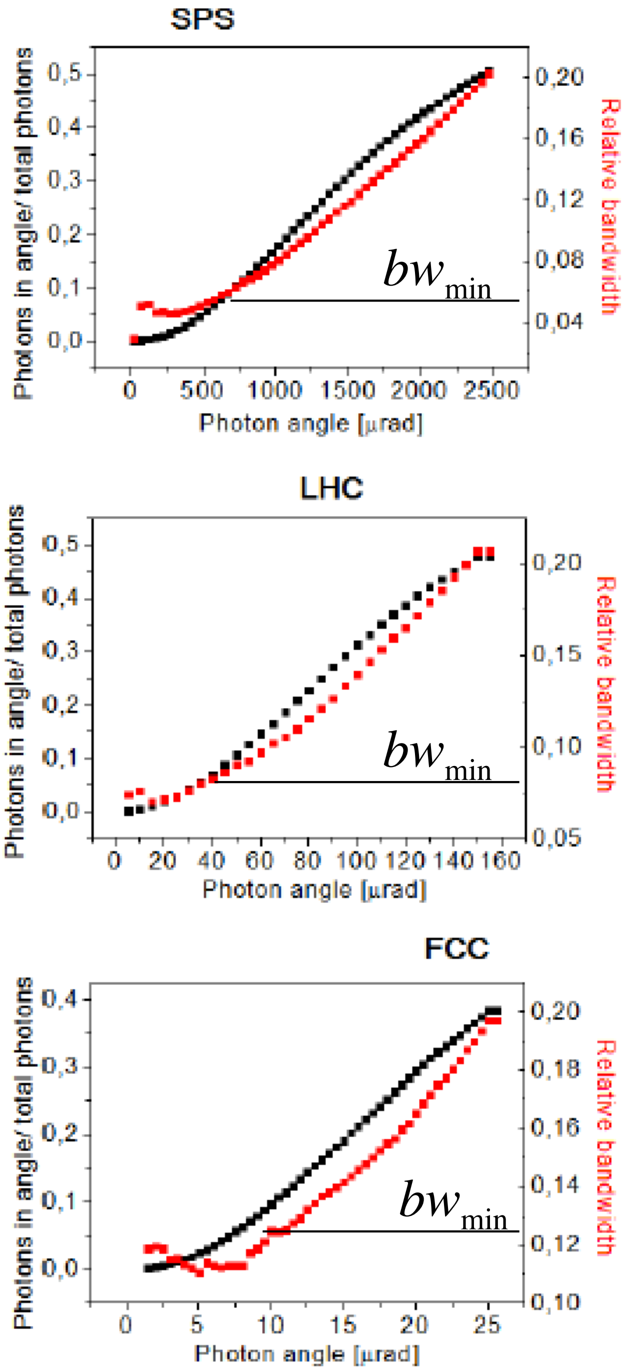

Figure 11: numero e banda caso magenta.

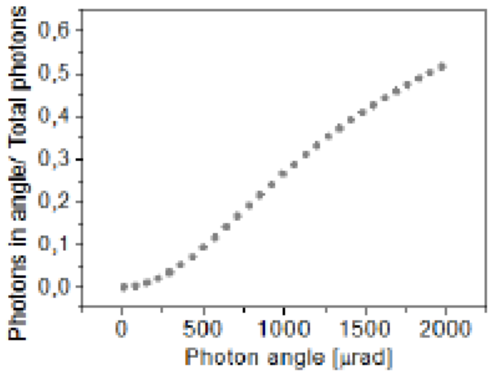

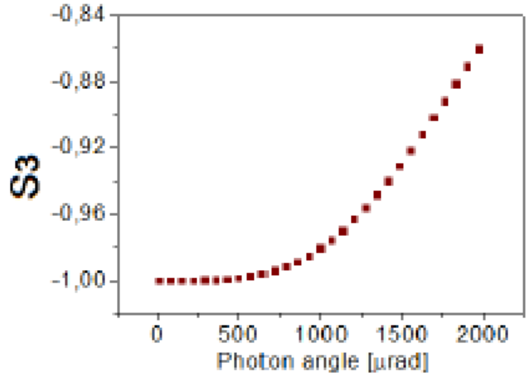

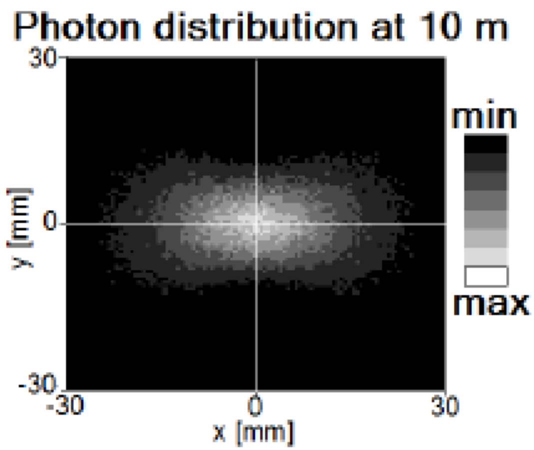

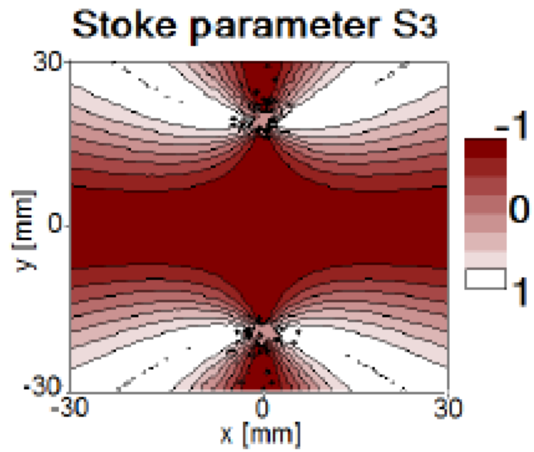

SPS

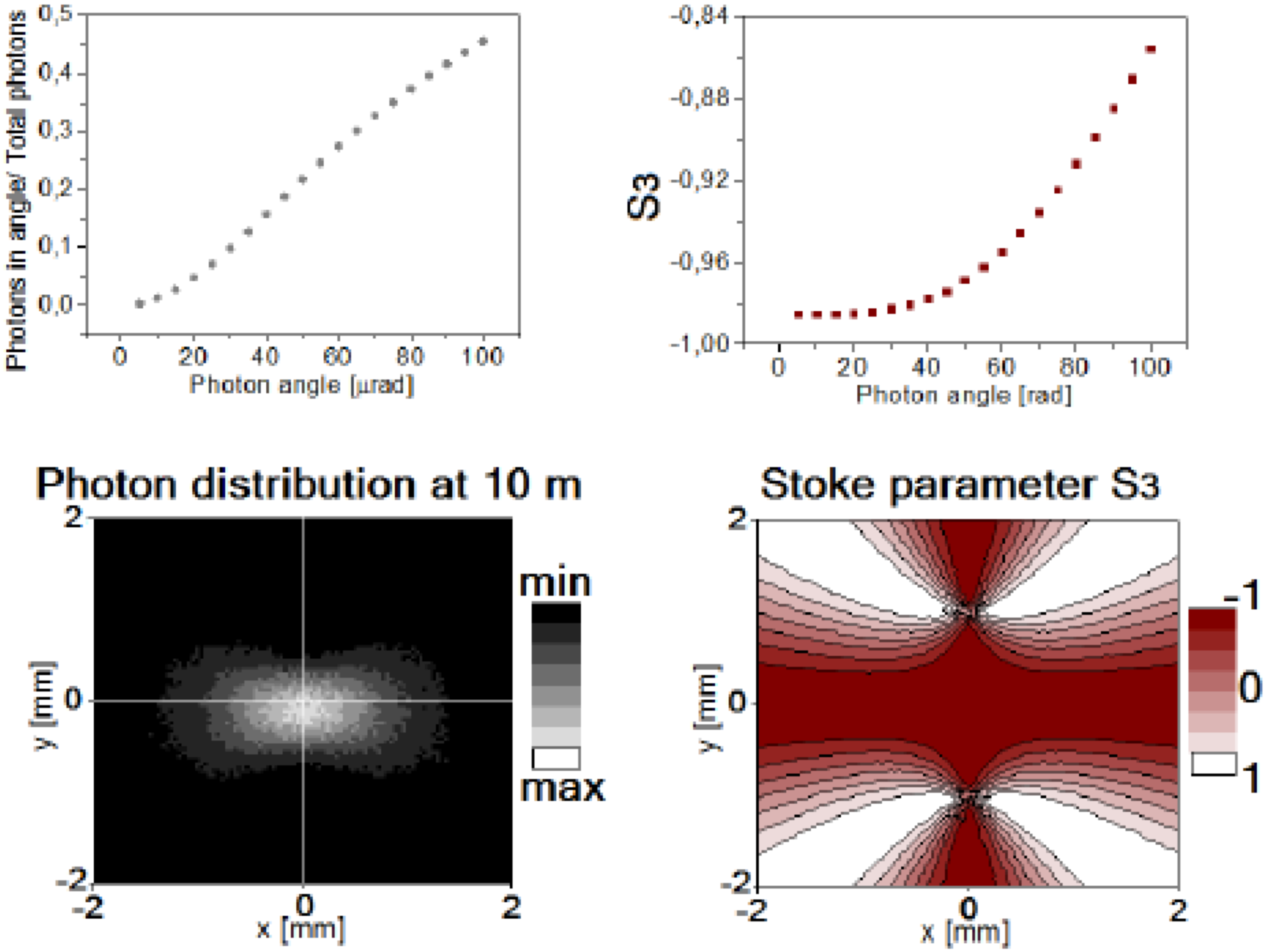

Figure 13: Equivalente LHC.

Table 2: Rate of events per second for $E_p = 50$ TeV, $\mathcal{L} = 3.1 \cdot 10^{38}$ cm^{-2}s^{-1} and various photon beam energies.

$h\nu$ [keV]	$\mathcal{N}_\pi$ [s^{-1}]	$\mathcal{N}_{\mu^-\mu^+}$ [s^{-1}]	$\mathcal{N}_{e^-e^+}$ [s^{-1}]
1.43	$1.86 \cdot 10^{10}$	0	$4.5 \cdot 10^{12}$
2.21	$3.72 \cdot 10^{10}$	$1.25 \cdot 10^{4}$	$5 \cdot 10^{12}$
3	$6.5 \cdot 10^{10}$	$4 \cdot 10^{5}$	$5.4 \cdot 10^{12}$
10	$8.6 \cdot 10^{9}$	$4.8 \cdot 10^{6}$	$6.5 \cdot 10^{12}$
12	$6.8 \cdot 10^{9}$	$5.6 \cdot 10^{6}$	$6.8 \cdot 10^{12}$

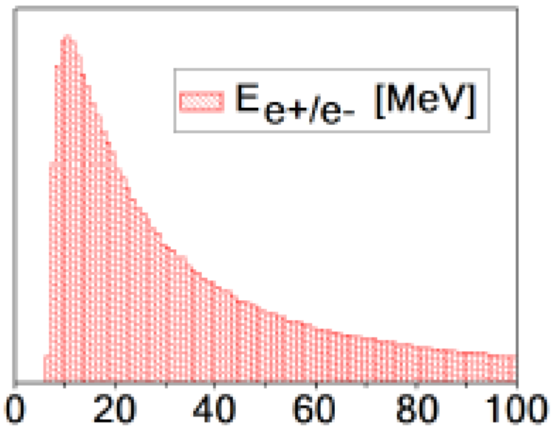

Figure 5: e^-e^+ energy spectrum [MeV] for $E_p = 50$ TeV and $h\nu = 10$ keV.

Hadron Photon Colliders as photo-cathode sources of low emittance muon beams

Camilla Curatolo*[1], Francesco Broggi[1], Luca Serafini[1]
[1] INFN Milan and University of Milan, via Celoria 16, Milan, Italy
*camilla.curatolo@mi.infn.it

INTRODUCTION

Muon colliders: highest lepton-antilepton collision energies for precision measurements of particles like the Higgs boson and for further study of their properties.

Main challenges of present muon collider design studies: capture and cooling stage of muons after generation by intense GeV-class proton beams impinging on solid targets producing pions further decaying into muons and neutrinos. Large emittance of pion beams, mapped into muon ones, mainly given by the mm-size beam source at the target and by Coulomb scattering of protons and pions propagating through the target.

We discuss the possibility to generate **low emittance muon beams at hundreds GeV by colliding high energy Large Hadron Collider/Future Circular Collider like protons and counterpropagating FEL keV photons**.

SCHEME & PARAMETERS

PROTON-PHOTON head-on collision

Energy and Lorentz factor of Center of Mass, assuming $E_p >> h\nu$, are

$$E_{CM} = \sqrt{2E_p h\nu - 2(\underline{p}_p \cdot \underline{k}) + M_p^2} \qquad \gamma_{CM} = \frac{E_{tot}^{LAB}}{E_{CM}} \simeq \frac{E_p + h\nu}{\sqrt{4E_p h\nu + M_p^2}}$$

where $E_p, \underline{p}_p$ and $h\nu, \underline{k}$ are energy, momentum of proton and photon in LAB. $M_p = 938$ MeV/c^2 is the proton mass.

Table 1: Collider performances in various scenarios.

Proton source	E_p	N_{pr}	spot size σ_0	Photon source	$h\nu$	N_{ph}
LHC	7 TeV	$2 \cdot 10^{11}$	7 μm	FEL	$10-20$ keV	10^{13}
FCC	50 TeV	10^{11}	1.6 μm	FEL	$1.43-12$ keV	10^{14}
SPS	400 GeV	$2 \cdot 10^{12}$	18 μm	ICS	$180-1450$ keV	10^{8-9}

ADVANTAGES

- Photon energy in proton rest frame is

$$h\nu' = h\nu\gamma(1 - \underline{\beta} \cdot \underline{e}_k) \simeq 2\gamma h\nu$$

  where $\underline{\beta}$ is the velocity of the proton, $\underline{e}_k$ is the direction of propagation of the photon and $\gamma = E_p/M_p$.
- The asymmetric collision of hadrons and FEL keV photons imparts a strong Lorentz boost to the secondary particles which are emitted at hundreds GeV energy in a small angle around the hadron beam propagation axis.

RELEVANT REACTIONS

$\mathrm{p} + \mathrm{h}\nu \rightarrow \mathrm{p}' + \mu^-\mu^+$	Best way to produce both signs muons. Threshold energy: $h\nu'^{th} = 235$ MeV.

$$p + h\nu \rightarrow n + \pi^+ \rightarrow n + \mu^+ + \nu_\mu$$

$$\left.\begin{array}{l} p + h\nu \rightarrow p' + e^-e^+ \\ p + h\nu \rightarrow p' + h\nu' \end{array}\right\} \text{side effects}$$

High Recoil of 12 keV photons scattering off 7 GeV electrons

$$\Sigma_{TH} = 670 \; mbarn \; 0-recoil$$

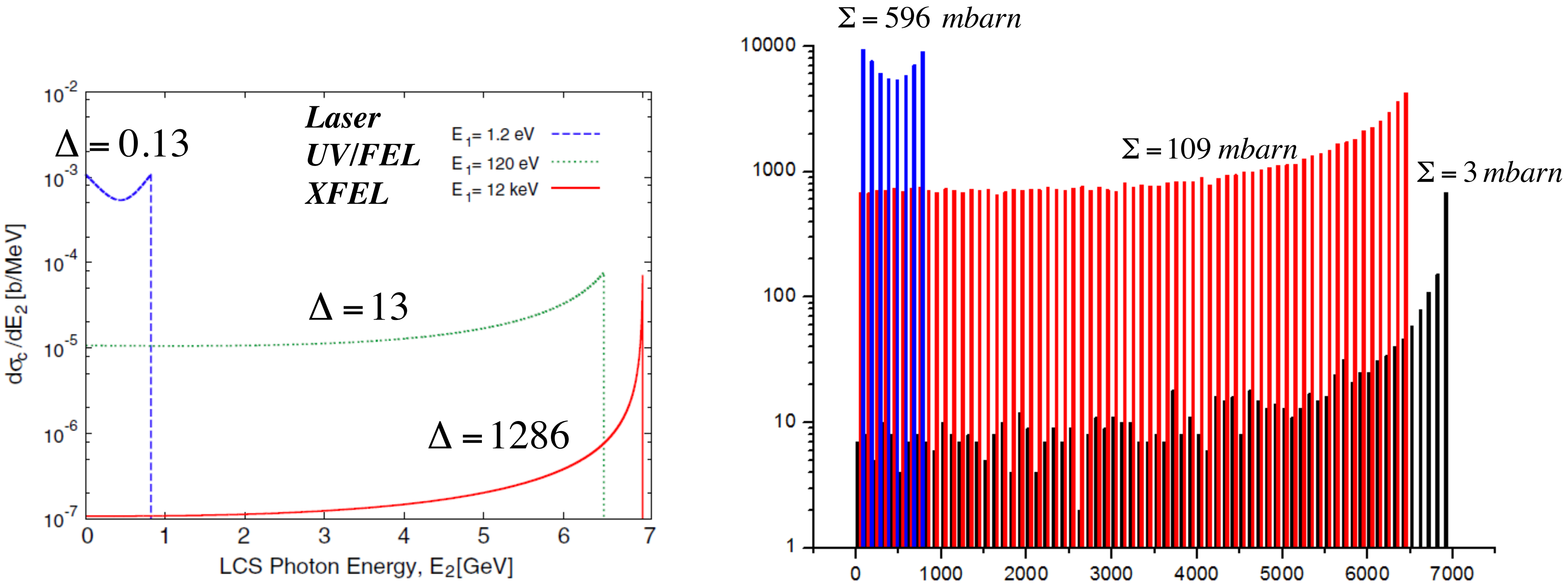

TABLE I. Parameters of the XFELO for the baseline design of XFELO-γ.

Electron beam	
Energy (E_e)	7 GeV
Bunch charge (Q)	40 pC
rms energy spread ($\sigma_{\Delta E}$)	1.4 MeV
Normalized rms emittance (ϵ_n)	0.082 mm-mrad
rms bunch length (τ_e)	2 ps
Bunch repetition (f)	3 MHz
Undulator	
Undulator parameter (K)	1.414
Pitch (λ_u)	1.88 cm
The number of periods (N_u)	3000
FEL	
Wavelength (λ)	1 Å
Energy (E_1)	12.3 keV
Cavity length (L_c)	100 m
Small signal gain	50%
Round-trip loss	17%
Out-couple	4%
rms pulse length (τ_X)	0.85 ps
rms energy spread ($\sigma_{\Delta E_1}$)	2.3 meV
Collision parameters	
Beta function (β^*)	10 m
Rayleigh length (Z_R)	10 m
Electron beam rms size (σ_e)	7.7 μm
Electron beam rms divergence (σ_e')	0.77 μrad
X-ray beam rms size (σ_X)	8.9 μm
X-ray beam rms divergence (σ_X')	0.89 μrad
The number of electrons (N_e)	2.5×10^8
The number of x-ray photons (N_X)	2.0×10^{10}

TABLE II. Calculated performance of the XFELO-γ with parameters listed in Table I.

Repetition	3 MHz
Peak energy	6.9922 GeV
Bandwidth (FWHM)	12 MeV
Flux (100% BW)	4900 ph/s
Flux (1% BW)	1700 ph/s
Flux (0.1% BW)	460 ph/s

0.0016 *photon scattered per bunch collision...*

$$\boxed{N_\gamma = \mathbf{L}\sigma_T} \qquad \sigma_T = 0.67 \cdot 10^{-24}\, cm^2 = 0.67 \ \ barn \qquad \boxed{\sigma_T = \frac{8\pi}{3} r_e^2}$$

(3)
$$L = \frac{N_{el} N_{las}}{2\pi\left(\sigma_0^2 + \frac{w_0^2}{4}\right)} f \cdot n_{RF} \cdot \delta_\phi$$

(4)
$$N_\gamma = 4.2 \cdot 10^8 \frac{U_L[J]Q[pC]f_{RF}n_{RF}\delta_\phi}{h\nu[eV]\left(\sigma_x^2[\mu m] + \frac{w_0^2[\mu m]}{4}\right)}$$

Formulas derived from Luminosity extensively tested vs. ELI-NP-GBS simulations

$$N_\gamma^{bw} = 0.7 \cdot 10^9 \frac{U_L[J]Q[pC]f_{RF}n_{RF}\delta_\phi}{h\nu[eV]\left(\sigma_x^2[\mu m] + \frac{w_0^2[\mu m]}{4}\right)} \cdot \gamma^2 \vartheta^2$$

$correction\ factor\ for\ collision\ angle\ \phi << 1$

$\delta_\phi = \frac{1}{\sqrt{\ldots}}$

$Assumptions: \quad weak\ \ diffraction\ \ c\sigma_t < Z_0 \equiv \frac{\pi w_0^2}{\lambda}$

$and\ \ \sigma_{z-el} < \beta_0 \equiv \frac{\gamma\sigma_0^2}{\varepsilon_n} \quad and\ \ ideal\ \ time-space\ \ overlap$

$implies: \quad \sigma_t < a\ \ few\ \ psec \quad \sigma_{z-el} < 300\ \ \mu m$

EPJ Web of Conferences **117**, 05002 (2016) DOI: 10.1051/epjconf/201611705002
NN2015

High intensity X/γ photon beams for nuclear physics and photonics

L. Serafini[1], D. Alesini[2], A. Bacci[1], N. Bliss[5], K. Cassou[3], C. Curatolo[1], I. Drebot[1], K. Dupraz[3], A. Giribono, V. Petrillo[1], L. Palumbo[4], C. Vaccarezza[2], A. Variola[2], F. Zomer[3].

[1] INFN, Sezione di Milano and Università degli Studi di Milano, Milano, Italy
[2] LNF-INFN, Frascati (RM), Italy
[3] LAL-Orsay, Orsay, France
[4]Università la Sapienza, Roma, Italy
[5] STFC Daresbury Laboratory, Warrington, UK

and references therein

Efficiency η of a Comtpon Source
(number of photons back-scattered per electron)

$$\eta \equiv \left.\frac{\left.N_\gamma^{bw}\right|_{fullspectrum}}{N_e}\right|_{shot} = 67\frac{U_L[J]\delta_\phi}{h\nu_L[eV]\left(\sigma_x^2[\mu m]+\frac{w_0^2[\mu m]}{4}\right)}$$

$ELI-NP \quad \eta \cong 0.025$

$STAR \quad \eta \cong 0.4$

$SPARC-LAB \ \eta \cong 1$

$\boxed{\eta \propto a_0^2 N_L}$

can exceed 1 when multiple scattering regime is reached

η measures the transparency of laser pulse to the electron beam

ELI-NP-GBS T. D. R.,http://arxiv.org/abs/1407.3669, (2014)

Vaccarezza C. and al., Proc. IPAC2014, Dresden, Germany, (2014)

Spectral broadening due to ultra-focused beams:
Thomson Source classically described as a
Laser Syncrotron Light Source

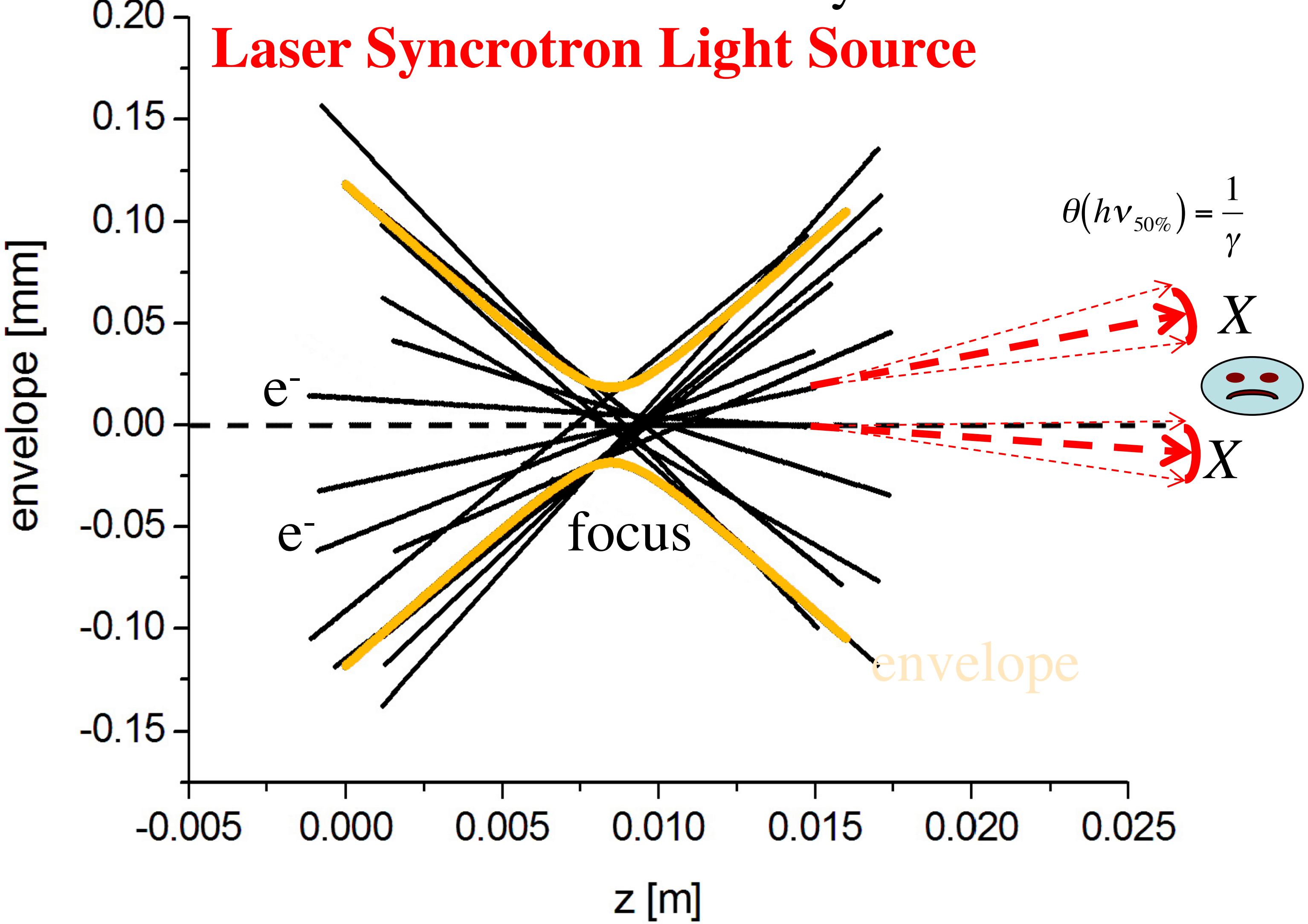

Scattering angle in Thomson limit (no recoil) is small, i.e. < $1/\gamma$

Spectral broadening due to ultra-focused beams:
Thomson Source classically described as a
Laser Syncrotron Light Source

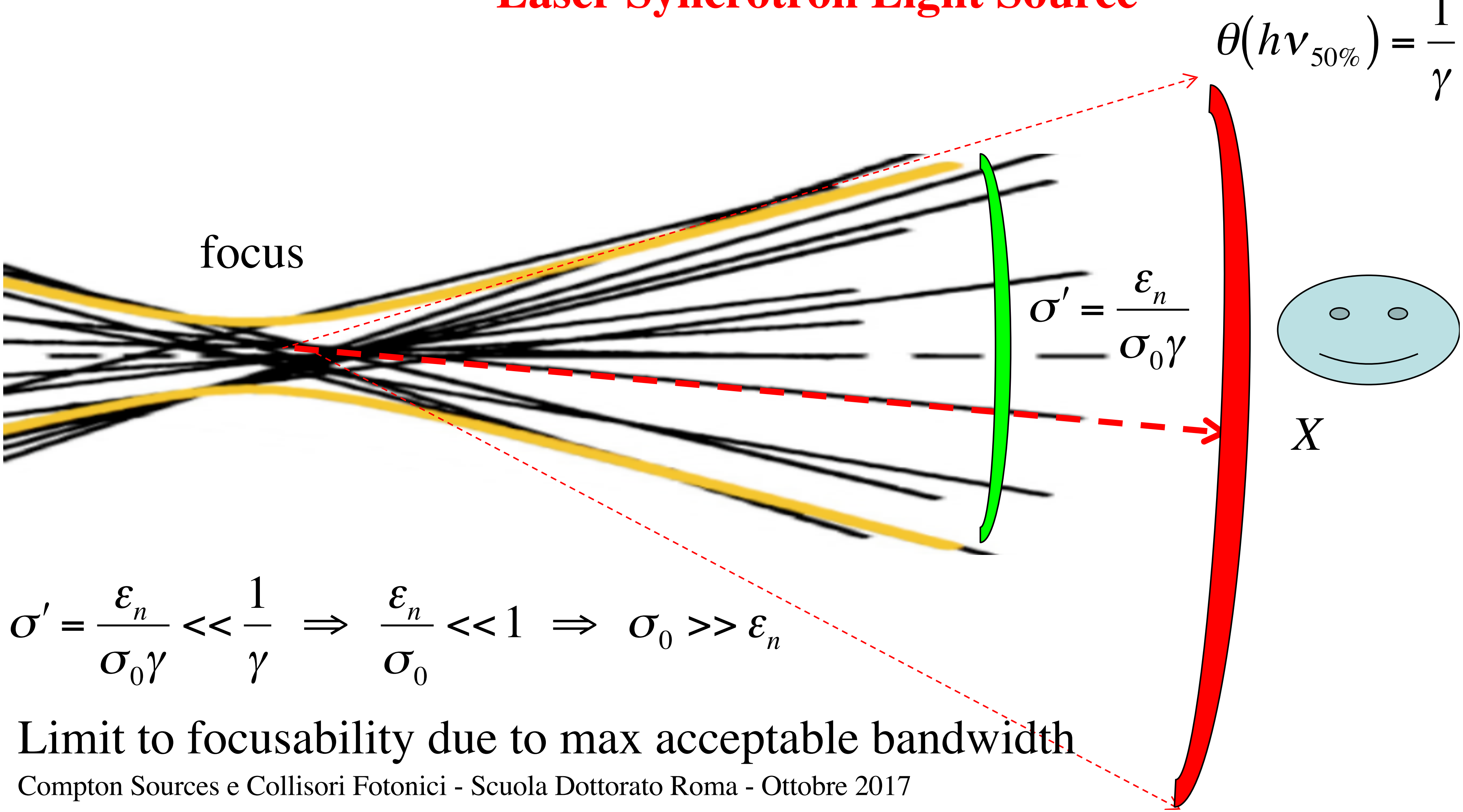

$$\sigma' = \frac{\varepsilon_n}{\sigma_0 \gamma} << \frac{1}{\gamma} \Rightarrow \frac{\varepsilon_n}{\sigma_0} << 1 \Rightarrow \sigma_0 >> \varepsilon_n$$

Limit to focusability due to max acceptable bandwidth

$$Peak\ \ Brilliance\ \ B_\gamma \equiv \frac{N_\gamma^{bw}}{\varepsilon_\gamma^2 \dfrac{\Delta\nu_\gamma}{\nu_\gamma}\sigma_t}$$

$$B_\gamma = 5.6\cdot 10^{19}\frac{\gamma^2 U_L[J]Q[pC]}{h\nu[eV]\dfrac{\Delta\nu_\gamma}{\nu_\gamma}\sigma_0^2 w_0^2\sigma_t}$$

UH-FLUX
Advanced Compton/THz source based on novel design of coupled SC RF cavities

A. Seryi, JAI

Collaboration of UK centers JAI, CI, STFC and UK industry

- Three patents on the technology, publication prepared
- Develop in collaboration
  - With Cockcroft and STFC, most recently with Fermilab
- Working with ISIS Innovation and companies
  - Niowave company USA and Sheakespear Engineering, UK
- Developing IPS, PRD, Innovate UK grant proposals
- Positive review by JAI AB and peers

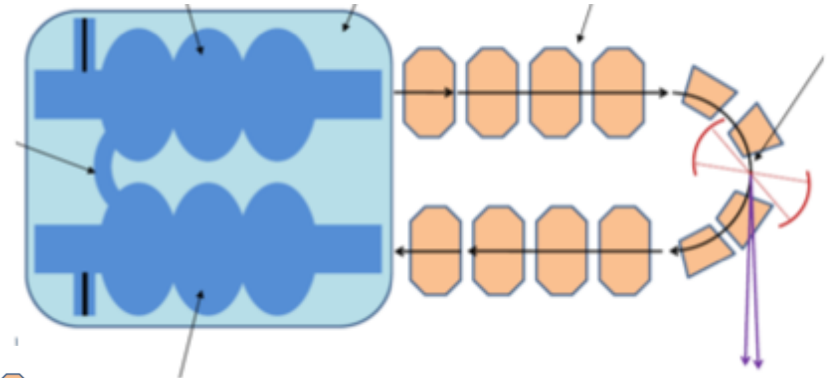

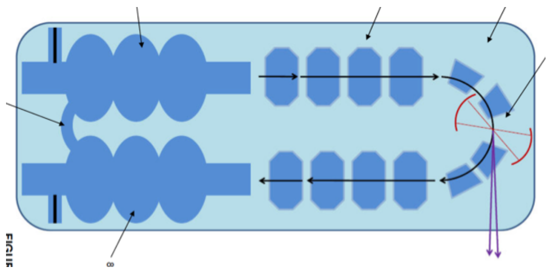

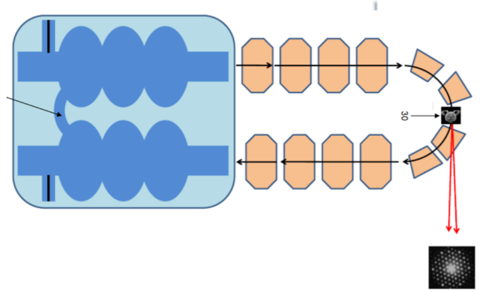

Compton or Coherent Smith Purcell (THz)
Recovery linac

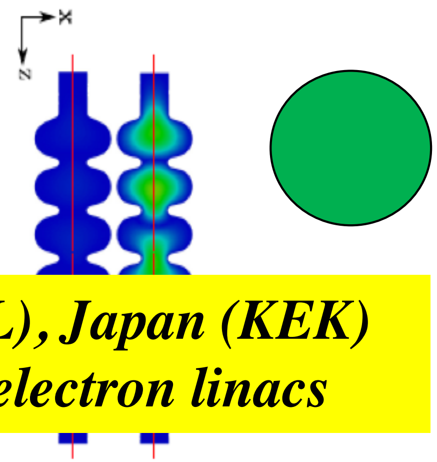

[1] International (PCT) Patent Application No. PCT/GB2012/052632 (WO2013/061051) filed on the 26th October 2012

[2] Oxford University Isis Project No. 11330 – "Asymmetric superconducting RF structure" (UK Priority patent application 1420936.5 titled 'Asymmetric superconducting RF structure' filed on the 25th November 2014

New Generation High Flux (10^{14}-10^{15} ph/s) Sources in the US (BNL), Japan (KEK) and UK (STFC) based on Energy Recovery Super-Conducting CW electron linacs

UH-FLUX

Advanced Compton/THz source based on novel design of coupled SC RF cavities

A. Seryi, JAI

Possible parameters

Typical parameters, range	[		]	
Electron beam E, MeV	10	20	30	
Electron bunch charge, nC	0.2	0.5	1	
e-bunch repetition rage, MHz	50	200	1000	
e-beam average current, A	0.01	0.1	1	
e-beam reactive power, MW	0.1	2	30	
e-beam energy at dump, MeV	0.2	0.1	0.1	
laser wavelength	1000	600	300	
X-ray max energy, keV	2	12	60	
X-ray min wavelength, nm	0.6	0.1	0.02	
X-ray flux, ray/s	1.E+15	8.E+15	4.E+16	
approx peak brilliance	2.E+20	2.E+21	8.E+21	ph/(s mm^2 mrad^2 0.1%bw)
approx RF power, kW	2	10	100	
e-Energy recovery coefficient	50	200	300	

Table from the Patent No. PCT/GB2012/052632 (WO2013/061051) filed on 26th October 2012

High flux X-ray/THz compact SCRF Compton Light Source

With unprecedented and outstanding foreseen performances, at all similar to Synchrotrons, but with higher energy X-rays

-- developing plans for realization of the prototypes of key systems

Quantum beam project – KEK/ATF

Compact (less than 10m) quasi-monochromatic (less than 1%)

High Flux (100 times than Compact normal Linac X-ray : 10^{11} photons/sec 1% b.w.)

High Brightness (10^{17} photons/sec mrad² mm² 0.1% b.w.)

Ultra-short pulse X-ray (40 fs ~)

J. Urakawa, Quantum Beam Project

Key: SCRF acceleration technology

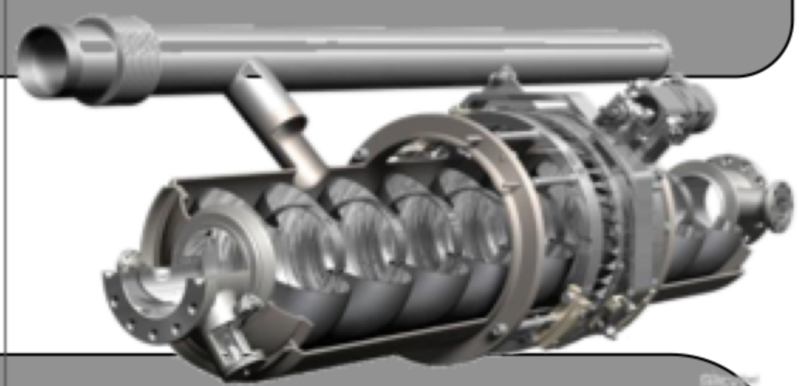

Structural genetic analysis,

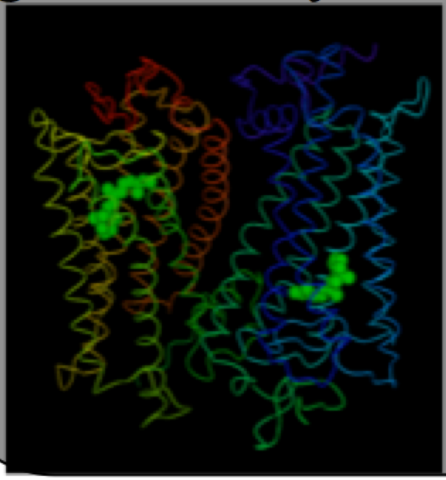

Nano-material evaluation,

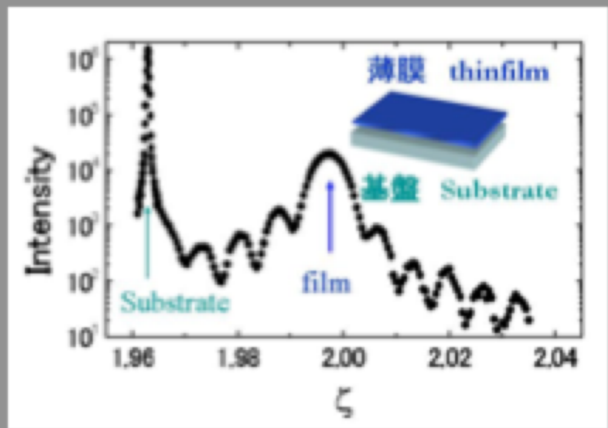

Highly fine X-ray Imaging

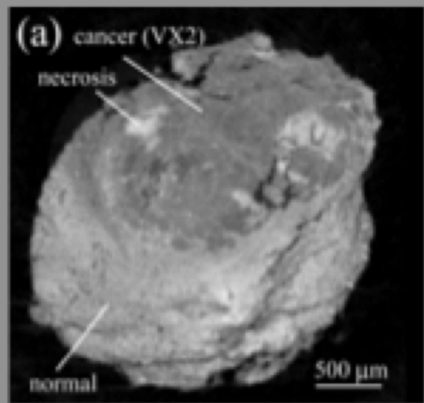

http://mml.k.u-tokyo.ac.jp/

J. Urakawa at KEK-ATF

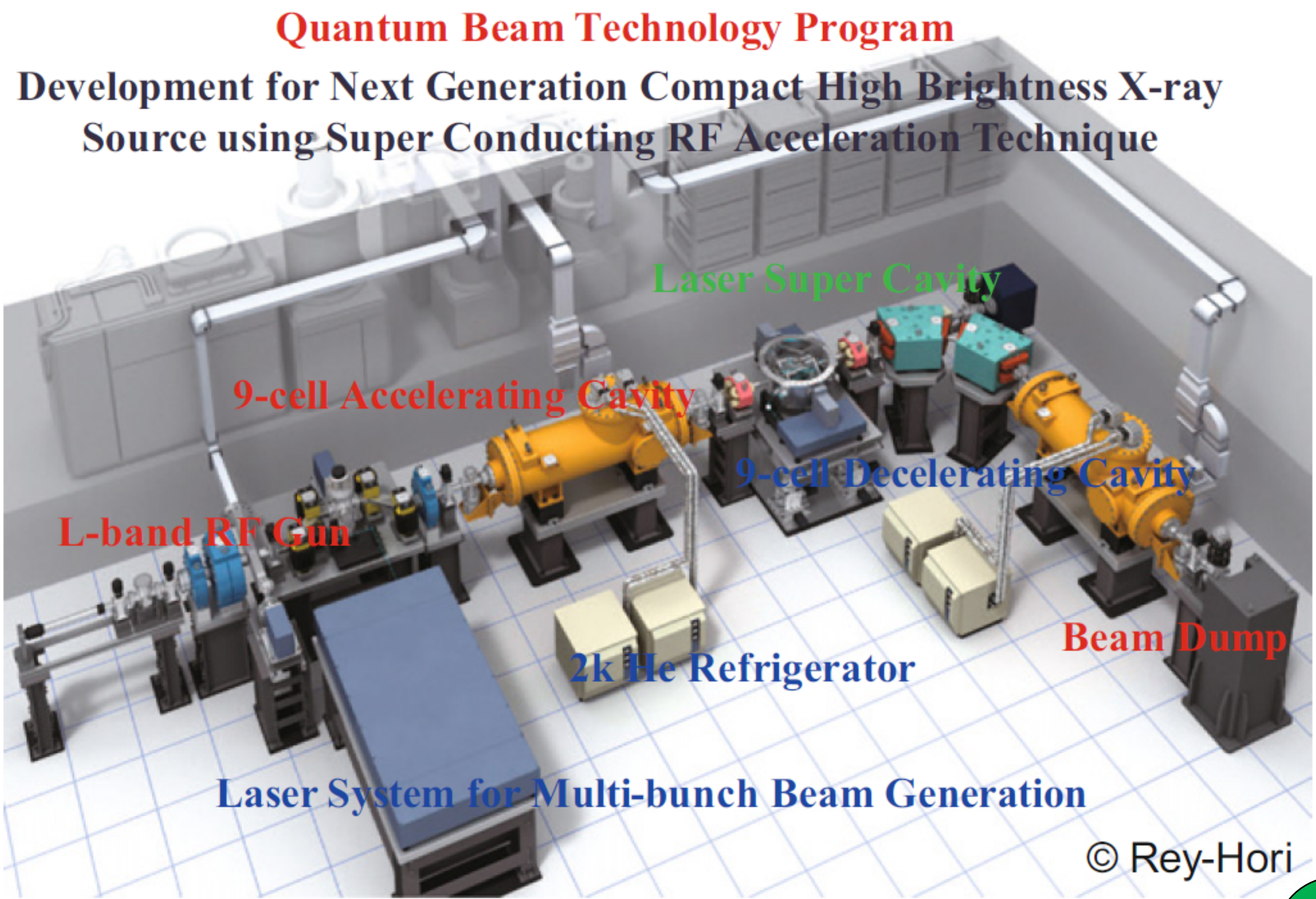

J. Urakawa, Nucl. Instr. and Meth. A (2010), doi:10.1016/j.nima.2010.02.019